AUSTRALIAN INSTITUTE OF NUCLEAR SCIENCE & ENGINEERING

AINSE CONFERENCE ON RADIATION BIOLOGY & CHEMISTRY

16-18 NOVEMBER 1994

CUMING THEATRE, CHEMISTRY DEPARTMENT
THE UNIVERSITY OF MELBOURNE

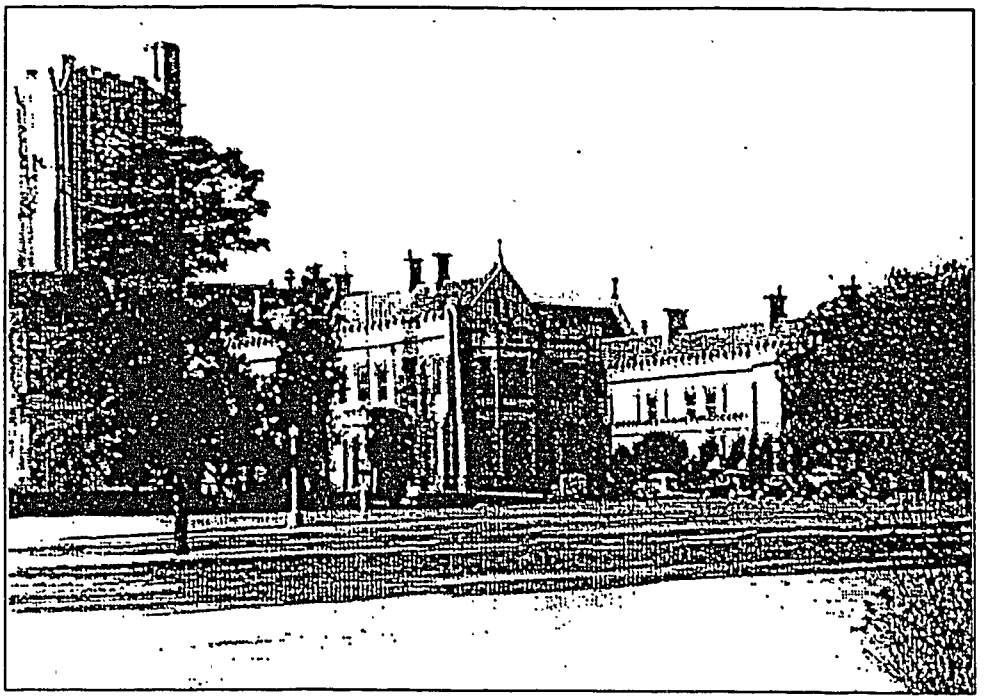

CONFERENCE HANDBOOK

(PROGRAM, ABSTRACTS AND LIST OF PARTICIPANTS)

AUSTRALIAN RADIOISOTOPES

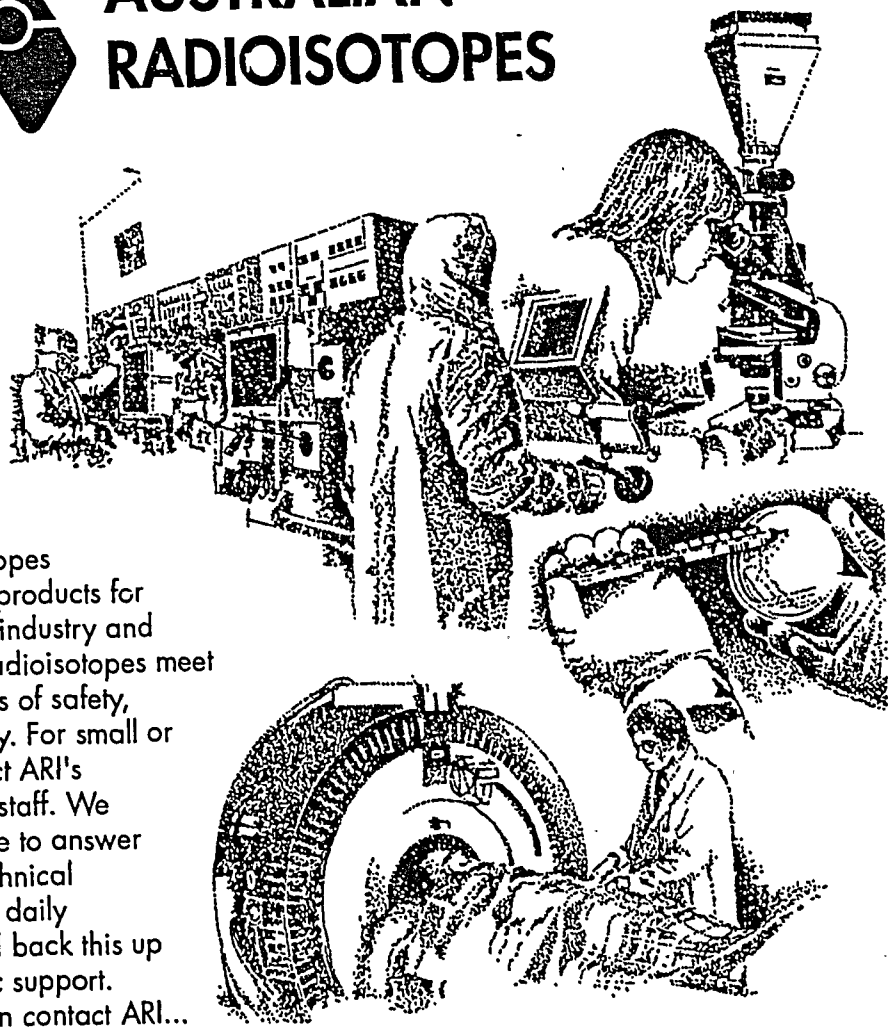

Australian Radioisotopes provide radioactive products for medicine, research, industry and education. All ARI radioisotopes meet the highest standards of safety, reliability and quality. For small or large sources contact ARI's qualified marketing staff. We are always available to answer any questions or technical enquiry. ARI have a daily delivery service and back this up with strong scientific support. For more information contact ARI...

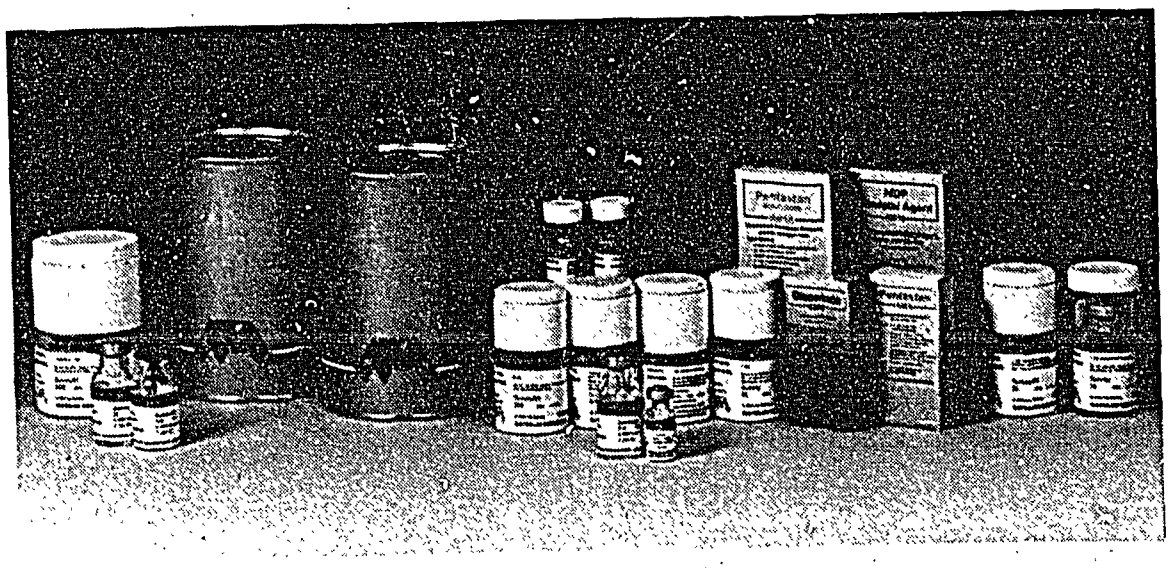

Australian Nuclear Science and Technology Organisation
Lucas Heights Research Laboratories
Private Mail Bag 1, Menai, 2234
Telephone: (02) 717 9008 Facsimile: (02) 543 6511

AUSTRALIAN RADIOISOTOPES

ISBN 0 9598472 3 5

AUSTRALIAN INSTITUTE OF NUCLEAR SCIENCE AND ENGINEERING

AINSE CONFERENCE ON RADIATION BIOLOGY AND CHEMISTRY

CUMING THEATRE, CHEMISTRY DEPARTMENT,
THE UNIVERSITY OF MELBOURNE

16-18 November 1994

Conference Chairman

Dr Roger Martin (The Peter MacCallum Cancer Institute)

Conference Committee

A/Professor Ron Cooper (The University of Melbourne)
Dr John Baldas (Australian Radiation Laboratory)
Dr Henri Tochon-Danguy (PET Centre, Austin Hospital)
Dr Roger Gammon (AINSE)

Conference Manager

Mrs Margaret Lanigan

PROGRAM

WEDNESDAY 16 NOVEMBER

Cuming Theatre, Chemistry Department, The University of Melbourne

TIME	PAPER	
1030		**WELCOMING ADDRESS:** Conference Chairman: Dr R Martin, Peter MacCallum Cancer Institute
Session 1		**Chairman:** **A/Professor Ron Cooper** (The University of Melbourne)
1035		Invited Speaker - Professor K-D Asmus
Plenary	1	**"Radiation and Photochemical Studies on C_{60} and Substituted Fullerenes"** K-D Asmus, D Guldi and H Hungerbühler, Hahn-Meitner-Institut, Berlin
1115		Presentation by Australian Radioisotopes
1120		**MORNING TEA**
Session 2		**Chairman:** **Dr Roger Martin** (Peter MacCallum Cancer Institute)
1140	2	**"The Use of Radiation in Studies of Oxidation of Blood Components"** J M Gebicki, A V Babiy and A Baoutina, Macquarie University
	3	**"Abnormality in Cyclin-Dependent Kinase Activities in Ataxia-Telangiectasia Cells Post-Irradiation"** H Beamish, R Williams and M F Lavin, The University of Queensland/QIMR
	4	**"Mechanistic Studies of Sensitisation of Radiation Induced DNA Strand Breakage by Halogenated DNA Ligands"** P Nel, R Cooper and R F Martin, The University of Melbourne
1240		**POSTER TALKS**
	5	**"Monte Carlo Calculation of Microbeam Radiation in a Tissue/Lung/Tissue Phantom"** F Z Company, B J Allen and P Miskelly, University of Western Sydney, Nepean
	6	**"An ESR Study of the Polymerisation of Acrylates"** G J Gaut, R W Garrett and A P Lang, ANSTO
	7	**"Effect of Proton Irradiation on Mechanical Properties of Polyimides"** J L Hopewell, D J T Hill, J H O'Donnell and P J Pomery, The University of Queensland

Session 2 Cont'd

TIME	PAPER	
	8	**"Investigation of γ-Irradiated Syndiotactic Poly(octyl methacrylate) by Using Multidimensional NMR Spectroscopy,"** L Dong, D J T Hill, J H O'Donnell, P J Pomery and I Brereton, The University of Queensland
	9	**"Radiation Chemistry of Polybutene-1"** G Watson and W K Busfield, Griffith University
	10	**"Radiation Induced Conductivity in X Irradiated Semiconductors"** D Edmondson, The University of Melbourne
1300		**LUNCH**
Session 3		**Chairman: Dr Dieter Asmus** (Hahn-Meitner-Institut, Berlin)
1400		Invited Speaker - Dr Ajit Singh
	Plenary	Sponsored by: Polymer Division, The Royal Australian Chemical Institute
	11	**"Electron Processing - Current and Emerging Applications"** A Singh, AECL Research, Canada
	12	**"Plankton as Monitors of Radionuclides in the South Pacific"** J R Twining, C Poletiko and R A Jeffree, ANSTO
	13	**"Synthesis and Evaluation of C-11 Labelled Radiotracers for Studying Dopamine D1 Receptors Using PET"** H J Tochon-Danguy, M Kassiou, K S Phan, J Sachinidis, S Y Chai, T Jenkins, J G Chan, A Katsifis, W J McKay and F A O Mendelsohn, PET Centre, Austin Hospital
1520		**POSTER TALKS**
	14	**"Correction for the Effect of Radionuclidic Impurities in Ionisation Chamber Measurements of ^{201}Tl"** S M Buckman, ANSTO
	15	**"Extent of K-Characteristic Photon Transport in X-ray Imaging Cassettes"** D McLean, The University of Sydney
	16	**"Oxygen-15 Labelled Water Production for Positron Emission Tomography"** H J Tochon-Danguy, A Janus, J I Sachinidis and G F Egan, PET Centre, Austin Hospital
	17	**"The Legal Measurement of Commonly Used Radionuclides"** H A van der Gaast and S M Buckman, ANSTO

Session 3 Cont'd

TIME	PAPER	
	18	**"The Contribution of ^{210}Po to the Radiation Dose Rate of Marine Organisms"** J D Smith and P H Towler, The University of Melbourne
	19	**"Sonochemical Reduction of $AuCl_{4\,(aq)}^-$"** R Hobson and F Grieser, The University of Melbourne
	20	**"The Effect of Anionic Polymers on the Radiation Induced Nucleation of Silver Particles in Aqueous Solution"** P Mulvaney, The University of Melbourne
1540		**AFTERNOON TEA**
Session 4		**Chairman:** **Dr Peter Wardman** (CRC Gray Laboratory, Mt Vernon Hospital, London)
1600	21	**"New Approaches to the Treatment of Cancer: Photoactivation, Microbeam Irradiation and Growth Factors"** B J Allen, St George Cancer Care Centre
	22	**"Effect of Additives on Radiation Graft Modification of N-Vinyl-2-pyrrolidone onto Ethylene-propylene Rubber"** V Haddadi-asl, R P Burford and J L Garnett, The University of New South Wales
1640		**POSTER TALKS**
	23	**"Mechanistic Studies of Sensitisation by Incorporation of BrU Into DNA"** G C D'Cunha, J Camakaris and R F Martin, Peter MacCallum Cancer Institute
	24	**"Cell Culture Studies of Radiation Sensitisation by Iodinated DNA Ligands"** R F Martin, S Broadhurst, J Humphries and J Camakaris, Peter MacCallum Cancer Institute
	25	**"Evaluation of Radioprotectors Using the Pig Skin Model"** R Budd, S D'Abrew, R Slocombe, S Broadhurst and R F Martin, Peter MacCallum Cancer Institute
	26	**"Increasing the Susceptibility of the Rat 208F Fibroblast Cell Line to Radiation-induced Apoptosis Does Not Alter Its Clonogenic Survival Dose Response"** D R Aldridge, M A Arends and I R Radford, Peter MacCallum Cancer Institute

Session 4 Cont'd

TIME	PAPER	
	27	**"Preliminary Evidence for a Radiation-Induced Adaptive Response *In Vivo*"** J S Prosser, B E Izard, M W Wallace and D Strain, ANSTO
	28	**"Preclinical and Clinical Trials in Boron Neutron Capture Therapy"** B J Allen, St George Cancer Care Centre
	29	**"Alpha and Beta Emitting Radionuclides for Cancer Therapy"** B J Allen, St George Cancer Care Centre
	30	**"Radiation-induced Peroxidation of Proteins and Amino Acids and its Effect on Other Biomolecules"** S Gebicki, R T Dean and J M Gebicki, Macquarie University
	31	**"Synthesis, Characterisation and Effects of Ionising Radiation on Linear Aromatic Polyesters"** E-J Choi, D J T Hill, K Y Kim, J H O'Donnell, P J Pomery and A K Whittaker, The University of Queensland
	32	**"The Impact of Gamma-irradiation on a Series of Polyurethane Thermoplastics Having Differing Structural Components and Compositions"** M I Killeen, F Kroesen and J H O'Donnell, The University of Queensland
	33	**"The Simulation of the Effects of Low Earth Orbit on Some Linear Aromatic Polyimides"** J S Forsythe, D J T Hill, J H O'Donnell, P J Pomery and F A Rasoul, The University of Queensland
	34	**"Irradiation Degradation of Poly(hydroxy ethyl methacrylate) and Poly(ethoxy ethyl methacrylate)"** D J T Hill, J H O'Donnell, P J Pomery and G Saadat, The University of Queensland
	35	**"Polymerisation of Monomers Inside Zeolites"** J Kwiatkowski and A J Whittaker, The University of Queensland

Session 5

1730-1830	**POSTERS/WELCOME DRINKS** Chemistry Dept, The University of Melbourne
1900	**SPIT ROAST** Janet Clarke Hall, The University of Melbourne

THURSDAY 17 NOVEMBER

Morning Sessions:
Peter MacCallum Cancer Institute, St Andrews Place, East Melbourne

TIME	PAPER	
Session 6		**Chairman: Dr R Martin (Peter MacCallum Cancer Institute)**
0900		Invited Speaker - Dr P Wardman
	36	**"Radiation Chemistry at the Interface of Chemistry and Biology"** P Wardman, L P Candeias, M F Dennis, S A Everett, L K Folkes, K B Patel and M R L Stratford, CRC Gray Laboratory, Mount Vernon Hospital, London
	37	**"A Linac Based Absorbed Dose Calibration Facility"** D V Webb, R B Huntley, K Wise and J F Boas, Australian Radiation Laboratory
	38	**"Chemistry of ^{99m}Tc Nitrido Complexes"** J Baldas, Australian Radiation Laboratory
	39	**"Gamma-initiated Radiation Studies of Chain-Length-Dependent Termination Rate Processes in Free-Radical Polymerizations"** P A G M Scheren, G T Russell, D F Sangster, R G Gilbert and A L German, The University of Sydney
1040		**MORNING TEA**
Session 7		**Chairman: Professor Martin Lavin** (The University of Queensland/QIMR)
1100	40	**"Mode of Cell Death and Radiosensitivity"** I R Radford, Peter MacCallum Cancer Institute
	41	**"Dosimetry for Boron Neutron Capture Therapy"** M G Carolan, S A Wallace, H A Meriaty, A B Rosenfeld, B J Allen and J N Mathur, The University of Wollongong
	42	**"Defect in Radiation Signal Transduction in Ataxia Telangiectasia"** M F Lavin, K K Khanna, H Beamish, R Williams J Yan and D Watters, The University of Queensland/QIMR
	43	**"Radium-226 in Skeletal Material of Marine Fishes"** R A Tinker and J D Smith, The University of Melbourne
1220		**LUNCH**

Afternoon Sessions:
Australian Radiation Laboratory, Yallambie

TIME	PAPER	
Session 8		**Chairman: Dr John Baldas (Australian Radiation Laboratory)**
1400	44	**"ARL's National Oversight of Radiation, its Uses and Effects"** Dr K Lokan, Australian Radiation Laboratory
	45	**"The Standardisation of Fluorine-18 and Americium 241"** H A van der Gaast, ANSTO
	46	**"Radiation Crosslinking and Grafting of a Swollen Polymer"** P Hidi, D H Napper and D F Sangster, The University of Sydney
	47	**"Sequence Analysis of Ionizing Radiation-induced DNA Rearrangements"** H Forrester, N Deacon and I Radford, Peter MacCallum Cancer Institute
1530		**AFTERNOON TEA**
Session 9		**Chairman: Professor Bob Gilbert (The University of Sydney)**
1550	48	**"Molecular Structure and Radiation Sensitivity of Elastomers"** T Bremner, D J T Hill, J H O'Donnell, M C Senake Perera, P J Pomery and A K Whittaker, The University of Queensland
	49	**"Dissolution of MnO_2 Colloids by Radicals Generated from Ultrasound"** J Sostaric, P Mulvaney and F Grieser, The University of Melbourne
	50	**"Ion Recombination Rate Constants in Irradiated Gases"** R N Bhave and R Cooper, The University of Melbourne
1700-1800		CONCURRENT TOURS - ARL Accelerator - Austin Hospital PET Facility
1830	CONFERENCE DINNER Janet Clarke Hall, The University of Melbourne	

FRIDAY 18 NOVEMBER 1994

Cuming Theatre, Chemistry Department, The University of Melbourne

TIME	PAPER	
Session 10		**Chairman:** **Professor Barry Allen** (The University of Wollongong)
	51	**"Pulse Radiolysis Studies on the Reaction Between DNA-targeted Compounds and .OH Radical-damaged DNA in Aqueous Solution"** R F Anderson, W A Denny, K B Patel and W R Wilson, The University of Auckland
0900	52	**"Formation of Q-State CdS Colloids Using Ultrasound"** F Grieser, R A Hobson and P Mulvaney, The University of Melbourne
	53	**"Semi-automated Carbon-11 Radioligand Synthesis for Positron Emission Tomography"** K S Phan, H J Tochon-Danguy, J I Sachinidis and D Howells, PET Centre, Austin Hospital
	54	**"Calculations of Yields of Radiation-induced Scission and Crosslinking Yields from Variations of Molecular Weights of Polymers with Dose"** K A Milne and J H O'Donnell, The University of Queensland
	55	**"Mechanism of Radiation Vulcanisation of Natural Rubber Latex Sensitised by Monoacrylates"** D J T Hill, J H O'Donnell, M C S Perera and P J Pomery, The University of Queensland
1040		MORNING TEA
Session 11		**Chairman:** **A/Professor R Cooper** (The University of Melbourne)
1100	56	**"Radiation Dosimetry above 1 Gray: A Comparison of Electron-Spin Resonance and Thermoluminescence Dosimetries"** J F Boas and J G Young, Australian Radiation Laboratory
	57	**"Rates of Energy Migration in Supramolecular Assemblies"** G D Scholes and K P Ghiggino, The University of Melbourne
	58	**"The Radiation Chemistry of Organic Herbicides"** I Bokor, K Cornelius and G S Laurence, The University of Adelaide

Session 11 Cont'd

TIME	PAPER	
	59	**"Monte Carlo Neutron Photon Treatment Planning Calculations: Modelling from CT Scans"** S A Wallace, J N Mathur and B J Allen, The University of Wollongong
	60	**"Recent Advances in Radiation Chemistry and Physics"** R Cooper, The University of Melbourne
1240		**CLOSING REMARKS AND PRESENTATION OF AWARDS**

ABSTRACTS

AUPS15020

Radiation and Photochemical Studies on C_{60} and Substituted Fullerenes

Klaus-Dieter Asmus, Dirk Guldi, and Hartmut Hungerbühler
Hahn-Meitner-Institut Berlin, Glienicker Str. 100, 14109 Berlin, Germany

Redox and alkylation (radical addition) reactions with C_{60} have been investigated by means of radiation chemical methods, particularly time-resolved pulse radiolysis measurements. The primary radical products, $C_{60}^{\bullet -}$, $C_{60}^{\bullet +}$, and radical adducts $(C_{60}\text{-R})^{\bullet}$ exhibit distinct absorption bands in the IR at 1080, 980, and (depending on R) around 900nm, respectively. Reductions, to yield the $C_{60}^{\bullet -}$ radical anion could be achieved by solvated electrons and $(CH_3)_2C(OH)^{\bullet}$ radicals in 2-propanol solutions and toluene/acetone/2-propanol mixtures. The reaction of a water-soluble C_{60}-γ-cyclodextrin complex (C_{60}/γ-CD) with ∝-hydroxyalkyl radicals also involves electron transfer, as indicated by the dependence of the rate constants on the redox potential of the reducing radicals: 2.7×10^8 M^{-1} s^{-1} for $(CH_3)_2C(OH)^{\bullet}$, 1.4×10^8 M^{-1} s^{-1} for $CH_3CH(OH)^{\bullet}$, and 0.5×10^8 M^{-1} s^{-1} for $^{\bullet}CH_2(OH)$. Efficient electron transfer has also been observed between C_{60} and a series of reduced metal porphyrins.

Oxidation of C_{60} to yield $C_{60}^{\bullet +}$ can be achieved through radiation-generated solvent radical cations (1,2-dibromocthane, dichloro- and dibromomethane, c-hexane) or arene radical cations (in CH_2Cl_2). The decay of the $C_{60}^{\bullet +}$ radical cation appears to proceed via a $(C_{60})_2^{\bullet +}$ dimer complex.

Addition of radicals (e.g., $^{\bullet}CH_3$, $^{\bullet}CH_2Br$, $^{\bullet}CH_2CH_2Cl$, and $^{\bullet}CH_2C(CH_3)_2OH$ to the π-system of C_{60} occurs with rate constants on the order of 10^9 M^{-1} s^{-1}. The decay of the adduct radicals involves both a second order component (presumed to be radical dimerization) as well as a pseudo-first order reaction dependent on the C_{60} concentration. The latter (1.0×10^8 M^{-1} s^{-1} for the $^{\bullet}CH_2CH_2Cl$-adduct) is suggested to be an initial step of a polymerisation process.

In further experiments it has been shown that C_{60} can be incorporated into micelles (Triton x 100) and, by means of ultrasonication, also into vesicles (DODAB, lecithin and DHP). Both systems are water soluble and exhibit yellow-brownish colour. Optical absorptions in the VIS are similar to those of C_{60} solutions in alcohols indicating that the C_{60} is probably located near to the polar head groups of the membrane. A concentration dependent UV band in case of the vesicle systems suggests C_{60} aggregation in this type of membranes. The membrane-incorporated C_{60} could be reduced via electron transfer from propan-2-ol radicals, generated

radiolytically in the surrounding water phase. The reduction efficiency was highest for the positively charge DODAB and lowest for the negatively charged DHP.

Solubility of the fullerenes can be enhanced by introduction of substituents. Addition of malondiester units, $>C(COOR)_2$, across one, two or three C_{60} double bonds, for example, leads to compounds which, upon hydrolysis, yield even water soluble $C_{60}[>C(COO^-)_2]_n$ molecules. Most interestingly, the monosubstituted $C_{60}[>C(COO^-)_2]$ does practically not react with hydrated electrons which is taken as evidence for clustering of these fullerenes in aqueous environment.

Complementary studies on most reactions mentioned above have been carried out with time-resolved laser photolysis. They include the investigation of excited states and, in particular, reductive quenching of the excited states to yield the reduced fullerenes. In the case of the substituted fullerenes the IR-absorptions of the one-electron reduced forms reflect a strong influence of the substitution pattern on the electronic structure of these species.

AU PS15021

THE USE OF RADIATION IN STUDIES OF OXIDATION OF BLOOD COMPONENTS

Janusz M. Gebicki, Alexander V. Babiy and Anna Baoutina
School of Biological Sciences, Macquarie University, Sydney, NSW 2019

There is conclusive evidence that formation and reactions of free radicals have significant consequences for the normal functioning and for the pathology of living organisms [1]. The most important of the primary biological radicals are the superoxide, hydroxyl and the nitric oxide, and much is already known about their formation and reactions in living organisms [2]. However, major difficulties exist in the unambiguous identification of cause/effect relatonships in events which begin with the release of free radicals and end with biological changes. These difficulties are caused mainly by the transient nature of the primary radicals, the chemical complexity of living systems and lack of methods for direct studies of reactions which follow radical release. For example, although the superoxide is probably the most commonly generated and abundant primary biological free radical, knowledge of its chemistry suggests that it can only cause biochemical changes after conversion to the hydroxyl radical or after reacting with bound transition metals [3,4]. However, convincing experimental evidence showing which of these, or of other possible mechanisms, operates in living organisms is almost never available. The derivation of reaction mechanisms is complicated by lack of information on the concentrations of potential reactants in tissues, so that even the extensive existing knowledge of reaction rate constants is not usually sufficient to show the relative significance of the many possible competing reactions. It is also seldom possible to identify the radicals and other reactive intermediates formed in any particular biological situation and to measure their yields. The common practice therefore is to isolate a tissue, or a less complex system derived from a living organism, expose it to free radicals and measure some selected end-point of the radical-initiated processes. Final mechanistic interpretation usually requires information from studies of chemically pure systems exposed to similar conditions.

This is a useful approach, but its outcomes are often made more ambiguous than necessary by the use of radical-generating systems which do not allow control of the nature or amounts of the reactive species [5]. The use of ionising radiation can often overcome these uncertainties. Radiation can generate precise quantities of radicals selected for their biological relevance, giving the experimenter control over parameters such as time, temperature, chemical composition and pH. There is no limit to the complexity of the systems investigated, which can vary from pure chemicals to living animals. The main disadvantages are the availability of suitable sources of ionising radiation and lack of familiarity on the part of many biological and medical researchers with the basic concepts of radiation chemistry

In recent studies we have used human blood and its components to obtain information on some biologically relevant effects of radiation-generated free radicals. Blood is an easily obtainable biological fluid which contains a wealth of information on the condition of the donor. In the first study we exposed lipoproteins isolated from blood to free radicals in order to measure their resistance to oxidation. Such information is relevant to the prediction of the susceptibility of individuals to atherosclerosis [6,7] and it may also help in assessment of the effectiveness of preventive treatments or of therapy. This was tested by the use of samples obtained from patients undergoing various treatments [8]. The use of radiation also allowed us to settle the question of the roles of formation and breakdown of lipoprotein peroxides in the generation of atherogenic forms of these blood components [9]. In a related study we are developing a test for the ability of the donor to resist stresses induced by free radicals or by other oxidants. The test relies on the measurement of the formation of peroxides in whole plasma or serum exposed to increasing doses

of radiation-generated free radicals. The kinetics of the process show a distinctive lag period during which the antioxidants present are consumed, followed by a linear rise in peroxide content. Further development of the test is required before it can be generally applied, but we believe that, as suggested in other studies [10], the lag period can be used as a measure of the total antioxidant status of the donor.

1. Halliwell B, Gutteridge JMC and Cross CE. Free radicals, antioxidants, and human disease: where are we now? J. Lab. Clin. Med. 119: 598-620 (1992)
2. Sies H. Strategies for antioxidant defense. Eur. J. Biochem. 215: 213-219 (1993)
3. Walling C. Fenton's reagent revisited. Acc. Chem. Res. 8: 125-131 (1975)
4. Samuni A, Aronovitch J, Godinger D, Chevion M and Czapski G. On the cytotoxicity of vitamin C and metal ions. A site-specific Fenton mechanism. Eur. J. Biochem. 137:119-124 (1983)
5. Fucci L, Oliver CN, Coon MJ and Stadtman ER. Inactivation of key metabolic enzymes by mixed-function oxidation reactions: Possible implication in protein turnover and ageing. Proc. Natl. Acad. Sci. USA 80:1521-1525 (1983)
6. Gebicki JM, Jurgens G and Esterbauer H. Oxidation of low-density lipoprotein in vitro. In "Oxidants and Antioxidants" (Sies H, Ed.) pp371-397, Academic Press, 1991.
7. Babiy AV, Gebicki JM and Sullivan DR. Vitamin E content and low density lipoprotein oxidizability induced by free radicals. Atherosclerosis 81: 175-182 (1990)
8. Babiy AV, Gebicki JM, Sullivan DR and Wiley K. Increased oxidizability of plasma lipoproteins in diabetic patients is not due to glycosylation and can be reduced by probucol treatment. Biochem. Pharmacol. 43: 995-1000 (1992)
9. Gebicki JM and Babiy AV. Roles of formation and decomposition of lipid and protein peroxides in generation of atherogenic low density lipoprotein. In "Frontiers of Reactive Oxygen Species in Biology and Medicine" (Asada K and Yoshikawa T, Eds) pp513-516, Elsevier Science BV, 1994
10. Wayner DDM, Burton GW, Ingold KU, Barclay LRC and Locke SJ. The relative contributions of vitamin E, urate, ascorbate and proteins to the total peroxyl radical-trapping antioxidant activity of human blood plasma. Biochim. Biophys. Acta 924:408-419, 1987.

AU PS15022

ABNORMALITY IN CYCLIN-DEPENDENT KINASE ACTIVITIES IN ATAXIA-TELANGIECTASIA CELLS POST-IRRADIATION

H Beamish, R Williams and M F Lavin
Queensland Cancer Fund Research Unit, Queensland Institute of Medical Research, Bancroft Centre, 300 Herston Road, Brisbane, Qld 4029

Ionizing radiation has an inhibitory effect on cell cycle progression. While cells are susceptible to radiation damage in all phases of the cycle it is important that they repair this damage before progressing through critical stages. In order to achieve this a number of checkpoints exist at G1/S, during S phase and at G2/M. A number of yeast mutants have been described for proteins involved in checkpoint control which are characterized by radiosensitivity, genome instability and abnormal cell division. Many of the phenotypic characteristics of the human genetic disorder ataxia-telangiectasia (A-T) can be explained by abnormalities in cell cycle control. Cells from patients with this disease fail to arrest at the G1/S and G2/M checkpoints after irradiation, exhibit radioresistant DNA synthesis and in the longer term are blocked at G2/M where they die. Failure to observe the G1/S delay post-irradiation appears to be responsible for the genetic instability seen in this syndrome. As outlined in the previous presentation the p53 response to radiation is delayed and/or reduced in A-T cells and as a consequence so too is the cyclin kinase inhibitor WAF1 (p21). In this report we demonstrate that the defect in the p53 response results in a failure of radiation to inhibit the activity of cyclin-dependent kinase activities in A-T cells.

Exposure of asynchronous control cells to ionizing radiation caused a marked decrease in cdk2/cyclin E, cdk2/cylin A cdc2/cyclin A and cdc2/cyclin B activities. In contrast in A-T cells no reduction in any of these activities was observed after exposure of cells to radiation. Reduced activity (cdk2/cyclin E and cdk2/cyclin A) was also observed in control cells synchronized at G1/S but again this reduction in activity was not seen in A-T cell lines. Failure to observe a radiation-induced decrease in cyclin-dependent kinase activities in A-T cell lines correlates with the lack of checkpoint control in these cells post-irradiation.

AUPS 15 023

Mechanistic Studies of Sensitisation of Radiation Induced DNA Strand Breakage by Halogenated DNA Ligands

by

Petronella Nel *#, Ronald Cooper *, Roger F. Martin #

* Department of Chemistry, The University of Melbourne, Parkville, VIC, Australia, 3052

Research Division, Peter MacCallum Cancer Institute, St. Andrews Place, East Melbourne, VIC, Australia, 3002

Abstract

It is well established that the incorporation of iodouracil, sensitizes DNA to cleavage by UV light and to a lesser extent, by ionizing radiation. The accepted mechanism for photosensitization involves photo-dissociation of the carbon-halogen bond, generating a carbon-centered radical on the uracil. This radical, abstracts an H-atom from a 2'-deoxyribosyl carbon, on a neighbouring nucleotide. Subsequently the deoxyribose is degraded via a series of non-enzymatic free radical reactions, generating a DNA strand break.

We have extended this concept in the design of radiosensitizers. In this instance, a halogenated substituent is incorporated onto a DNA binding ligand instead of to a DNA base. It is required that the carbon-centered radical which is anticipated to be generated on the ligand, be appropriately located to induce a DNA strand break, in a similar fashion to the halogenated DNA system described in the first paragraph. This idea is currently being pursued in a collaborative effort between Peter MacCallum Cancer Institute, The University of Melbourne and Latrobe University. Halogenated analogues of the commercially available dye Hoechst 33258 have been synthesized as potential sensitizers.

Current work aims to determine the basis of the large difference in sensitization activity between the isomeric ligands o-I Hoechst and m-I Hoechst. Various experimental systems have been employed to investigate this problem. Ligands have been spectroscopically characterized when free in solution and when bound to DNA. Results suggest that the compounds (like their parent Hoechst compound) interact with DNA.

The relative yields of dehalogenation and DNA strand breakage when irradiating with UV or ionizing radiation have been quantitated. A method has been developed to separate reaction products from DNA after irradiation so that dehalogenation can be quantitated by HPLC. DNA damage is assayed by agarose gel electrophoresis.

Under UV conditions o-I Hoechst dehalogenates and induces DNA strand breaks more efficiently than m-I Hoechst. Under aqueous conditions, when all of the compound is in the minor groove of DNA, both compounds are approximately equally efficient at inducing a strand break for a given number of dehalogenation events (ie. 0.3 strand breaks per dehalogenation event). Therefore, the major difference between the two isomers appears to be a difference in UV induced dehalogenation efficiency.

Under steady state ionizing radiation conditions, dehalogenation could not be demonstrated in the aqueous buffer, due to the chromophores of the ligand being destroyed via hydroxyl radical attack. As a result, no sensitisation of DNA strand breakage is observed for either compound in the aqueous buffer.

Hydroxyl radicals were removed by employing a buffered solvent system which contained 20% ethanol. As a result the radiation induced DNA strand breakage process is dramatically slowed down. Under these conditions o-I Hoechst, not m-I Hoechst, is a sensitizer. When electrons are scavenged by nitrate which was added to the 20% ethanol buffer, both sensitisation and dehalogenation of o-I Hoechst becomes less efficient. Therefore electron capture by the ligand plays a role in the dehalogenation - sensitization process.

Pulse radiolysis experiments confirm that hydroxyl radicals react with these particular Hoechst analogues, destroying the compounds. Both m-I Hoechst and o-I Hoechst also form electron adducts, however, the electron adduct species observed for o-I Hoechst is far more pronounced.

These results will be reported and discussed in further detail.

AUPS15024

MONTE CARLO CALCULATION OF MICROBEAM RADIATION IN A TISSUE/LUNG/TISSUE PHANTOM

F.Z. Company[1], B.J. Allen[2], P. Miskelly[3]

1 *Faculty of Science and Technology, Department of Physics, University of Western Sydney, Nepean, Kingswood 2747, NSW, Australia*
2 *Cancer Care Centre, St George Hospital, Kogarah 2217, NSW, Australia*
3 *Australian Nuclear Science and Technology Organization, Menai 2234, NSW, Australia*

Abstract

Recent advances in synchrotron generated X-ray beams with high fluence rate, small divergence and sharply defined microbeam margins permit investigation of the application of an array of closely spaced, parallel or converging microbeams in radiotherapy.

The proposed technique takes advantage of the hypothesis repair mechanism of capillary cells between alternate microbeam zones, which regenerates the lethally irradiated capillaries. Unlike a pencil beam, more accurate dose calculation, beam width and spacing are essential to minimise radiation damage to normal tissue cells outside the target. The absorbed dose between microbeam zones should be kept below the threshold for radiation damage. Thus the peak-to-valley ratio for the dose distribution should be optimized.

The absorbed dose profile depends on the energy of the incident beam and the composition and density of the medium. In this study, using Monte Carlo computations, the radial absorbed dose of single 24 x 24 μm^2 cross-section X-ray beams of 100 and 300 keV in a tissue/lung/tissue phantom are investigated. Two parallel, 100 keV, 24 x 24 μm^2 cross-section beams, using 200 μm center-to-center spacing, give similar peak-to-valley ratio in both media at the same depth. These results indicate that at 100 KeV, closely spaced microbeam therapy can be applied to the lung as well as the tissue.

It is found that in the 300 keV region the peak-to-valley ratio decreases 200 times compared with 100 KeV. At the center of a bundle of a 1 x 1 cm^2 cross-section, 200 μm center-to-center microbeams, the ratio approaches unity, indicating the unsuitability of this energy region when using closely spaced microbeam therapy.

In the 33 KeV region the peak-to-valley ratio is similar to the 100 KeV. The relatively high surface absorbed dose of 33 KeV microbeam ruls out its possible application in the deep microbeam therapy.

AUPS150 25

AN ESR STUDY OF THE POLYMERISATION OF ACRYLATES

by

Gavin J Gant [1], R Wayne Garrett [1] and Anthony P Lang [2]

1. Applications of Nuclear Physics Program, ANSTO, PMB 1 Menai NSW 2234
2. School of Chemistry, University of Sydney NSW 2006

Abstract

Acrylic monomers have found industrial applications as reactive diluents in the coatings industry. Few studies have been carried out to examine the mechanism by which the polymerisation reaction proceeds in these systems. In the present study, purified monomer samples were solidified at 77K and irradiated with gamma-radiation from a ^{60}Co source. The radicals produced as a result of irradiation were examined using ESR spectroscopy.

Initial spectra recorded at 77K have been attributed to a combination of signals from several species including the initiating acrylate radical, the spectrum of which has been simulated theoretically. Warming the samples produced changes in the observed ESR spectra which have been attributed to the formation of the acrylate propagating radical. The structure of this radical has been proposed and the theoretical spectrum of such a radical compared with that obtained experimentally.

Changes in the total radical concentration with temperature have been followed and rationalised. G-values for radical production have been calculated for several monomers. It was noted that there was a trend toward increasing G-values with increasing length of the acrylic ester side-chain. Prerequisites and precautions necessary for future work in this area have been identified.

AU PS15026

Effect of Proton Irradiation on Mechanical Properties of Polyimides

Jefferson L. Hopewell, David J.T. Hill, James H. O'Donnell and Peter J. Pomery

INTRODUCTION

Polyimide films are widely used in the aerospace industry, mostly as coatings for electrical applications. Polyimide films have been exposed to the general radiation flux existing in low-earth orbit (LEO) as part of the long-duration exposure facility (LDEF) project, in addition to various experiments using generated UV, electron beam and γ-radiation. However one result of space-based experiments has been the detection of a significant flux of high energy protons. The effects of proton radiation on polymers has received little study to date. As a result it was decided to investigate what effect high energy protons has on the mechanical properties of two commercially-available polyimide films, Kapton and Ultem.

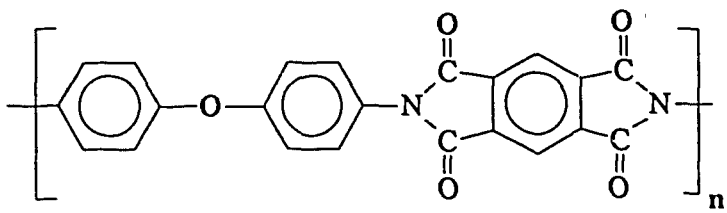

Kapton

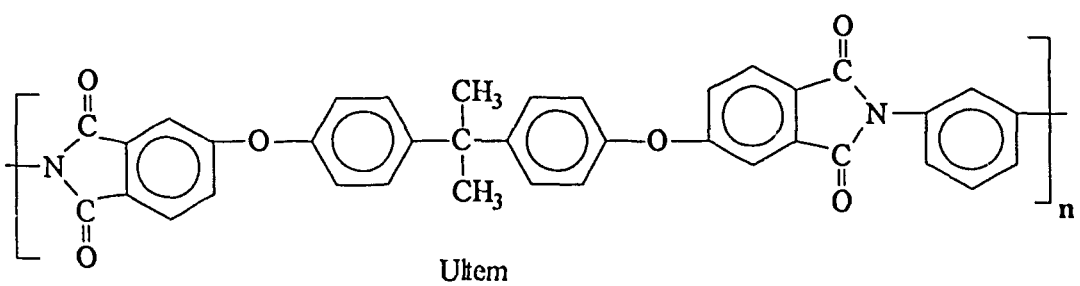

Ultem

MATERIALS AND METHODS

Kapton and Ultem films (obtained from NASA) were used. Chemical structures are given above in Figure 1. Proton beam irradiations were performed using the 3 MeV Van deGraff accelerator at Lucas Heights Research Laboratories. Samples were irradiated as dogbones, 30 mm long with a neck width of 3 mm. Mechanical testing of the samples were then performed on an Instron model 1026, using a crosshead speed of 5 mm/min and a gauge length of 16 mm. Tensile properties were calculated from the resulting stress - strain curves.

RESULTS AND DISCUSSION

There is a general decreasing trend in all mechanical properties, except for the tensile modulus of Kapton. For example, there is a clear decrease in the ultimate elongation (Figure 2) for both Kapton and Ultem polyimides with proton irradiation. which falls considerably with comparatively low dose. This change in the fracture mode from being predominantly 'tough' to 'brittle' is thought to be the result of crosslinking.

High proton dose results in decreasing toughness in both Kapton and Ultem, in that the fracture energy and ultimate elongation both decrease markedly. It is suggested that proton irradiation induced crosslinking is the reason for this embrittlement.

AU9515027

Investigation of γ-Irradiated Syndiotactic Poly(octyl methacrylate) by Using Multidimentional NMR Spectroscopy

Limin Dong, David J. T. Hill, James H. O'Donnell, Peter J. Pomery and Ian Brereton*

Polymer Materials & Radiation Group, Department of Chemistry and Centre for Magnetic Resonance, The University of Queensland, QLD 4072, Australia*

ABSTRACT

It is well known that the irradiation of poly(methyl methacrylate) results in the formation of main chain scission-type radicals which might initiate depolymerization. However, little attention has been given to the poly(methacrylates) with a long side chain in the ester group. It is more interesting that the radiation chemistry of long side chain poly(methacrylates) appears to present new information since decomposition occurs both in the main chain and the extended side chain, which will be different from PMMA. In the present work, the γ-irradiated syndiotactic poly(octyl methacrylate) has been studied by NMR spectroscopy in order to examine the effect of octyl side chain in the γ-irradiation.

In this study, the NMR peaks of ^{1}H and ^{13}C nuclei for the γ-irradiated syndiotactic poly(octyl methacrylate) sample were assigned by using 2D and DEPT techniques. The spin-echo pulse had been introduced in order to modify ^{1}H-^{1}H shift-correlated (COSY) NMR and proton-detected ^{1}H-^{13}C heteronuclear shift-correlated (hetero-COSY) NMR. Thus, some signals from small molecules which were formed during γ-irradiation and from long-distance couplings in the γ-irradiated syndiotactic poly(octyl methacrylate) sample could be observed in the 2D spectra while the signals from macromolecules with short T_2 and from the coupling with greater coupling constants would be attenuated.

Figure 1 shows the ^{1}H detected hetero-COSY spectrum which can be used to assign the resonances in the polymer chain. Figure 2 shows the spin-echo modified COSY spectrum which provides some information for couplings in small molecule and long-distance coupling. Detailed results and discussion will be given in this poster.

REFERENCES

1. Miller, K. J.; Hellman, J. H.; Moore, J. A. *Macromolecules*, **1993**, *26*, 4945.
2. Beshah, K. *Macromolecules*, **1992**, *25*, 5597.

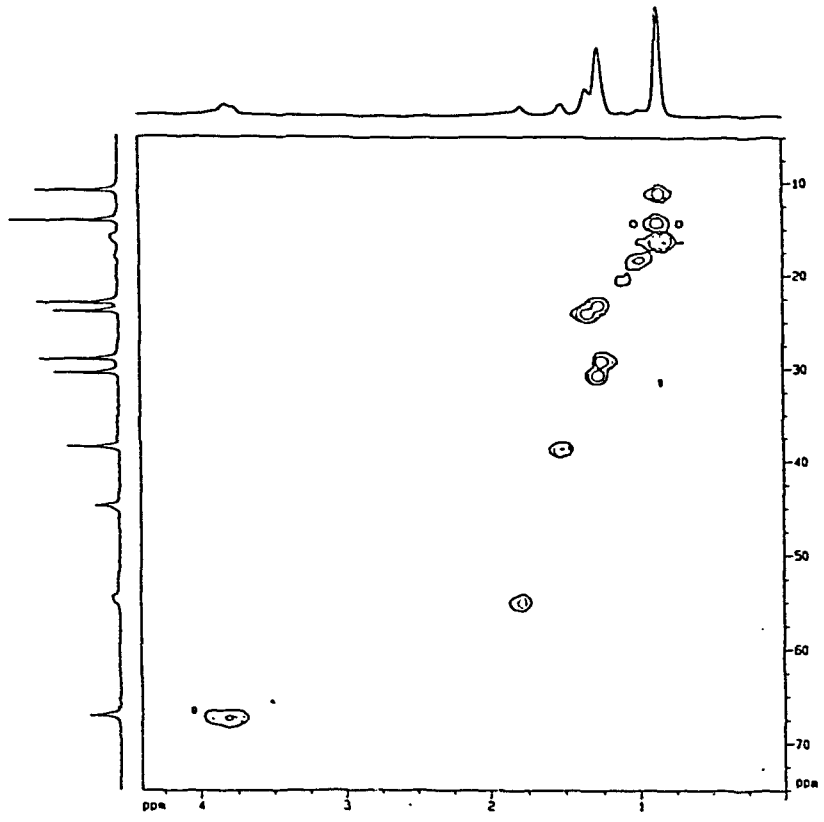

Figure 1. The ^{1}H detected hetero-COSY spectrum of γ-irradiated syndisotactic poly(octyl methacrylate).

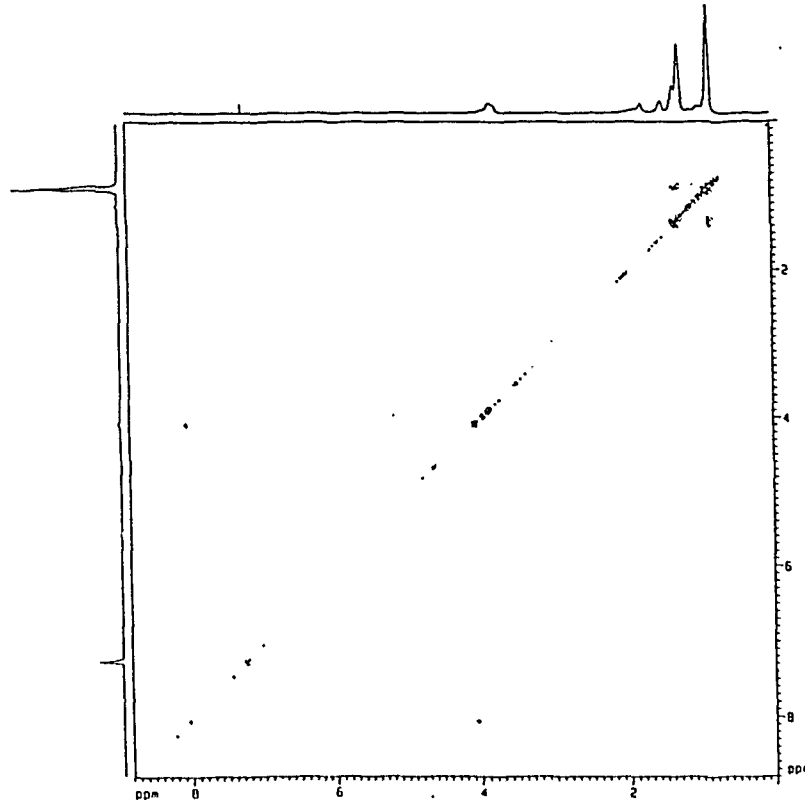

Figure 2. The spin-echo modified COSY spectrum of γ-irradiated syndisotactic poly(octyl methacrylate)

AUPS 15028

RADIATION CHEMISTRY OF POLYBUTENE-1

Greg WATSON and W.Ken BUSFIELD

School of Science
Griffith University
Nathan Qld 4111
Australia

A recent investigation of the effect of high energy irradiation on the stereoregularity of isotactic polypropylene[1] showed dramatic effects. Gamma radiation produced a G value for the loss of isotactic pentad sequences of 94 at ambient temperature and 220 if the irradiation was carried out above the melt temperature. With a knowledge of the mechanism, deduced from changes in the full pentad distribution, the ambient temperature value translates into a G value for configurational inversion of >21 $(100\ eV)^{-1}$. This value is considerably higher than the G value for any other chemical event in polypropylene, e.g. G (crosslinking) and G(scission) have values of about 0.9 and $G(H_2)=2$. The suggested explanation is that the irradiation promotes many more chain scission events than G(scission) suggests, but a large proportion are nullified by recombination in the cage. With stereoregular polymers however, there is sufficient time between scission and recombination for bond rotation and configurational inversion of the free radical end, leading to extensive loss of stereoregularity. In contrast, a previous investigation of the effect of irradiation on isotactic polymethylmethacrylate[2] showed that even a 2 MGy dose produced only minor changes in tacticity.

In this paper we report our preliminary findings on the influence of gamma irradiation on isotactic polybutene-1, a polymer of commercial interest which has a chemical structure similar to that of polypropylene. The irradiation chemistry of polybutene-1 has not been extensively studied previously. Mark and Flory[3] found that irradiation produced predominant crosslinking in isotactic films and that the extent of crosslinking was much reduced in atactic polymer.

The sample used in this work is moderately isotactic, 68.8% mm triads, and low MW, 20,900. Gelation does occur after moderate doses and this limits the dose range for high resolution ^{13}C NMR analysis. However, a satisfactory spectrum of a sample irradiated to 750 kGy has been obtained. An analysis of the fine structure of the signal due to side chain methylene C indicates a decrease of isotactic pentad sequence concentration from 55.5% to 48.7%. This is equivalent to a G value of $-16.1\ (100eV)^{-1}$, considerably less than that in polypropylene.

References

[1] W.K. Busfield and J.V. Hanna, Polymer J. **23**, 1253 (1991).
[2] E. Thompson, J.Polym.Sci., Letters Edit., **3**, 675 (1965).
[3] J.E. Mark and P.J. Flory, J.Amer.Chem.Soc. **87**, 1423 (1965).

AVPS15029

Radiation Induced Conductivity in X Irradiated Semiconductors

D. Edmondson

Radiation Chemistry Group,
The School of Chemistry,
The University of Melbourne,
Parkville, 3052,
Australia.

Irradiation induced conductivity changes in titanium dioxide and cadmium sulphide were detected with a time resolved microwave conductivity technique. Conductivity changes were induced in the semiconducting titanium dioxide and cadmium sulphide with high energy X-rays. A linear dependence of the induced conductivity on the radiation dose was detected for both cadmium sulphide and titanium dioxide with doses of 0.04 - 0.40 Gy.

Previous experiments[1,2,3,4] detected the mobilities and recombination kinetics of the major charge carriers in electron irradiated titanium dioxide in air and with adsorbed liquids.

In the present experiments the effects of air, nitrogen, oxygen, hydrogen, helium and sulfur hexafluoride were distinguished from the induced conductivity of an anatase titanium dioxide sample evacuated of gases. Charge scavenging and charge trapping by physisorbed and chemisorbed gases were detected.

Increases in the dimensions of the titanium dioxide particles are directly related to increases in the lifetime of the irradiation induced conductivity change. Lesser effects were detected with larger sized particle samples. These samples were produced at the Advanced Mineral Products Centre in the University of Melbourne. The particles, which were a rutile structure, were photographed with a transmission electron microscope. The average particle dimensions were calculated from the photographs; submicron and nanometer sized particle samples were irradiated in these particle size experiments.

References:
1. J. M. Warman, M. P. de Haas, M. Graetzel, P. P. Infelta, Nature 1984, 310, 306-308.
2. K. M. Schindler, M. Kunst, J. Phys. Chem., 1990, 94, 8222-8226.
3. J. M. Warman, M. P. de Haas, P. Pichat, T. P. M. Koster, E. A. van der Zouwen-Assink, A. Mackor, R. Cooper, Radiat. Phys. Chem., 1991, 37, 433.
4. J. M. Warman, M. P. de Haas, P. Pichat, N. Serpone, J. Phys. Chem., 1991, 95, 8858-8861.

AUPS 15030

ELECTRON PROCESSING – CURRENT AND EMERGING APPLICATIONS

AJIT SINGH

Research Chemistry Branch, AECL Research
Whiteshell Laboratories, Pinawa, Manitoba, Canada ROE ILO

The interaction of high-energy radiation with organic and biological systems produces very reactive, short-lived, ionic and free-radical species. The chemical and biological changes brought about by these species are very useful in several systems, and are the basis of the growth of the electron processing industry. The availability of reliable (availability, >95%), high-power, electron accelerators has contributed to this growth. The number of electron accelerators in industrial use for processing exceeds 800. Some of the traditional areas of the use of these accelerators in the plastic industry are (i) crosslinking of wire and cable insulation, (ii) manufacture of heat-shrink items, including thin films and electric connectors, (iii) crosslinking of polyethylene pipe, (iv) curing of coatings, (v) manufacturing of plastic foams, and(vi) partial curing of rubber products. Some of the biological applications include sterilising medical devices and sewage treatment.

The emerging applications of electron accelerators include production of advanced composites for the aerospace industry, modification of the process to produce viscose, production of immobilised enzymes and pharmaceutical's, wastewater treatment, and treatment of gaseous effluent's.

Traditionally, the graphite-, aramid- and glass-fibre-reinforced composites with epoxy matrices are produced by thermal curing. However, equivalent composites with acrylated-epoxy matrices can be made by electron curing. Cost estimates suggest that electron curing could be more economical than thermal curing.

During traditional viscose production, high concentrations of alkali, acid and carbon disulfide are used in a multi-step process. Electron irradiation of pulp can lead to (i) a significant reduction in the required amounts of alkali and acid, (ii) a large reduction in the required amount of carbon disulfide, (iii) a significant reduction in the emissions of carbon disulfide and hydrogen sulfide, and (iv) elimination of the ageing step, with a large overall reduction in the cost of viscose production.

In this paper, the fields of industrial radiation chemistry and radiation biology will be reviewed, with emphasis on the work performed at Whiteshell Laboratories.

AUPS1501 31

Plankton as Monitors of Radionuclides in the South Pacific.

J. R. Twining[1], C. Poletiko* & R. A. Jeffree[1]
[1] Environmental Science Program, ANSTO, Australia
* ISPN, CEA, France

Extended Abstract

Aims & Rationale

Zooplankton are known for their ability to accumulate a variety of elements to levels up to 10^4 times higher than their concentration in associated water. Thus, they have been sampled for use as biomonitors of radionuclides in the waters surrounding the French nuclear test sites at Mururoa and Fangataufa as well as in the more populated areas of French Polynesia (Figure 1). Given the global distribution of fallout from atmospheric testing in past decades it was important to determine background levels within similar latitudes. For this reason, sampling was also undertaken in Australian coastal waters.

Figure 1. Plankton sampling regions.

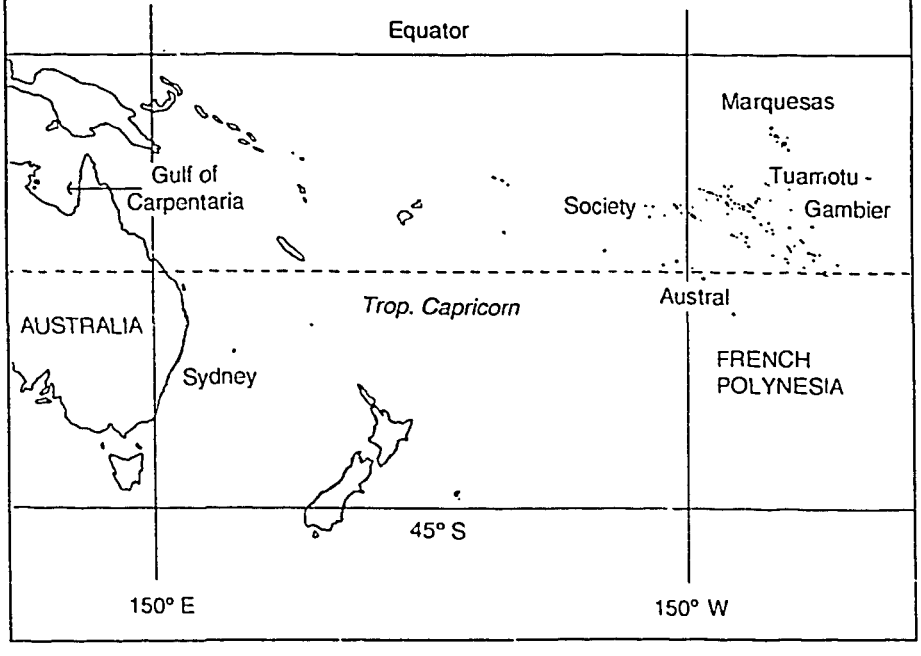

These organisms also have a fundamental importance in marine foodchains, particularly in relation to biomagnification of isotopes such as polonium to humans, and are also significant factors in the biogeochemistry of radionuclides in the marine environment.

This paper summarises our results to date on the concentrations of natural and artificial radionuclides in zooplankton from the two regions, and discusses the implications of the findings to dose assessment in areas of low planktonic productivity.

Methods

Samples were collected between 18/8/90 and 29/6/92 from waters of the Maquesas (n = 12), Society (10), Tuamotu-Gambier (6) and Austral (2) island groups in French Polynesia as well as from the Gulf of Carpentaria (27) and the waters off Sydney (3) (Figure 1). Depths between the surface and 100m were sampled by trawled plankton nets and the filtered volumes determined using meters positioned at the opening of the nets. Samples were dried at 60°C for 7 days to give an average FW/DW ratio of 7.5. The dried samples were split between laboratories for replicant analyses and quality control. Gamma analyses were performed using shielded, HP Ge, coaxial detector systems and efficiencies determined using mixed nuclide standards in similar geometry to the samples. For the alpha emitters, $^{239/240}$Pu and ^{210}Po, extra replicates were also analysed by the Service Centrale de Protection Contre les Rayonnments Ionisants, France as part of our quality assurance program. Detection efficiency was determined using ^{238}Pu or ^{208}Po yield tracers.

Results and Discussion

Average zooplankton densities varied from 0.47 to 50.0 mg (DW)/m^3. The lowest densities were recorded in samples from French Polynesian waters which were between 1 and 2 orders of magnitude lower than those measured in Australian samples. In all regions Copepods (primarily Calanoid then Podoploid) numerically dominated the taxonomic composition of the samples.

As part of the quality assurance program, the results for replicate sample analyses for individual isotopes were linearly regressed between each laboratory. In all comparisons the regression coefficients were highly significant ($p < 0.005$, $r = 0.54$ to 0.95). These results imply good quality control despite the errors implicit in such low level determinations and the fact that split, not homogenised, samples were used.

The results for specific activities detected by each laboratory showed that:

- ^{134}Cs, ^{137}Cs, ^{60}Co and ^{90}Sr were not detected. This in part reflects the low concentration factor for some elements, but also indicates that levels of these isotopes in French Polynesian waters were not high enough to generate significant concentrations in the plankton;
- $^{239/240}Pu$ was detected in some samples from each region except the Austral Archipelago and the waters off Sydney. The measured low levels ranged from 0.05 to 2.15 Bq/kg DW with the highest levels consistently found in the Tuamotu-Gambier group. Subsequent observations showed that these high values were from samples collected during a single trip in 1991;
- ^{228}Ac was only detected in samples from the Gulf of Carpentaria which is consistent with their collection from a shallow coastal environment. Its progenitor, ^{232}Th, is derived from erosion of continental masses but is quickly adsorbed onto particles and drops out of solution once it enters the marine environment; and
- Average ^{210}Po concentrations were inversely correlated with plankton density (figure 2). This result was consistent with the greater removal rate for Po by adsorption onto sinking biogenic particulates (eg faecal pellets) which are produced more frequently in higher productivity regions. This is combined with the major source of ^{210}Po being decay of atmospheric ^{222}Rn and aerial deposition of its progeny ^{210}Pb directly into the oceans. Ingrowth of ^{210}Po then occurs with a 138 day half-life. It is proposed that plankton in lower productivity regions are exposed to and thus accumulate higher concentrations of ^{210}Po.

Figure 2. The inverse relationship between ^{210}Po and plankton density.

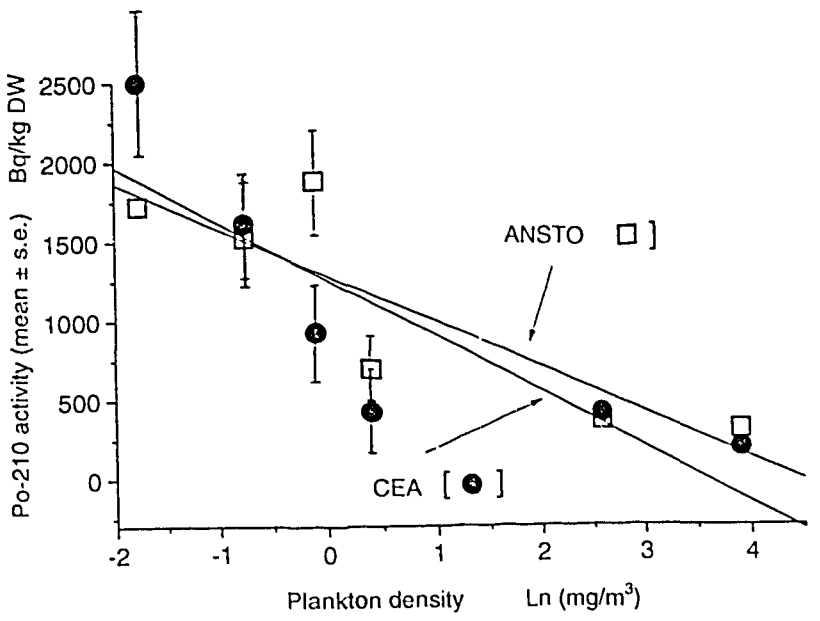

One hypothesis arising from the higher concentration of ^{210}Po in plankton is that secondary consumers, eg fish, could be expected to have similarly increased ^{210}Po concentrations in lower productivity areas. It follows that humans consuming these fish could therefore be expected to be exposed to higher dose from ^{210}Po due to consumption of these fish. Some support for this hypothesis can be found in the limited data bases for edible fish in low productivity regions around the Marshall Islands, located in the mid North Pacific Ocean. The values from two studies, when compared with global averages for commercial fisheries, indicate higher concentrations in both pelagic and reef fish from the low productivity area. When this result is compounded by the higher intake of fish as a proportion of total diet in these environments and by the proposed changes in the transfer factors for ingested polonium in the latest ICRP models, then the dose from ^{210}Po may become radiologically significant.

SYNTHESIS AND EVALUATION OF C-11 LABELLED RADIOTRACERS FOR STUDYING DOPAMINE D1 RECEPTORS USING PET.

TOCHON-DANGUY H.J., KASSIOU M.*, PHAN K.S., SACHINIDIS J., CHAI S.Y., JENKINS T., CHAN J.G., KATSIFIS A.*, McKAY W.J., MENDELSOHN F.A.O.
Centre for PET & Department of Medicine, Austin Hospital, Heidelberg VIC 3084; and *Biomedicine and Health Program, Ansto, Sydney NSW.

A Positron Emission Tomography (PET) facility has been recently established within the Department of Nuclear Medicine at the Austin Hospital in Melbourne. This non-invasive imaging technique is based on the use of biologically relevant compounds labelled with short-lived positron-emitting radionuclides. The basic equipment consists of a whole body scanner (model ECAT 951) from Siemens/CTI, a small cyclotron (cyclone 10/5) from IBA and six shielded hotcells for the production of radiolabelled pharmaceuticals.

In clinical applications, the radiotracer is introduced into the patient usually by injection and the concentration in tissue measured by PET. The time course of the tracer uptake may be followed and related to biochemical pathways, when the precise localisation of the tracer may provide important clinical information. Recent developments in PET and in radioligand specificity, have allowed the possibility of visualising the distribution of neuroreceptors in the living human brain (1). The receptors for brain neurotransmitters are of fundamental importance for psychiatrists since most of the currently used pharmacological drugs induce their effects by interacting with neuroreceptors.
In the dopaminergic system, communication between neurons takes place through the liberation of dopamine, a neurotransmitter stored in pre-synaptic vesicles which binds to post-synaptic receptors. Through PET studies, it is now possible to relate changes in neurotransmitter function to clinical features.
In order to fulfil the Austin Hospital's PET potential in neuroreceptor mapping of the central dopaminergic system, [^{11}C]-radiosynthesis of two relevant ligands were investigated: [^{11}C]-SCH23390, a specific D_1 radioligand (2) extensively used in clinical PET studies; and [^{11}C]-A69024, a more biologically stable D_1 radioligand (3) recently investigated overseas. In this work we report the first Australian experience in the [^{11}C] labelling of pharmaceuticals, and discuss our preliminary in vivo animal studies.

It is obvious that radiosynthesis of such compounds, performed in a hot cell by remote control, are rather delicate, and protocols of chemical manipulations differ from one author to another. Due to the rapid radioactive decay throughout the procedure (because of the short half-life of the radionuclides, for example 20 minutes for ^{11}C), time is an important constraint on synthesis. In addition, to produce useful amounts of the final product, considerable amounts of radioactivity have to be used initially.

[^{11}C]-SCH23390

The labelling of SCH23390 is carried out by N-alkylation of the desmethyl compound with [^{11}C]-iodeomethane. After HPLC purification, the solution is sterilised by filtration (Millipore 0.22μm), to give 50-100mCi of pure [^{11}C]-SCH23390. The total time of synthesis was 30min including HPLC purification, and the average specific activity of the tracer calculated at the end of synthesis was 500mCi/μmol.

[^{11}C]-A69024

The labelling of the non-benzazepine ligand A69024 was carried out using the same automated [^{11}C]-methylation procedure. The average yield of production was 50mCi of purified product with a specific activity close to 500mCi/μmol at the end of synthesis.

Preliminary biodistribution of both tracers in Wister rats was observed at 30min and 60min after the intravenous injection of 0.5mCi of the radiopharmaceutical. The tissue radioactivity was measured with a gamma counter, and was corrected for decay. Both tracers showed a high binding in the dopamine-rich caudate-putamen: for the [^{11}C]-SCH23390 compound, a striatum/cerebellum uptake ratio of 10.2 and 17.7 was found at 30min and 60min respectively; for the [^{11}C]-A69024 compound, the striatum/cerebellum uptake ratio was found to be 4.0 at 30min. These results are in good agreement with data from the literature, and further [^{11}C]-labelling is now under progress.

In conclusion, we have shown that the production of [^{11}C]-radioligands has been successfully carried out at the Austin Hospital PET Centre, and that in the near future we should be ready for clinical PET studies of cerebral D_1 receptors in the human brain.

References.

1. Maziere M., Berger G., Comar D. 11C-radiopharmaceuticals for brain receptor studies in conjunction with positron emission tomography. In: Applications of Nuclear and radiochemistry; Lambrecht and Morcos ed. Pergamon Press, New York (1982) pp 251-270.
2. Dejesus O.T., Van Moffaert G.J.C., Friedman A.M. Evaluation of Positron-emitting SCH 23390 Analogs as Tracers for CNS Dopamine D1 Receptors. Nucl. Med. Biol. 1989;16:47-50.
3. Kassiou M., Scheffel U., Ravert H.T., Mathews W.B. et al. [11C]A-69024: A Potent and Selective Non-benzazepine Radiotracer for In Vivo Studies of Dopamine D1 Receptors. Nucl. Med. Biol. 1994 (in press).

AUPS9150 33

Correction for the Effect of Radionuclidic Impurities in Ionisation Chamber Measurements of ^{201}Tl

by Mr S.M.Buckman
Ansto-Physics, PMB 1, Menai, New South Wales, 2234.

The National Medical Cyclotron (NMC) in Sydney commenced commercial production of ^{201}Tl in May 1993[1]. From the locally produced ^{201}Tl, Australian Radioisotopes (ARI) produces radiopharmaceuticals which are supplied to the nuclear medicine community. Under the National Measurement Act, 1960[2] the activities quoted on products supplied by ARI must be legally traceable to National standards of measurement. The Australian primary standard of measurement for radioactivity is the legal responsibility of the Radiation Standards Project at ANSTO[3].

The Radiation Standards Project, in collaboration with the Quality Control section at ARI, has established an on-going calibration program to ensure that ARI's activity measuring equipment is traceable to National standards.

Soon after the production of ^{201}Tl commenced at the NMC, inconsistencies were observed in ionisation chamber measurements of ^{201}Tl solutions. The cause for these inconsistencies was shown to be the presence of the radionuclidic impurities, ^{200}Tl and ^{202}Tl.

Even though the levels of these impurities were well below the recommended limits[4], their effect on ionisation chamber measurements could be relatively large. In order to correct for the effect of these impurities, calibration factors for ^{200}Tl and ^{202}Tl were determined using two independent methods.

In the first method[5], the calibration factors were calculated from the decay scheme of the nuclides and the response curve of the ionisation chamber. However, this method can only be applied when the response curve of the ionisation chamber is reasonably well known and where there is no significant contribution due to bremsstrahlung.

An alternative and more reliable method was developed which used statistical modelling techniques[6] to obtain maximum likelihood estimates of the calibration factors. This method can be used in cases where there may be significant bremsstrahlung production or where the gamma-energy response curve is unknown.

By using these methods, calibration factors were determined for two TPA chambers and a Vinten IV dose calibrator. The results from the two methods were in agreement to within the measurement uncertainties.

By incorporating these calibration factors into the measurement systems of both the Quality Control and Production sections at ARI, the effect of these impurities on ionisation chamber measurements was successfully eliminated.

The accuracy of the Australian standard of measurement for ^{201}Tl has now been confirmed by International intercomparison through the international reference system for gamma-emitting nuclides[7].

References:

1. Wood, N.R. "Thallium-201 production at the National Medical Cyclotron." Newsletter of the Australian and New Zealand Society of Nuclear Medicine. Sept 1993.

2. "National Measurement Act, 1960." Australian Commonwealth Government, amended to 1989.

3. Buckman, S.M. "The Australian national standard of measurement for radioactivity." Newsletter of the Australian and New Zealand Society of Nuclear Medicine. Dec 1992.

4. British Pharmacopoeia 1988, addendum 1989. p1204

5. Urquhart, D.F. "Calibration and operation of the AAEC working standard of measurement for the activity of radionuclides. Part 1: The measurement system." **AAEC/E627** (1987)

6. Buckman, S.M. "Metrology and statistical analysis for the standardisation of ^{60}Co by $4\pi\beta$-γ coincidence counting." PhD thesis (in progress), Macquarie University.

7. Rytz, A. "The international reference system for activity measurements of γ-ray emitting nuclides." *Int. J. Appl. Radiat. Isot.*, **34**(8) 1047-1056.

AUPS15034

Extent of K-Characteristic Photon Transport in X-ray Imaging Cassettes

Donald McLean

School of Medical Radiation Technology

University of Sydney, East Street Lidcombe, NSW 2141, Australia

Abstract:

Image quality in diagnostic screen-film radiography is degraded by the presence of non-primary photons. These photons, generated either within or without the x-ray intensifying cassette, reduce both contrast and resolution. Visible light photons, scattered or transported across the base of a double emulsion film have recently been minimised by a number of new techniques. X-ray photons, originating within the cassette, may also reduce image contrast and resolution. The purpose of this paper is to explore the extent of this effect for (i) some standard x-ray cassettes at a variety of exposure conditions, and (ii) multiple detector cassettes (that is, cassettes containing two or more films or imaging plates).

The transport of K-characteristic photons, generated within an intensifying phosphor, has been mathematically modelled. The validity of this model as a function x-ray energy, phosphor composition, field size and detector geometry has been established. Measurements of resolution degradation, using a high contrast line pair phantom, have been made (i) for a standard x-ray cassette as a function of x-ray energy and (ii) for a multiple detector cassette. Calculations show that for a Lanex Medium cassette, over 8% of the absorbed energy in the cassette can be attributable to K-characteristic x-ray transfer at high kVp. This results in a measurable drop in image resolution for both standard x-ray cassettes and multiple detector cassettes.

K-characteristic x-ray transfer has been identified as having a significant effect in diagnostic energy x-ray imaging systems. The effect is phosphor dependent and may be particularly significant in multiple detector cassettes.

AUPS150035

OXYGEN-15 LABELLED WATER PRODUCTION FOR POSITRON EMISSION TOMOGRAPHY

H.J. Tochon-Danguy, A.Janus, J.I.Sachinidis, G.F.Egan
Centre for Positron Emission Tomography, Department Nuclear Medicine, Austin Hospital.

Introduction:
A Positron Emission Tomography (PET) facility has been established at the Austin Hospital in Melbourne. PET is a non-invasive technique based on the use of biologically relevant compounds labelled with short-lived positron emitters such as $^{18}F(t_{1/2}=110min)$, $^{11}C(20min)$, $^{13}N(10min)$ and $^{15}O(2min)$. PET enables the *in vivo* study of dynamic physiological and biochemical processes since the labelled molecules are metabolically equivalent to the natural unlabelled analogues.

The short half-life of oxygen-15 allows for multiple administration to a patient without exceeding acceptable levels of absorbed radiation dose and without excessive delay between administrations. The clinical usefulness of [^{15}O]-labelled water for cerebral blood flow measurements has been well established.[1] Here we report the development and construction of an [^{15}O]-water generator based on a design by Clark and Tochon-Danguy.[2] The present system has been in operation for nine months and has been used for clinical evaluation of stroke patients and for brain activation research.

Radionuclide production:
The cyclotron produces a continuous flow of [^{15}O]-O_2 gas by the irradiation of a target mixture of 1% oxygen in nitrogen. The ^{15}O-radionuclide is produced via the nuclear reaction of nitrogen with a 5MeV deuteron beam ($^{14}N(d,n)^{15}O$). The radioactive gas is then mixed with 5% hydrogen and piped to the water generator in the scanner room (figure 1).

Water generator:
The water generator (figure 2) sits in a lead-shielded cylinder situated under the patient bed and is connected to the radioactive gas line from the cyclotron. The O_2/H_2 gas mixture is reacted over a palladium catalyst at 150°C to produce [^{15}O]-H_2O vapour. This passes through the exchanger where it diffuses across a semi-permeable membrane (cellulose acetate) into saline solution. At the optimum gas flow-rate of 500ml/min, more than 95% of the radioactive oxygen is converted to radioactive water. Waste radioactive gas is piped back to the cyclotron vault to allow decay before release to the atmosphere.

The saline solution (0.9% NaCl) is pumped continuously through the system at 6ml/min with an infusion pump (3M AVI470). The flowpath through the generator is controlled by two 3-way electrovalves and is determined by the mode of delivery to the patient. In continuous mode operation, the saline flows through the membrane exchanger and is then directed either to the patient line for infusion, or to the waste decay line. In bolus mode, the flow bypasses the exchanger for a period of time to allow buildup of radioactivity before delivery to the patient. The system is capable of delivering up to 80mCi/min in continuous mode or 50mCi/ml in bolus mode. The delivered radioactivity is measured by an integrating ratemeter connected to a Geiger-Muller tube along the patient infusion line and allows accurate monitoring of patient dose. The dose can be varied by changing either the flow-rate of target gas, the intensity of the deuteron beam or the flow-rate of the infused saline solution.

All functions are monitored and operated by a remote control-board situated outside the scanner room within view of the patient bed.

1. M.E. Raichle, *Handbook of Physiology, Sec 1, Vol V: The Nervous System*, (V.B. Mountcastle, ed), Bethesda, American Physiological Society, pp 643-674, (1987)
2. J.C.Clark, H.Tochon-Danguy, *Targetry 91 Workshop on Targetry & Target Chemistry*, 1992, 234.

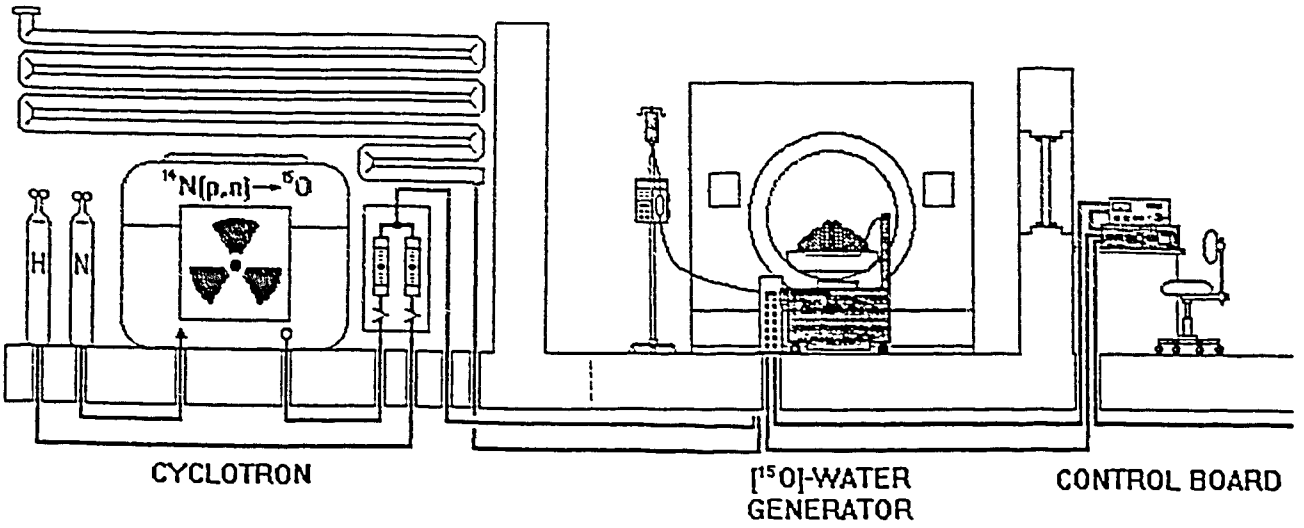

Figure 1. Layout of [^{15}O]-water facility at the Austin Hospital.

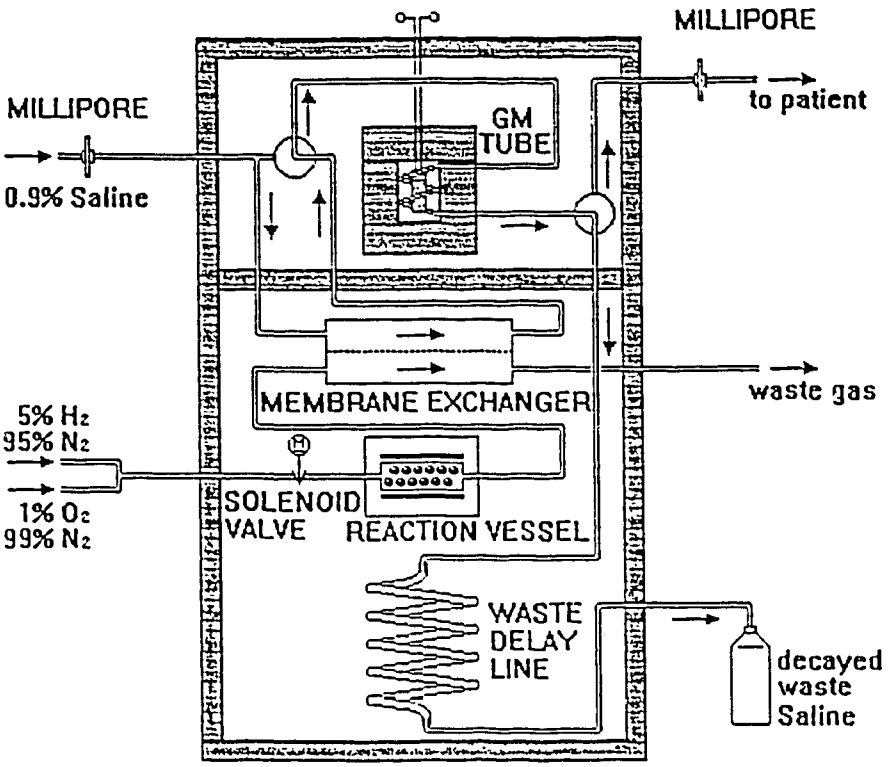

Figure 2. Schematic of the [^{15}O]-water generator

The Legal Measurement of Commonly used Radionuclides

by
H.A van der Gaast and S.M. Buckman
ANSTO-Physics, PMB 1, Menai, New South Wales, 2234.

The Australian Nuclear Science and Technology Organisation (ANSTO) maintain and disseminate the Australian primary standard of measurement for radio-activity. The standard includes all γ – emitters used in nuclear medicine departments.

Calibration factors for the ANSTO 4π ionisation chamber (the Australian secondary standard) have been determined from primarily standardised solutions of β–γ emitters (1). A number of different nuclides can be used to construct a calibration curve of ionisation chamber response for gamma energy (1, 2, 3, 4 & 5). Such curves can then be used to determine ionisation chamber calibrations for nuclides not previously standardised using the $4\pi\beta$–γ coincidence counting. A calibration for a nuclide can generally be interpolated provided a nuclide decays via a mode where a sufficiently energetic β particle or γ or X– ray is emitted (1).

Absolute radio-activity measurements of β–γ emitting radionuclides are carried out using the $4\pi\beta$–γ coincidence counting method (the Australian primary standard for the measurement of radioactivity). Coincidence methods can also be used to determine the activity of nuclides that decay via other modes than β–γ emission (6, 7 & 8).

The curve was recently re-evaluated with the restandardisation of sodium-22 and cobalt-60 (8, 9 & 10). The equation that describes the ionisation chamber response was determined for γ–energies in the range 400 keV to 1400 keV (11).

The ionisation chamber calibration was tested for 6 different nuclides. Three calibrations had been previously determined using absolutely standardised nuclides (1). The other three calibrations were interpolated using the ionisation chamber response calibration curve (these calibrations had an arbitrary uncertainty of ±5% assigned for ionisation chamber activity estimates). The activities of representative solutions of each radionuclide were measured. Each solution was sent to the Bureau International des Poids et Mesures (BIPM, the international organisation of weights and measures at Sevres, France) so that the activity estimate could be compared internationally using the facility provided by (4) the Systeme International de Reference (SIR, the international reference system for activity measurements).

The $4\pi\beta$–γ coincidence counting method and the 4π ionisation methods of activity estimation will be presented. The results of the international activity intercomparison and the effect of these measurements on the Australian legal measurements will be discussed.

References

1) Urquhart, D.F. (1986) - "Calibration and Operation of the AAEC Working Standard of Measurement for the Activity of Radionuclides Part 1: The Measurement System". AAEC/E627.

2) Weiss, H.M. (1973) - "4π Ionisation Chamber Measurements". Nucl Inst and Meth, 112, pp 291-297.

3) Schrader, H. and Weiβ H. M. (1983) - "Calibration of Radionuclide Calibrators". Int. J. Nucl. Med. Biol. 10: 2/3, PP 121-124.

4) Rytz, A. (1983) - "The International Reference System for Activity Measurement of γ-Ray Emitting Nuclides". Int. J. Appl. Radiat. Isot., 34:8, pp 1047 - 1056.

5) Suzuki, A., Suzuki, M. and Weis, A.M. (1976) - "Analysis of a Radionuclide Dose Calibrator". J. Nucl. Med. Tech. 4, 4, pp193 - 198.

6) Sherlock, S.L. (1987) - "The Absolute Determination of Activity by the Efficiency Extrapolation Method". AAEC/E654.

7) Koskinas, M.F. and Dias, M.S. (1989) - "A Coincidence System for Radionuclide Standardisation using Surface Barrier Detectors". Nucl. Inst. Meth. in Phys. Res., A280, pp327- 331.

8) van der Gaast, H.A. (1994) - "Development of Australian Commonwealth Standards of Measurement for Cyclotron Produced Radionuclides". (Thesis to be Presented).

9) Buckman, S.M. (1994) - "Standardisation of Cobalt-60". - (Thesis to be presented).

10) van der Gaast, H.A., Buckman, S.M., and Sherlock, S.L. (1993) - "The development of the National Radionuclide Dose Calibrator Standardisation Service". Australasian Physical and Engineering Sciences in Medicine, Vol. 16, No. 1.

11) van der Gaast, H.A. (1992) - "Ion Chamber Calibration by Interpolation Part 2: Ion Chamber Response for Gamma Energies Between 400 keV and 1400 keV". ANSTO AP/TN 246.

AU PS15037

AINSE Conference on Radiation Biology and Chemistry
University of Melbourne, 16-18 November 1994

The contribution of ^{210}Po to the radiation dose rate of marine organisms

J D Smith and P H Towler
Marine Chemistry Laboratory
School of Chemistry, University of Melbourne
Parkville, Victoria 3052

The major source of internal radiation dose to many marine organisms is polonium-210. This is a result of the concentration of this radionuclide from seawater to the digestive organs. Most of the data on ^{210}Po in marine organisms refers to crustaceans and molluscs (Cherry *et al.* 1983) and most of the measurements of ^{210}Po in fishes refers to the bony fishes. There are few studies of the concentration of ^{210}Po in cartilaginous fishes (including sharks, rays, dogfish and elephant fish).

We have analysed (Smith and Hamilton 1984) the livers of cartilaginous fishes (Chondrichthyes) caught by trawling in Port Phillip Bay in 1991. Five elasmobranch species and one holocephalian species, the elephant fish (*Callorhynchus milii*) were examined. The five elasmobranch species had ^{210}Po concentrations in the range 1 - 31 Bq kg^{-1} (wet weight) (Smith and Towler 1993). The elephant fish was exceptional with ^{210}Po in the range 60 - 270 Bq kg^{-1} (n = 3, mean 180 Bq kg^{-1}). Lead-210 was present at $<$1 - 10 Bq kg^{-1} in all specimens. In every case the activity concentration of ^{210}Po exceeded that of the grandparent ^{210}Pb, indicating that the ^{210}Po could not have grown in from in *situ decay* of ^{210}Pb within the liver. The intermediate radionuclide ^{210}Bi that occurs between ^{210}Pb and ^{210}Po was not included in this study.

As ^{210}Po is an alpha-emitter (5.305 MeV) its contribution to the weighted absorbed dose is enhanced by a high quality factor (Q). We have used a value of Q = 20. Both ^{210}Pb and ^{210}Bi are beta-emitters for which we use Q = 1.

The mean concentration of ^{210}Po measured in Port Phillip Bay water was 0.32 mBq kg^{-1}. This yields concentration factors of 3,500 to 900,000 for unsupported ^{210}Po in the livers of the Chondrichthyans.

The external dose from the seawater for mid-water fishes (about 0.003 μGy h^{-1}) is dominated by decay of ^{40}K. The bulk of the internal dose originates from ^{40}K and ^{210}Po. The potassium concentration in soft tissues of marine organisms is relatively constant and is responsible for about 0.02 μGy h^{-1}.

Dose rate and weighted absorbed dose calculations for cartilagineous fishes with a high and a low concentration of ^{210}Po are summarised in the table. When the weighted absorbed dose is calculated using a quality factor of 1 for ß- and γ-emitters and 20 for α-emitters, then in the elephant fish ^{210}Po contributes up to 140 mGy y^{-1} (16 μGy h^{-1}), which is >99% of the total internal weighted absorbed dose and three orders of magnitude greater than the weighted absorbed dose from external sources. We have called [dose rate x Q] the *weighted absorbed dose* in μGy h^{-1} for the fishes. This is analogous to the *dose equivalent* in μSv h^{-1} in humans.

	Port Jackson Shark	Elephant Fish
^{210}Po		
Concentration, Bq kg^{-1}	1.2	270
Dose rate, μGy h^{-1}	0.0036	0.82
Weighted Absorbed Dose, μGy h^{-1}	0.072	16.4
^{210}Pb		
Concentration, Bq kg^{-1}	0.09	0.9
Dose rate, μGy h^{-1}	0.0003	0.003
Weighted Absorbed Dose, μGy h^{-1}	0.006	0.06
^{40}K		
Dose rate, μGy h^{-1}	0.02	0.02
Weighted Absorbed Dose, μGy h^{-1}	0.02	0.02
Total Dose Rate, μGy h^{-1}	0.056	0.84
^{210}Po (%)	15	97
^{210}Pb (%)	1	0.4
^{40}K (%)	83	2.4
Total weighted absorbed dose, μGy h^{-1}	0.098	16.48
^{210}Po (%)	73	99.5
^{210}Pb (%)	6	0.4
^{40}K (%)	20	0.1

References

Cherry, R. D., Heyraud, M. and Higgo, J. J. (1983). Polonium-210: its relative enrichment in the hepatopancreas of marine invertebrates. *Marine Ecology Progress Series* 13, 229-236.

Smith J.D. and Hamilton, T.F. (1984). Improved technique for recovery and measurement of polonium-210 from environmental materials. *Analytica Chimica Acta* 160, 69-77.

Smith J.D. and Towler, P.H. (1993). Polonium-210 in Cartilaginous Fishes (Chondrichthyes) From South-East Australian Waters. *Australian Journal of Marine and Freshwater Research* 44, 727-33.

SONOCHEMICAL REDUCTION OF $AuCl_4^-(aq)$

by
Rachel Hobson and Franz Grieser

School of Chemistry,
University of Melbourne,
Parkville, VIC., 3052
Australia.

ABSTRACT

The absorption of high intensity ultrasound by water is known to produce H· and ·OH radicals in solution[1]. This is due to a phenomenon known as acoustic cavitation; the formation, growth and collapse of small bubbles in the sonicated solution. These primary radicals can then be scavenged by other chemical species in solution to produce secondary radicals and subsequently further chemical reactions may occur. The scavengers used in this study are alcohols and surfactants, molecules known to have a preference for the interfacial phase rather than the bulk solution. Hence these scavenging molecules should be at the bubble interface. The water soluble metal ion, $AuCl_4^-$, when sonicated in the presence of these surfactants is reduced generating colloidal gold particles[2]. It has been found that by altering the type and quantity of the surfactant in solution the yield of the gold particles also changes. The efficiency of gold formation is dependent on the air/water surface activity of the surfactant used, implying that the scavenging of the primary radicals occurs at the cavitation bubble liquid interface.

1. K. S. Suslick, *Scientific American*, 1989, **260**, 80.
2. S. Au Yeung, R. Hobson, S. Biggs and F. Grieser, *J. Chem. Soc., Chem. Commun.*, 1993, 378.

THE EFFECT OF ANIONIC POLYMERS ON THE RADIATION INDUCED NUCLEATION OF SILVER PARTICLES IN AQUEOUS SOLUTION

by

Paul Mulvaney

Advanced Mineral Products Research Centre, University of Melbourne, Parkville, VIC., 3052, Australia.

Abstract

It is well established that the reaction of hydrated electrons and hydrogen atoms with silver ions in aqueous solution leads to the formation of silver atoms. These silver atoms dimerize and then further aggregate to form colloidal silver.

In the absence of steric or electrostatic stabilization, the colloidal metal eventually settles out of the solution after several minutes. In the presence of anionic polymers such as poly(vinyl sulfonate) poly(acrylic acid) or sodium hexametaphosphate, the colloidal silver is stabilized at very small particle sizes. At high concentrations, the growth processes take place along the chains, rather than in free solution. In some cases, the polymer freezes the growth process when the nascent silver nuclei contain less than ten atoms [1-3]. Extremely reactive silver clusters can be prepared this way.

We discuss here the effect of poly(acrylic acid) on the kinetics of nucleation, and the first few aggregation steps. It will be shown that many of the aggregation processes are slowed down by an order of magnitude in the presence of polymer. Some positively charged clusters are stabilized indefinitely by adsorption to the polymer chains.

References

1. Mulvaney, P.; Henglein, A.; J. Phys. Chem. 94, 4182 (1990).
2. Mulvaney, P.; Henglein, A.; Chem. Phys. Lett. 168, 391 (1990).
3. Linnert, T.; Mulvaney, P.; Henglein, A.; Ber. Bunsenges. Phys. Chem. 94, 1449 (1990).

AUPS1503 8

NEW APPROACHES TO THE TREATMENT OF CANCER: PHOTOACTIVATION, MICROBEAM AND GROWTH FACTORS

Barry J Allen
St George Cancer Care Centre
Gray St Kogarah 2217 NSW Australia

Binary therapies hold the promise of improved cancer cell kill while sparing normal tissue. Two such therapies are Boron Neutron Capture and Photodynamic therapy which are already being used for the treatment of melanoma and high grade tumours with encouraging results. Further down the track are new approaches which are at the in vitro research stage. These involve photoactivation, microbeams and growth factors.

Photoactivation Therapy (PAT) is also a binary modality which makes use of the higher mitotic rate of cancer cells which might then selectively take up IdUdr as a thymidine analogue. Auger electron emission can then be induced by an external x-ray beam or x-ray brachytherapy. Laster el al[1] have demonstrated that a differential dose between normal and cancer cells can be achieved through the use of halogenated pyrimidine analogues of DNA precursors which radiosensitise cells populations with higher mitotic rates. In PAT, iodine becomes the target atom which can be activated by x-rays above the K shell edge, emitting low energy Auger and Koster-Kronig electrons. Because of the short range of these particles, high LET damage is imparted to cells by direct ionisation of DNA. Biological damage results from both radiosensitation and Auger electron emission. Studies using monochromatic photons above the K shell edge at the Brookhaven National Synchrotron Light Source showed a therapeutic gain of 3.3. The penetration of external beam x-rays is poor, so for deep seated tumours, implanted Sm-144 seeds could be used in a binary brachytherapy mode.

Microbeams exploit the potential for a differential response to narrow beams of radiation between elongated endothelial cells (50 um in length) and glioma cells (10 um dia). This differential response may explain heavy ion microbeam experiments on mouse brains to test the effect of cosmic rays on astronauts when it was found that mice could sustain very high doses of microbeam radiation. In radiotherapy of brain tumours, the capillaries may be the dose limiting organ. If these can be spared radiation damage, much greater doses could be delivered to the tumour. Thus the objective is to stimulate repair of endothelial cell damage between dose fractions, such that the capillaries have no memory of the such damage. Microbeams would be 20 um wide with 50 um spacing, such that only one nucleus of contiguous endothelial cells would be damaged. This cell would undergo apoptosis and slough off into the lumen, allowing contiguous cells to expand, maintaining capillary integrity. These cells would then be stimulated to undergo mitosis, returning the capillary to normal cell density. In this way the capillary would have no memory of the insult, and further doses could be delivered. Micro-positioning would not be necessary as it would not be necessary to ensure that the same sections are not irradiated again.

We have grown bovine capillary endothelial cells to confluence and subjected them to physical trauma by scoring or by microbeam irradiation with x-rays[2]. The endothelial cells promptly grow back into the cleared area and align with the other cells. Thus we have established the principle of contiguous replacement in vitro.

Growth factors could be used to speed up endothelial repair between dose fractions in radiotherapy. A human endothelial model is being developed for testing cell response to various growth factors, relative to that for glioma cells[3]. The cells will be challenged with radiation and cell proliferation, migration and protease production will be measured in response to potential modulators on brain endothelial regeneration. Agents are given in table 1 below.

Table 1 Potential stimulators of brain endothelial regeneration

Basic fibroblast growth factor bFGF	Transforming growth factor B TGF-B
Acidic fibroblast growth factor aFGF	Tumour necrosis factor a TNF-a
Vascular endothelial cell growth factor VEGF /vascular permeability growth factor VPF	Angiogenin
Platelet derived endothelial growth factor PD-ECGF	Platelet derived growth factor PDGF
Transforming growth factor a TGF-a	Interleukin-1 and 8 IL-1, IL-8
Epidermal growth factor EGF	Heparin and related sulphated polysaccharides
Platelet activating factor PAF	

While the use of growth factors in vivo might be seen to stimulate angiogenesis and tumour growth, the glioma is normally removed surgically and the target for therapy are peripheral subclinical tumour and micrometastases without vascular support. It is the differential concentration of growth factors in the lumen compared to that around the isolated cancer cells then will result in an improved therapeutic ratio.

References

1 B H Laster, W C Thomlinson, R G Fairchild, Photon activation therapy of iododeoxyuridine: biological efficacy of Auger electrons, Radiat Res 133 219-224 1993

2 B J Allen, P White, M Geso, L Poolewarren, Potential of microbeam radiotherapy, National Workshop on Experimental Radiation Oncology, Sydney August 1994

3 C J Jackson, B J Allen, Regeneration of brain endothelium using growth factors: an in vitro model, ibid.

AUPS1503P

EFFECT OF ADDITIVES ON RADIATION GRAFT MODIFICATION OF N-VINYL-2-PYRROLIDONE ONTO ETHYLENE-PROPYLENE RUBBER.

V. Haddadi-asl, R.P. Burford and J.L. Garnett

School of Chemical Engineering & Industrial Chemistry
University of New South Wales, PO Box 1
Kensington, NSW 2033 Australia

Rubbers based on ethylene-propylene are widely used due to their good mechanical properties, highly saturated structure and associated resistance to aging and ozone deterioration. Whilst they strongly resist acids and alkalis, they suffer from low wettability and low biocompatibility. This limitation can be reduced by introducing suitable monomers to polyolefins using either chemical or radiation graft copolymerisation, initiated by high energy radiation and UV.

Radiation grafting of NVP onto ethylene-propylene elastomers (EPM rubbers) by the simultaneous method was studied. The present work centres upon gamma radiation-induced grafting of N-vinyl-2-pyrrolidone(NVP) onto four different EPM rubbers. The results of grafting yield obtained for different EPM rubber grades are shown in Figures 1. As shown in Table 1, the ethylene content of these rubbers increases in the order Vistalon 808 > Vistalon 504 > Vistalon 404, while their molecular weights are similar. The grafting efficiency of these rubbers are in the order as: Vistalon 808 > Vistalon 504 > Vistalon 404, indicating that increasing the ethylene content increases the grafting yield. The extent of graft copolymerisation of the monomer was examined as a function of monomer concentration. As shown in Figure 1, grafting yield increases with increasing monomer content up to a maximum. This optimal monomer concentration occurs at about 80wt%, regardless of which EPM rubber is used and corresponds to a Trommsdorff peak in grafting. A further increase in monomer concentration, however, results in a decrease in graft yield.

Metal based homopolymerisation inhibitors including Mohr's salt, $Cu(NO_3)_2$ and $FeSO_4$ were evaluated and found to prevent homopolymerisation and significantly increase graft yield. Lithium nitrate was also evaluated as a graft promoter. The effect of multifunctional acrylic additives include TMPTA, PEGDA and PGTA was also studied. Addition of polyfunctional additives such as multifunctional acrylates can significantly enhance the grafting yield of the polar monomer onto EPM rubber.

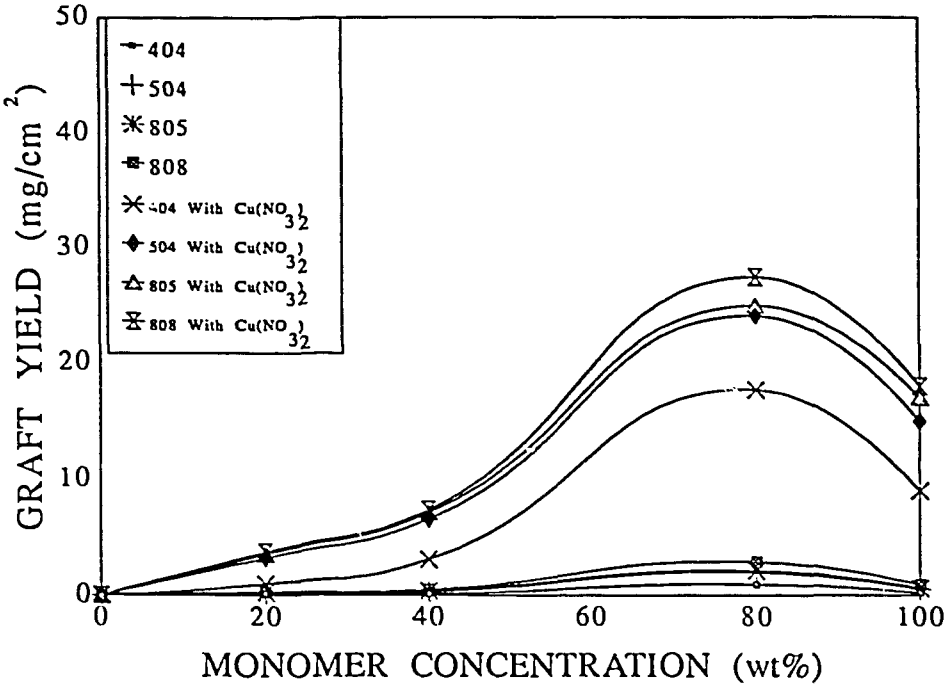

Fig.1 Comparison of EPM Types, Monomer Concentrations and Additives, Effects on Radiation Grafting of (NVP) onto EPM Rubber. (0.005M $Cu(NO_3)_2$). Dose rate = 0.4 KGY/hr, Total dose = 7.5 KGY.

AU PS15040

Mechanistic studies of Sensitisation by incorporation of BrU into DNA;

G.C. D'Cunha, J. Camakaris*, and R.F. Martin, Peter MacCallum Cancer Institute, Melbourne Australia, *Department of Genetics, University of Melbourne.

DNA that has iodine or Bromine substituted for its analog thymidine has an enhanced sensitivity to UV-induced, strand breakage than unsubstituted DNA. There is considerable evidence to support the mechanisms that mediate this sensitisation (Hutchinson, F. 1973). It is assumed that similar mechanisms may be involved with ionizing radiation and hence there is an interest in the use of IUdR and BrUdR as sensitisers in cancer radiotherapy.

We have undertaken a study that uses ^{32}P end labelled synthetic oligonucleotides with BrU incorporated at defined sites (fig. 1).

Br
5' TCACTCGGCUCCGGT
GTGAGCCGAGGCCAT

Cleavage products from UVB induced lesions were identified and characterised on the basis of their electrophoretic mobility relative to the mobility of the Maxam-Gilbert sequencing reactions. Two major types of lesions were identified, both were converted to breaks under mild basic conditions (ie, 1.0M piperidine, 50°C, 10'). However, both lesions produced are very different with respect to their size and the nature of their terminii. The smaller and faster migrating fragment, F, has been shown to have 3' phosphoryl terminus (fig. 2).

The larger and slower migrating fragment, S, requires stringent base treatment (ie, 1.0M piperidine, 90°C, 30') before it is converted to a phosphoryl terminating species. HPLC and NMR studies are being carried out to further characterise the intermediate species of S.

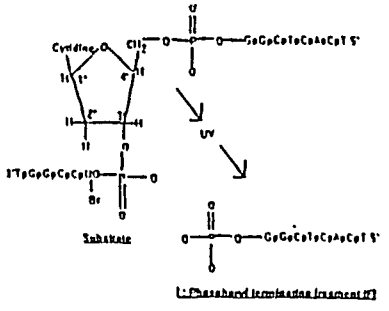

Similar experiments have been done with oligonucleotides that have a known Hoechst 33258 binding site (Martin and Holmes 1983) as well as the single (or multiple) BrU site (fig. 3).

Br
5'ACAAGAATTCUCACT
Hoechst 33258 binding site

Irradiations were then carried out with UVA to specifically excite the Hoechst ligand, damaged products were then analysed by PAGE. Damage induced by UVA-light leads to similar cleavage products to those detected with UVB. The mechanisms that lead to strand cleavage together with the yield of the products relative to the Hoechst binding site will be discussed.

1. Hutchinson, F. 1973, The lesions produced by Ultraviolet light in DNA containing 5-Bromo uracil. *Quarterly Review of Biophysics* v:66, No.2, p202-246.

2. Martin, R.F., and Holmes, N. 1983, Use of an ^{125}I-labelled DNA ligand to probe DNA structure. *Nature 302, p452-454.*

Cell culture studies of radiation sensitisation by iodinated DNA ligands.

R.F. Martin, S. Broadhurst, J. Humphries[1] and J. Camakaris[1].

Peter MacCallum Cancer Institute and [1]Department of Genetics, University of Melbourne.

Introduction

It is well established that incorporation of bromo- or iodouracil into DNA markedly increases the sensitivity of DNA and cells to UV_B and ionising radiation. The sensitisation is mediated by the carbon-centered radical left on the uracil after dissociation of the carbon-halogen bond. The uracilyl radical abstracts a deoxyribosyl H-atom, resulting in DNA strand breakage. This mechanism of sensitisation has inspired the investigation of the potential of iodinated DNA ligands as radiosensitisers, using minor-groove binding bibenzimidazoles; the carbon-centred radical on the ligand in the minor takes the role corresponding to that of the uracilyl radical in the major groove. The first compound evaluated (1) was iodoHoechst 33258 (structure **1**: R_2 = I; R_3 = OH), originally synthesised by direct iodination of Hoechst 33258 (**1**: R_3 = OH), and this compound clearly sensitised DNA strand breakage by UV_A irradiation. DNA sequencing gel analysis demonstrated that the sites of cleavage induced by UV_A/iodoHoechst reflected discrete ligand binding sites. Also, iodoHoechst markedly sensitised cell kill by UV_A-irradiation (1).

More recently, a series of iodoHoechst analogues have been synthesised (2) in which the phenyl ring of the bibenzemidazole is substituted with just a single iodine atom, at different sites. The three isomers are denoted:

ortho-iodoHoechst (**1**: R_1 = I),
meta-iodoHoechst (**1**: R_2 = I) and
para-iodoHoechst (**1**: R_3 = I).

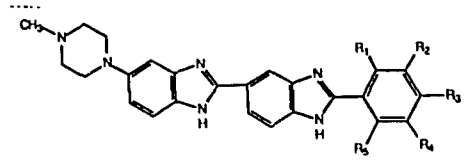

Comparison of the iodinated ligands with respect to UV_A-induced DNA single-strand breaks in plasmid DNA shows the following trend of decreasing activity (3):

ortho -> *meta* -, *para* -> iodoHoechst 33258

DNA sequencing gel analysis has shown that the sites and chemistry of breakage by *ortho*-iodoHoechst is different from that of the other 3 compounds, for which breakage is attributed to abstraction of a H-atom from a 5'-deoxyribosyl carbon. Indirect evidence (4) indicates that cleavage by *ortho*-iodoHoechst may involve attack at the 1'-carbon, but this is not yet substantiated. More detailed mechanistic studies, focussing on the comparison of *ortho*- and *meta*-iodoHoechst are the subject of an accompanying presentation (P. Nel *et al*). Preliminary cell culture studies indicate that *ortho*-iodoHoechst is also more active than its isomers for UV_A-induced cell kill (4). Also, unlike all the other iodoHoechst analogues, which while showing marked sensitisation for UV_A-induced breakage do not sensitise ionising radiation, there is some evidence that *ortho*-iodoHoechst does sensitise cell kill by ionising radiation. This presentation updates the results of our cell culture studies with *ortho*-iodoHoechst.

Experimental

Standard procedures were used for propagation of V79 cells and for assay of clonogenic survival. The UV_A source (a 4W BLB fluorescent tube) and UVX-36 detector (UV Products California USA) were the same as used previously (1), except that the vertical distance between the source and the culture flask was increased to produce a lower dose-rate.

After UV_A-irradiation, the medium was removed and the monolagers rinsed with 2 x 3ml medium and incubated for 60 minutes in 5ml of fresh medium. The subseqent rinsing and

dispersion for clonogenic assay followed standard procedures. For all the post-irradiation procedures, ambient lighting was minimised, for example the boxes containing the dishes that were incubated for 7 days for clonal growth were covered in black paper/tape.

The ionising radiation source was a ^{137}Cs-gamma cell and the same post-irradiation measures were used to reduce the effects of ambient light, as described for UV_A-irradiation.

Results

It was clear from preliminary experiments with *ortho*-iodoHoechst 33258, that lower ligand concentrations were required to bring the UV_A fluence and cell survival into workable ranges. Also, in earlier experiments, the ligand-only controls (no UV_A) gave erratic results, unless ambient light was carefully eliminated. It was also important to use extensive washing procedures to remove cell-bound ligand, which might otherwise be subsequently activated by ambient light.

Table 1- Sensitisation of V79 cells to UV_A-irradiation: Comparison of *ortho* -iodoHoechst and iodoHoechst 33258.

Conditions	UV_A Fluence (J/M^2)	Survival
4μM iodoHoechst 33258	75	52%
1μM *ortho*-iodoHoechst	5	2.4%
1μM *ortho*-iodoHoechst	15	0.9%

The greater activity of *ortho*-iodoHoechst is clear form the comparison shown in Table 1. For ionising radiation, the survival of cells irradiated on the presence of 20μM *iodo*-Hoechst at a dose of 12Gy was 0.9% compared to 2.3% for the radiation-only control.

Conclusions

Although further quantitative data is required, it is clear that *ortho*-iodoHoechst is a potent sensitiser of UV_A. Similarly, data for a complete survival curve is required to quantitate the extent of sensitisation of ionising radiation.

References

1. Martin, R. F., V. Murray, G. D'Cunha, M. Pardee, A. Haigh, E. Kampouris, D.P. Kelly, and G.S. Hodgson. Radiosensitisation by an iodine-labelled DNA ligand. **Int. J. Rad. Biol. 57**, 939-946 (1990).

2. Kelly, D.P., Bateman, S.A., Hook, R.J., Martin, R.F., Reum, M. E., Rose, M., and Whittaker, A.R.D., DNA binding compounds VI.[1] Synthesis and Characterization of 2,5'-disubstituted bibenzimidazoles related to the DNA minor groove binder, Hoechst 33258. **Aust. J. Chem. 47**, 1751-1769 (1994)

3.. Martin, R.F., Kelly, D.P., Roberts, M., Green, A., Denison, L., Rose, M., and Pardee, M., Comparative studies of UV-induced DNA cleavage by structural isomers of an iodinated DNA ligand. **Int. J. Radiat. Oncol. Biol. Phys. 29**, 549-553 (1993).

4.. Martin, R.F., Kelly, D.P., Roberts, M., Nel, P., Tursi, J. , Denison, L., Rose, M, and Pardee, M., Comparative studies of UV-induced DNA cleavage by analogues of iodoHoechst 33258. **Int. J. Radiat. Biol.** in press (1994)

AUPS15042

Evaluation of radioprotectors using the pig skin model

R. Budd, S. D'Abrew, R. Slocombe[1], S. Broadhurst, R.F. Martin,

Peter MacCallum Cancer Institute, and [1]School of Veterinary Science, University of Melbourne.

Introduction

A possible clinical use of DNA-binding radioprotectors such as Hoechst 33342, is in protecting normal tissues by topical application - for example to skin in the peri-anal region of patients undergoing pelvic irradiation.

Our initial aim in using the pig skin model is to test investigate whether adequate concentrations can be achieved by topical application. In this poster we present our progress in setting-up the pig skin model.

Experimental

The methods essentially follow those developed by Hopewell and collaborators at Oxford (eg 1, 2). Briefly, 3-4 month-old female pigs (Large White and Land Race) from a Halgene negative herd were acclimatised in the experimental facility in individual pens. Approximately 1 week prior to irradiation, the flanks of the animals are shaved with electric clippers and field positions marked in three rows of 5 fields on each flank. The animals were anaesthetised by intubation using a Halothane/oxygen mixture, during which time the marked fields received the required radiation dose using ^{90}Sr discs of 2.25cm diameter.

At weekly intervals the skin reactions at each site were evaluated by teams of 3-5 scorers, for the most part using the scoring system devised by Hopewell and colleagues. Erythema was scored according to skin colouration, and in the first wave of reaction (4 - 6 weeks after irradiation) the colours described as pink, red and bright red, were ascribed scores of 1, 2 and 3 respectively. The second stage erythema reactions (10 - 14 weeks after iradiation) were described as brick-red or deep crimson, and scored as 1 and 2, respectively. Dry desquamation was scored simply a positive or negative (ie. 1 or 0), whereas moist desquamation, usually detected as a scab, was scored according to the percentage of the radiation field affected.

Results

The Hopewell group have found that moist desquamation is the most reliable skin reaction endpoint. For each field, the moist desquamation score is taken as positive if the majority of scores note it as such. Then, for each radiation dose, the percentage of fields scored as positive is plotted. The overall dose response is then described by the ED_{50} value which is defined as the radiation dose at which 50% of the fields are scored as positive moist desquamation. With these criteria, our preliminary results showed a somewhat higher ED_{50} than the Hopewell group. In our first experiment, the highest dose of 34Gy corresponded to approximately 50% of moist desquamation, whereas the Hopewell group reported values of about 28 Gy (1). Our current experiments are aimed at defining the dose response for radiation-only (i.e. no radioprotector) fields.

References

1. Aardweg van den, G.J.M.J., Hopewell, J.W., and Simmons, R.H., **Radiother. Oncol., 11**, 73-82, (1988).

2. Hopewell, J.W., Robbins, M.E., van den Aardweg, G.J., Morris, G.M., Ross, G.A., Whitehouse, E., Horrobin, D.F., Scott, C.A., **Brit. J. Cancer, 68**, 1-7, (1993).

Increasing the susceptibility of the rat 208F fibroblast cell line to radiation-induced apoptosis does not alter its clonogenic survival dose-response

David R Aldridge[a,b], Mark J Arends[c] and Ian R Radford[a]

a. Research Division, Peter MacCallum Cancer Institute, Melbourne, 3000 Australia
b. Walter and Eliza Hall Institute of Medical Research, Parkville, 3052 Australia.
c. Cancer Research Campaign Laboratories, Department of Pathology, University Medical School, Teviot Place, Edinburgh, EH3 8AG, U.K.

Abstract

Recent work has focused attention on the possibility that susceptibility of normal or transformed cells to radiation-induced apoptosis may be an important indicator of radiosensitivity. Using a panel of mouse lymphoid or myeloid cell lines, all of which underwent apoptosis after irradiation, a correlation between the rapidity of induction of apoptosis and the clonogenic survival dose-response of a particular cell line has been shown (Radford, 1994). The greater sensitivity of these haemopoietic lines to radiation-induced DNA double-strand breaks as compared with fibroblast lines such as V79, which die by necrosis, suggested that radiosensitivity may be related to the mode of death (Radford, 1991; Radford, 1994). Similarly, *in vivo* studies with transplantable murine tumours showed that elevation of both spontaneous and radiation-induced apoptosis correlated positively with growth delay and negatively with TCD_{50} (Meyn *et al.* 1993).

Because the cell lines used in the above studies have different origins, we were interested in investigating the relationship between mode and rapidity of cell death and radiosensitivity in cell lines with a common origin. Accordingly, we examined the response to γ-ray and DNA-associated ^{125}I decay-induced damage of two transfectants of the rat lung fibroblast line 208F which express either human c-*myc* (cell line RBM7) or activated Ha-*ras* (cell line T1). We found that increasing the rate of induction of apoptosis in the fibroblast line 208F, by transfecting it with human c-*myc*, did not lead to a change in its clonogenic survival dose-response for either γ-irradiation or ^{125}I-induced DNA damage. It was also found that expression of mutant (T24) Ha-*ras* in the 208F line appeared to decrease the level of apoptosis per mitosis after irradiation. As a consequence, significant population expansion relative to the parental cell line was observed up to 72 h post irradiation. While expression of this gene (Ha-*ras*) also inhibited the formation of nucleosomal ladders it did not affect the onset of the morphological features of apoptosis or the clonogenic survival dose-response of the cells to either γ-irradiation or ^{125}I-induced DNA damage. These findings suggest that it may be incorrect to make predictions about the radiosensitivity of cells based only on knowledge of their mode of death.

References

Meyn, R.E., Stephens, L.C., Ang, K.K., Hunter, N.R., Brock, W.A., Milas, L. & Peters, L.J. (1993). Heterogeneity in the development of apoptosis in irradiated murine tumours of different histologies. *Int. J. Radiat. Biol.*, **64**, 583-591.

Radford, I.R. (1991). Mouse lymphoma cells that undergo interphase death show markedly increased sensitivity to radiation-induced DNA double-strand breakage as compared with cells that undergo mitotic death. *Int. J. Radiat. Biol.*, **59**, 1353-1369.

Radford, I.R. (1994). Radiation response of mouse lymphoid and myeloid cell lines. Part I. Sensitivity to killing by ionizing radiation, rate of loss of viability, and cell type of origin. *Int. J. Radiat. Biol.*, **65**, 203-215.

AUPS15044

Preliminary evidence for a radiation-induced adaptive response *in vivo*.

JS Prosser[1], BE Izard[1], MW Wallace[1] and D Strain[2]

[1]Biomedicine and Health Program, ANSTO, Lucas Heights Research Laboratories, Sydney.
[2]Faculty of Health Sciences, University of Sydney.

ABSTRACT

Evidence from *in vitro* experiments is quite conclusive that in some biological systems an adaptive response can be induced whereby a low level radiation dose reduces the response to a subsequent higher exposure. Information on the adaptive response *in vivo* is less well established although there is epidemiological evidence for lower radiation-linked health effects in areas of high natural background.

To investigate further the potential for an adaptive response *in vivo*, the mouse bone marrow micronucleus assay has been used as a measure of radiation-induced damage both with and without a preceding small "priming" radiation dose.

Preliminary results indicate some evidence of an *in vivo* adaptive response in the radiation-induced level of micronuclei in bone marrow reticulocytes. This has been observed after priming doses of 5 and 10 mGy and with an interval between doses of 2 hours. Priming doses of 2.5 or 20 mGy did not induce the same effect. There was also some indication of a possible adaptive response effect of a priming dose of 50 mGy and a time interval between doses of 24 hours.

The time characteristics of this response are to be further defined before examining the possible influence of specific inhibitors of DNA repair and of protein synthesis on the expression of the adaptive response *in vivo*.

Acknowledgements.
DS is in receipt of AINSE grant no. 94/018 BIO.
This work is part of an IAEA co-ordinated research program into the adaptive response.

AU9515045

PRECLINICAL AND CLINICAL TRIALS IN BORON NEUTRON CAPTURE THERAPY

B J Allen
St George Cancer Care Centre
Gray St Kogarah 2217 NSW Australia

After a decade of gestation, BNCT is set to move from animal and human studies to dose escalation trials. Animal studies with spontaneous or xenograft cancers show 60% survival in a wide range of models, and control is being obtained while sparing of normal tissue is being achieved [1].

In Japan, studies with thermal neutrons have demonstrated the efficacy of BNCT for the treatment of skin melanoma[2]. Intraoperative treatment of high grade gliomas has also shown promising results[3]. However, a more penetrating neutron beam is required if deep seated tumours are to be treated on an outpatient basis. This will be achieved with epithermal beams that provide skin sparing. Such facilities are now installed in Europe and the USA. Normal brain tolerance studies in dogs have been completed using BSH and the epithermal neutron beam at the JRC reactor at Petten, The Netherlands. These results delineate normal tissue tolerance with respect to blood boron concentration and neutron fluence[4]. A substantial therapeutic gain has been observed for BPA-BNCT of rat brain tumours in a comparative study with 250 keV x-rays [5]. Histological examination of brain and tumour sections showed that normal brain vasculature was spared while achieving superior control rates to the x-ray irradiations.

Uptake studies of BSH[6] and BPA[6,7] in glioma and melanoma patients show tumour to blood boron ratios of 1.4(0.4) and 4.3(1.8) respectively. However, because of the capillary dose factor of 0.3 for BSH, comparable doses to capillary endothelial cells will result [8].

In September 1994, the New England Medical Centre-Massachusetts Institute of Technology (MIT) clinical dose escalation study commenced using the MIT epithermal reactor beam with BPA for the treatment of metastatic melanoma of the extremities. Also in September, the Brookhaven National Laboratory (BNL) epithermal reactor beam was used, again with BPA, for the treatment of a patient with a high grade brain tumour (on compassionate grounds). Fractionated treatment has the advantage of reducing the concomitant gamma dose and the effect of restricted blood circulation in the hypoxic regions of the tumour. The optimal treatment scheme is recommended to be 4-5 fractions[9].

A key factor in the use of BPA for brain tumours is the effect of BPA-BNCT on the dopamine tracts in mouse brain. While short term effects are observed at 4 hours, recovery occur at 12 hours and up to 120 hours, exceeding the time required for apoptosis of neurons[10].

There is some debate about the relative merits of BSH and BPA, and the need for further compounds with improved uptake and incorporation properties. BSH will be effective only where the blood brain barrier (BBB) is incompetent, as in tumour vasculature, or in the peritumour region of excised tumours. BSH is therefore unlikely to reach more distant metastases in the brain which may become the sites of recurrence. BPA passes the BBB and as such can

reach these preangiogenic nests of cells. Thus there is a case for using different boron compounds with complementary properties.

References

1 B J Allen, D E Moore, B V Harrington, Progress in Neutron Capture Therapy for Cancer, Plenum Press 1992

2 Y Mishima et al, Advances in the control of human cutaneous primary and metastatic melanoma by thermal neutron capture therapy, ibid 577-584

3 H Hatanaka, K Sano, H Yasukochi, Clinical results of boron neutron capture therapy, ibid 561-568

4 K H I Phillip, R Huiskamp, J Casado, A Siefert, R L Moss, Healthy tissue tolerance studies in dogs after boron neutron capture therapy, In: I Auterinen, M Kallio: Proceedings of the CLINCT BNCT Workshop, Helsinki, TKK-F-A718 1994 94-94

5 J Coderre, P Rubin, A Freedman et al, Selective ablation of rat brain tumours by boron neutron capture therapy, Int J Radiation Oncology Biol Phys 28 5 1994 1067-1077

6 B J Allen, Maximum therapeutic depth in thermal neutron capture therapy, Strahlenther Onkol 1 34-41 1993

7 J L Mallesch, D E Moore, B J Allen, W H McCarthy, R Jones, W A Stening, The pharmacokinetics of p-boronophenylalanine.fructose in human patients with glioma and metastatic melanoma, Int J Radiation Oncology Biol Phys 28 5 1183-1188 1994

8 B J Allen, M Bilek, D E Charlton, Monte Carlo calculations of microdosimetry in nitrogen and boron neutron capture reactions, in Advances in Neutron capture Therapy, Ed A H Soloway et al, Plenum Press 1993 221-224

9 K J Durrant, J W Hopewell, Fractionation in boron neutron capture therapy, In: R G Fairchild et al, Clinical aspects of Neutron Capture Therapy, Plenum Press 1989 53-61

10 Y Setiawan, G Halliday, A Harding, D E Moore, B J Allen, Effect of L-10BPA. fructose and the boron neutron capture reaction on mouse brain dopaminergic neurons, submitted.

AU P5150 46

ALPHA AND BETA EMITTING RADIONUCLIDES FOR CANCER THERAPY

Barry J Allen
St George Cancer Care Centre
Fray St Kogarah 2217 NSW Australia

The efficacy of radionuclide therapy depends on the type and energy of radiation, the specificity of the carrier and the nature of the target cancer. The objective of this project is to develop experiments which strictly test the properties of the radionuclide against different classes of cancer, using radio lanthanides and monoclonal antibodies. Thus only the properties of the radionuclide will effect the outcome of the experiments.
Alpha and beta emitting radiolanthanides, the latter with different beta energies, will be produced, conjugated with monoclonal antibodies, and their efficacy tested in three models, viz in vitro leukaemia model, in vivo bladder cancer model, and the in vivo metastatic melanoma model. The alpha emitting lanthanide ^{149}Tb has already been produced at the Tandem accelerator at the Australian National University [1]. The aims of the project are therefore to:
a evaluate the efficacy of beta emitting lanthanides as a function of beta energy in a controlled experiment using the same chelator method and monoclonal antibody,
b compare the efficacy of these beta emitting lanthanides with that for an alpha emitter using the same monoclonal antibody,
c determine the appropriate class or stage of cancer most suitable for a specific radiolanthanide therapy.

Orthodox radionuclide therapy of cancer rests on a very limited quantitative basis. Traditionally ^{131}I labelled carriers are used, and more recently radiolanthanides are being applied for palliative treatment of bone cancer. With the exception of thyroid cancer, radionuclide therapy has been markedly unsuccessful in controlling cancer.

There are four stages of cancer which require quite different approaches to effect control. These are described below.
a Cells in transit:
Blood borne cancer cells from the primary tumour brake away and travel through the lymphatic system or vasculature, lodging in the lymph nodes or on the walls of capillaries. These cells may be in the G0 phase, in a dormant state, and as such are not receptive to chemotherapy which relies on high mitotic rates to enter the cell and cause damage to DNA. Thus to target these cell extremely short range toxicity is required with a highly selective carrier.
b Preangiogenic lesions:
Small nests of cells develop in appropriate sites which might stimulate cell division. However, the numbers of cells is insufficient to secrete growth factors which would induce angiogenesis in nearby capillaries.
c Subclinical lesions:
Sufficient cells are present to stimulate capillary growth which leads to rapid development of the tumour. However, it is still too small to be observable clinically. ie tumour diameter is less than say 3 mm, and the patient is asymptomatic.
d Clinical lesions:
The tumour now manifests itself clinically with symptoms and can be readily observed by various diagnostic methods. For malignant cancers, metastatic disease is widespread, and treatment is mostly palliative in nature.

Currently, the same approach is used for each of the above stages of cancer. This is the use of beta emitting radiolabels chelated to monoclonal antibodies. We propose to investigate these different stages with several cancer models, and to demonstrate the superior efficacy of one type of radionuclide vs others for a given cancer stage. This will be achieved by using radiolanthanides, all with the same chelation chemistry for binding to the same monoclonal antibodies. However the radiolanthanides will have different decay properties as shown below.

Table 1 Nuclear decay parameters of radiolanthanides

Parameter	149 Tb	161 Tb	153 Sm	166 Ho
radiation	alpha	beta	beta	beta
max energy MeV	3.97	0.5	0.81	1.96
<range> um	26	800	1000	3400
volume factor	1	26 000	57 000	2 200 000
hits to kill cell	1-4	400	400	
half life	4 h	165.6 h	1.95 d	26.8 h

From the table the effective interaction volume factor for each radiolanthanide is seen to vary by many orders of magnitude., even between ^{153}Sm and ^{166}Ho. Clearly, if a specific monoclonal antibody is used as a carrier which targets individual cancer cells, then the probability of cell kill relates to the fraction of energy deposited in the cell and the hits to kill a cell. These quantities therefore determine the required dose to be administered, which may exceed the critical normal tissue tolerance dose.

Three models will be used to test the above hypothesis.

a In vitro leukaemia model:

Monoclonal antibodies against acute myeloid leukaemia will be used and compared with a control . The therapeutic ratio, ie the dose to cancer cells vs dose to stem cells, will be very sensitive to the effective volume of interaction of the radiolanthanide.

b Bladder cancer model:

Monoclonal antibodies against the bladder cancer lines will be studied in in vivo experiments in which bladder cancer cells are incubated in mouse bladders. The radiolabelled MCA is then injected into the bladder and mice sacrificed , bladder resected and the extent of cancer determined.

c In vivo metastatic melanoma model:

MCA against malignant melanoma will be used to control metastatic disease after injection of melanoma cells into the peritoneum. After sacrifice, tumours will be resected and total weight and number of nodules determined.

References

1 B J Allen, N Blagojevic, H Meriaty, J Leigh, Role of alpha and beta emitting monoclonal antibodies in the therapy of subclinical metastases, Clinical Oncological Society Australia (COSA) Nov 1993 Abstract 90

AU 9515047

RADIATION-INDUCED PEROXIDATION OF PROTEINS AND AMINO ACIDS AND ITS EFFECT ON OTHER BIOMOLECULES

Silvia Gebicki*, Roger T. Dean# and Janusz M. Gebicki*

* School of Biological Sciences, Macquarie University, Sydney NSW 2109
# Heart Research Institute, 145 Missenden Rd., Camperdown, Sydney NSW 2050

Free radicals are a product of many biological reactions and have been implicated in an ever increasing number of pathological conditions. The superoxide free radical (O_2^-) and hydrogen peroxide (H_2O_2) are commonly occurring reactive oxygen species in organisms; in presence of transition metals, they can give rise to the very reactive hydroxyl free radical (HO·). The reaction between HO· and proteins leads to extensive protein damage such as cross-linking and scission, destruction of amino acids, increased susceptibility to proteolysis in some cases or intracellular accumulation in others, and loss of biological function (1). We have measured the formation of BSA-, lysozyme- and amino acid peroxides as markers of oxidative damage under a variety of conditions.

Hydroperoxide groups were formed on BSA, lysozyme and some amino acids in aqueous solution when they were subjected to free radicals produced by: gamma radiation(2,3); the reduction of hydrogen peroxide by ferrous ions (Fenton reaction) (2); the thermal decomposition of the azo-compound 2,2'-azobis(2-amidinopropane)hydrochloride (AAPH) (2); or the oxidation of xanthine by xanthine oxidase (4). The species responsible for initiating the peroxide formation was the hydroxyl or peroxyl radical (HO· or R-OO·). At temperatures higher than 0°C, there was a slow, exponential, temperature-dependent auto-decomposition of the protein and to a lesser extent the amino acid peroxides. However, the peroxides were relatively long-lived. After 8 days at 22°C, approximately 30% of BSA-peroxides were still intact with a plateau being approached by approximately 3 days. Valine-peroxides decomposed even more slowly (2). Decomposition can be accelerated by chemical or enzymatic means. Ascorbate and reduced glutathione (GSH) enhanced the rate of degradation, with large amounts of reducing agents being consumed. At 37°C, the addition of the enzyme glutathione peroxidase to the GSH sample had only a slight effect, however at O°C, the kinetics of degradation were significantly accelerated by the enzyme.

Obvious differences were found in the reactivity between added reagents and peroxide groups from different molecules. Valine peroxides were decomposed very rapidly, lysozyme peroxides were degraded more slowly, and the rate of reduction of the BSA peroxides was slowest of all. In the case of the two proteins, a significant percentage of the peroxide groups appeared to be resistant to degradation under our conditions, i.e. decomposition was not complete. The issue arose, therefore, whether intact peroxides which may form on proteins and may not be degraded *in vivo* could pose a threat to other biomolecules.

Incubating a number of sulfhydryl-sensitive enzymes with gamma-irradiated proteins, after reduction of radiolytically generated hydrogen peroxide by catalase, did not affect their catalytic activity; however the enzyme glutathione reductase which catalyses the reduction of oxidized glutathione, using NADPH as reducing substrate

$$GSSG + 2\ NADPH \rightarrow 2\ GSH + 2\ NADP^+$$

was partly inactivated by lysozyme-peroxides. When the peroxide groups were reduced by ferrous ions, by sodium borohydride or by spontaneous decomposition for 3 days at 22°C, inactivation did not occur. As large amounts of reducing agents such as GSH or ascorbate are consumed in the reduction of protein peroxides, the partial inhibition of an enzyme which ensures that one of these molecules is replenished could be of biological importance during periods of oxidative stress which may overwhelm the antioxidant machinery of the organism.

References

1. Wolff SP, Garner A and Dean RT. Free radicals, lipids and protein degradation. TIBS 11:27-31 (1986).

2. Gebicki S and Gebicki JM. Formation of peroxides in amino acids and proteins exposed to oxygen free radicals. Biochem.J. 289:743-749 (1993).

3. Simpson JA, Narita S, Gieseg S, Gebicki S, Gebicki JM and Dean RT. Long-lived reactive species on free-radical-damaged proteins. Biochem.J. 282:621-624 (1992).

4. Babiy AV, Gebicki S and Gebicki JM. Protein peroxides: formation by superoxide-generating systems and during oxidation of low density lipoprotein. In: Free Radicals: From Basic Science to Medicine (G. Poli, E. Albano and M.U. Dianzani eds.), pp. 340-348, Birkhauser Verlag, Basel (1993).

AU 9315048

SYNTHESIS, CHARACTERISATION AND EFFECTS OF IONISING RADIATION ON LINEAR AROMATIC POLYESTERS

E-JOON CHOI, DAVID J. T. HILL, KI YUP KIM, JAMES H. O'DONNELL, PETER J. POMERY, and ANDREW K. WHITTAKER

Polymer Materials and Radiation Group, Department of Chemistry, The University of Queensland, Brisbane, QLD 4072, Australia

Linear aromatic polyesters have been accepted as high performance polymers for many years, due to their excellent thermal and mechanical properties. Recently, it has been known that the aromatic polyesters not only have more useful properties derived from their unique structure, but they are also more resistant to high-energy ionising radiation than vinyl polymers.

In order to determine how changes in chemical structure would effect the response of polyesters to ionising radiation, six polyesters shown below have been synthesised by melt-polymerisation.

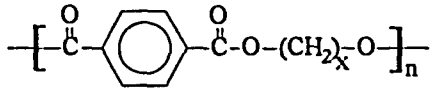

X = 2, 4 or 10

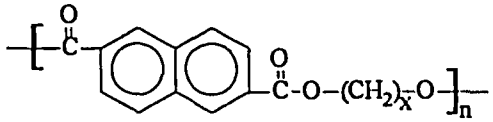

X = 2, 4 or 10

With these poly(ethylene terephthalate) analogues, the aliphatic length of the glycolic portion of the polymer was expanded, and the terephthalate segments were replaced with naphthalenedicarboxylate segments. Their structures were characterised by FT-IR and ^{13}C solid state NMR spectroscopy. The solution viscosities were measured using a phenol/1,1,2,2-tetrachloroethane mixture, and the thermal properties were evaluated by DSC and TGA under a nitrogen atmosphere.

In order to investigate the structural dependence on high energy radiation, the polyesters were irradiated with ^{60}Co gamma rays at the University of Queensland or the Australian Nuclear Science and Technology Organisation. Radiation sensitivity of the polyesters was investigated by ESR spectroscopy. Our measurements of ESR spectra indicated that on the expansion of the length of methylene unit the G-value was increased, whereas the polyesters containing the naphthalenedicarboxylate segment, in comparison with those containing the terephthalate segment, were about same in G-values.

AUPS1504P

THE IMPACT OF GAMMA-IRRADIATION ON A SERIES OF POLYURETHANE THERMOPLASTICS HAVING DIFFERING STRUCTURAL COMPONENTS AND COMPOSITIONS.

M. I. Killeen, F. Kroesen and J. H. O'Donnell.

Department of Chemistry, University of Queensland, Brisbane, Australia, 4067.

INTRODUCTION.

The effect of gamma radiation on polyurethane is of importance for two reasons: i) Gamma radiation may be useful for upgrading polyurethane properties by causing chemical crosslinking at low temperatures while the polymer is in a phase separated state[1,2]. ii) Gamma radiation is also important for sterilising polyurethane medical equipment, therefore the study of radiation damage is important in these applications[3]. In work presented here, five samples of polyurethane thermoplastics have been assessed for their susceptibility to gamma radiation. The five samples have a variety of hard and soft segments and differing ratios of hard to soft segment. The effects of gamma irradiation have been tested with respect to tensile properties, gel-sol fractions (Charlesby-Pinner plots) and G-values for trapped radicals at 77K (G[R·]) calculated from electron spin resonance (ESR) studies.

RESULTS AND DISCUSSION.

The five polyurethane thermoplastics have been obtained from commercial suppliers in pellet form (Dow, BASF, and Termedics Inc.). The structures of the soft and hard segments of these polymers were obtained from their proton nuclear magnetic resonance (NMR) spectra. NMR spectra were obtained at 80°C on a Jeol GX 400MHz spectrometer from a 0.5% (w/w) solution in deuterated dimethylsulphoxide (DMSO-d_6). The molecular weights of the soft segments and percentage hard segment (w/w) could also be calculated from these spectra[4].

The dependence of the polymers susceptibility to gamma radiation was assessed with respect to percent hard segment, ester verses ether soft segment and hydrated versus saturated hard segment. Results for all of the analyses suggest that;

i) Radiation activity is predominate in the soft segment of the polyurethane.
ii) Polyether soft segment is more prone to gamma degradation than polyester.
iii) Hydrogen saturation of the hard segment renders the polymer extremely radiation sensitive.

REFERENCES.

[1] S. N. Lawandy, C. Hepburn, *Elastomerics*, **112**, 12 (1980).

[2] R. A. Assink, *J. Appl. Polym. Sci.*, **26**, 3689 (1981).

[3] H. Shintani, H. Kikuchi, A. Nakamura, *J. Appl. Polym. Sci.*, **41**, 661 (1990).

[4] J. I. Mardel, A. J. Hill, K. R. Chynoweth, *Materials Forum*, **16**, 155 (1992).

THE SIMULATION OF THE EFFECTS OF LOW EARTH ORBIT ON SOME LINEAR AROMATIC POLYIMIDES

J.S. Forsythe, D.J.T. Hill, J.H. O'Donnell, P.J. Pomery, & F.A. Rasoul

Polymer Materials & Radiation Group
Department of Chemistry, The University of Queensland 4072

INTRODUCTION

Polyimides have been extensively used in space applications as advanced composites, encapsulation materials, high density multilayer packages, and UV protective coatings, due to their excellent mechanical properties, thermal and UV resistance. However polyimides have been restricted in their use as optical protective coatings eg. in solar cells and reflective mirrors, due to their dark yellow colour. Much research has been directed towards the reduction of the intramolecular charge transfer complex responsible for the colouring [1].

This has largely been achieved by the incorporation of kinks along the polyimide chain ie. the use of ortho and meta linkages, introducing electron withdrawing groups in the diamine and electron donating groups in the dianhydride moieties, integrating bulky units along the polyimide backbone and any combination of the above (Fig. 1.). However little is known about the effect of reducing the extent of charge transfer formation on the radiation resistance of the polyimides.

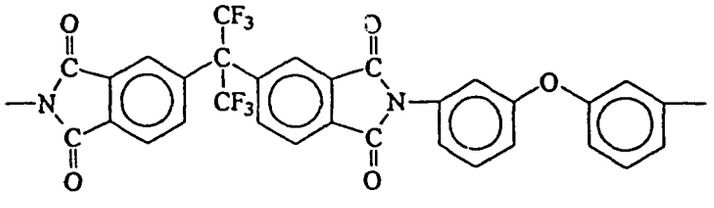

Figure 1 6FDA/3,3'-ODA showing incorporation of kinks and bulky units along the chain disrupting the charge transfer complex.

Four soluble, colourless polyimide films developed by T. St. Clair of the NASA Langley Research Centre are described and their stability determined under simulated Low Earth Orbit (LEO) conditions. LEO is described by orbits about 150 km above the earth's surface and is characterised by high levels of UV and VUV radiation as well as atomic oxygen particles. The photodegradation was studied using ESR, XPS, FTIR, UV/Visible spectroscopies, TGA and contact angle measurements. The synergistic effects of atomic oxygen and VUV radiation induced degradation were studied using XPS.

RESULTS AND DISCUSSION

UV exposure of the polyimides (at wavelengths greater than 200nm) produced slight colouring as evidenced by the red shifts in the UV/Visible spectra. After approximately 20hr UV exposure, the films had become opaque with a white residue on the surface that was able to be physically removed. It was believed that UV irradiation caused bond cleavage primarily on the surface of the films producing colour centres. Furthermore, thermal dynamic analyses showed a significant decrease in the thermal oxidative stability of the polyimide films with increased exposure to UV radiation.

Under vacuum, all of the polyimides gave a symmetrical ESR signal when irradiated in situ with UV radiation. Typical g values were about 2.004 and the peak to peak width was approximately 8 Gauss, which indicated the radical was delocalised over a significant proportion of the polymer chain and interacting with nitrogen and oxygen [2]. However when UV exposure was carried out in air, a much broader ESR signal was obtained with a peak to peak width of 15 Gauss and a typical g value of 2.005. In addition, shoulders appeared indicating oxygen was playing an important role in the radical formation on the surface of the films. These surface radicals could be alkoxy type radicals, whereas the radicals formed below remained unaffected by oxygen.

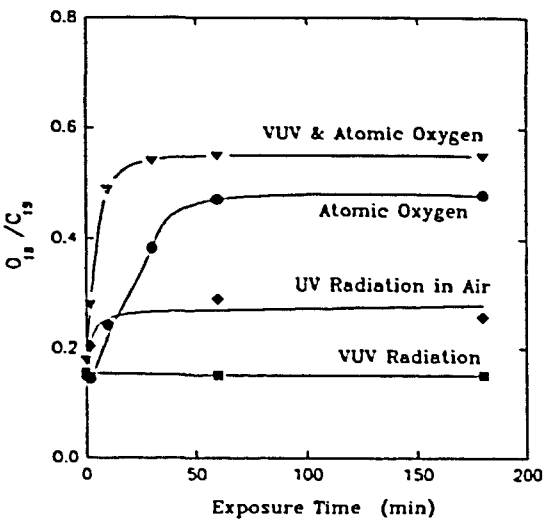

Figure 2 O1s/C1s vs Exposure Time for various radiation conditions

Evidence of surface oxidation was also obtained from XPS. After exposure to UV in air, new oxidised species were observed in the C1s and O1s peaks. The O1s/C1s ratio was determined (Fig. 2), and showed a rapid rise after which there was little change, suggesting an ablative degradation process occurring at the surface. This fact was further supported with transmission FTIR, which showed no new absorptions after UV exposure, but a significant drop in the relative intensities of all bands. Furthermore, contact angle measurements, using drops of water on the films exhibited decreasing contact angles, indicating an increasingly hydrophilic and hence highly oxidised surface.

The polyimide films were also irradiated with VUV, atomic oxygen, and VUV/atomic oxygen, and the surface chemistry analysed using XPS. The VUV irradiation showed no change in surface chemistry as shown in Fig. 2. Conversely, atomic oxygen and atomic oxygen/VUV exposure gave rise to rapid oxidation and ablation of the polymer surface. It was also apparent from Fig. 2. that a synergistic relationship existed between atomic oxygen and VUV. The level of oxidation on the surface strongly suggested that a ring opening mechanism was occurring, giving oxidised species from the aromatics.

REFERENCES

(1) T.L. St. Clair, Polyimides, Ed. D. Wilson, H.D. Stenzenberger, P.M. Hergenrother. Blackie, New York, (1990).

(2) M.A. George, B.L. Ramakrishna, & W. Glaunsinger. *J. Phys. Chem.* 1990, 94, 5159.

AUPS15050

IRRADIATION DEGRADATION OF POLY (HYDROXY ETHYL METHACRYLATE) AND POLY (ETHOXY ETHYL METHACRYLATE)

David J.T.Hill, James H. O'Donnell, Peter J. Pomery and Giti Saadat

Polymer Materials and Radiation Group
Department of Chemistry
The University of Queensland , Brisbane 4072, AUSTRALIA

ABSTRACT

Poly hydroxy ethyl methacrylate (PHEMA) and poly ethoxy ethyl methacrylate (PEEMA) are of biomedical and industrial interest due to their biocompatibility with living tissues[1]. In this paper the effect of high energy radiation on these polymers is reported.

PEEMA and PHEMA have similar molecular structures to poly methyl methacrylate (PMMA) and the γ irradiation of this polymer is well understood [2] . Therefore the radiation degradation of PMMA is used as a model system for the irradiation of these polymers.

Electron spin resonance (ESR) spectroscopy was used to study the mechanism of the irradiation induced degradation of these polymers. The radical yield per 100 eV energy absorbed , G(rad), of these polymers at 77 K , 195 K and room temperature were determined. The ESR spectrum of polymers at 77 K is the overlap of several components. Photobleaching and annealing techniques were used to identify the type of radicals present by taking advantage of the different reactivity of the radicals. The initial analysis of the γ irradiation of PEEMA indicated the presence of methacrylate propagating radical when the irradiated PEEMA at 77 K and 195 K , warmed to 273 K. At room temperature there are no radicals remaining. Methacrylate propagating radical was not found for the γ irradiated PHEMA.

G -value for chain scission and cross -linking , G(S) and G(X) respectively, was calculated using gel permeation chromatography (GPC) to examine the changes in molecular weight distribution and gas chromatography (GC) to determine the volatile gas products .

References:

1-B.D. Gupta, P.K. Tyagi, A.R. Ray and H. Singh, *J. Macromol. Sci. -Chem A* 27, 831 (1990).

2-T.G. Carswell Ph.D. Thesis, The University of Queensland (1991).

AUPS15031

POLYMERISATION OF MONOMERS INSIDE ZEOLITES

BY

GAMMA IRRADIATION

JOHANN KWIATKOWSKI* and ANDREW K. WHITTAKER

CENTRE FOR MAGNETIC RESONANCE
UNIVERSITY OF QUEENSLAND
QLD, 4072
AUSTRALIA

ABSTRACT

Zeolites have attracted wide interest because of their unique catalytic and molecular sieve properties. The structure of the zeolite is largely responsible for this. The structure contains molecular dimensional channels and cavities where cations are able to locate themselves.

Recently zeolites have been shown to be useful for the polymerisation of monomers inside the cavities and channels. This area of research has mainly centred on the formation of long molecular wires. In these systems the cations play an important role in the polymerisation process, as they increase the conductivity of the molecular wire. We aim to restrict the conformations of the monomer in the zeolite so that they polymerise to form stereo-regular polymers upon irradiation.

The initial experiments were concerned with the relation between zeolite channel size and the stereo-regularity of the polymers formed. Polymerisation is initiated via gamma-irradiation from a ^{60}Co source. It became apparent that the effects of the sample preparation had to be investigated in order to quantify the results obtained so far. Thus the aim of this poster is to examine the zeolite before, during and after treatment from gamma-irradiation as well as the effects of loading the zeolite with the monomers methyl methacrylate and styrene.

H-ZSM5 has shown itself to be an excellent catalyst as well as having moderate pore dimensions of approx. 5.4nm. The H-ZSM5 zeolite is made by thermal treatment (typically 500°C to 1000°C for several hours) of NH4-ZSM5, which in the process will produce free ammonia. The treatment will however induce Al migration out of the lattice structure to form octahedrally coordinated Al. This will lead to a loss in catalytic properties of the resulting zeolite and must therefore be monitored.

The samples were analysed mainly by ^{27}Al and ^{29}Si MAS NMR and powder diffraction. Initial studies of gamma-irradiation of 1MRad dosages indicate that free ammonia is produced and that no structural damage occurs to the lattice. This poster will discuss the effects of 1Mrad and 8Mrad irradiation dosages on the zeolite (the amount used to polymerise the monomer) as well as the structures of the polymers formed in-situ. Effects of the monomer on the zeolite structure will also be discussed.

AU PS15052

Radiation chemistry at the interface of chemistry and biology

P Wardman, L P Candeias, M F Dennis, S A Everett, L K Folkes, K B Patel and M R L Stratford

CRC Gray Laboratory, PO Box 100, Mount Vernon Hospital, Northwood, Middx HA6 2JR, UK

Radiation chemistry applied to biological problems has traditionally focused on studies of the radicals from DNA constituents, radical attack on proteins, etc. Applying radiation chemistry to quantify redox properties was also useful in developing quantitative structure-activity relationships for radiosensitizers. As methods to produce specific radicals by radiolysis have become routine, so the far wider application of radiolysis methods have become to be appreciated. This presentation will illustrate the present applications of radiolysis methods in the Gray Laboratory, and also outline the application of fluorescence quenching techniques to probe the interaction of oxygen and other radiation-chemical 'modifiers' of the radiobiological response with cellular DNA.[1]

The latter problem illustrates that whereas radiolysis techniques can easily measure reactivity in homogeneous solutions, the disposition of drugs or endogenous reactants at the microscopic level is frequently an unknown factor. We have examined targeting nitroaryl radiosensitizers to DNA by means of polyamino functions to exploit electrostatic targeting, and minor-groove binding moieties to induce tighter binding. Although fluorescence quenching techniques showed strong interaction with DNA, both approaches have been unsuccessful at the biological level,[2] and the possible reasons for this will be discussed.

Targeted antioxidants may be more succesful and our chemical studies of the properties of a perthiol analogue of the known radioprotector, WR1065 illustrates the logical approach to the chemical design of improved antioxidants with controlled pro-oxidant actvity.[3,4]

Much current interest in the role of free radicals in biology centres on the involvement of superoxide and nitric oxide in cellular oxidative stress. While Fenton chemistry is usually invoked as the basis for biological damage, our radiolysis studies have shown that the formation of hydroxyl radicals from superoxide and hypochlorous acid could be kinetically more favourable.[5,6] The role of antioxidants has often centred on superoxide dismutase to 'detoxify' superoxide, with thiols as intermediate radical repair agents, but radiation-chemical studies have quantified the reactivity of ascorbate and it is easily shown kinetically that ascorbate is probably the most important radical 'sink' in most tissues.[7]

Nitric oxide is known to be synthesised from arginine, via hydroxyargine, and producing citrulline (catalyzed by nitric oxide synthase). Citrulline is used as an indicator of nitric oxide synthase activity. However, our radiolysis studies have shown that nitric oxide can be produced on oxidation or reduction of hydroxyarginine, without generating citrulline. These results have important implications in nitric oxide research since much attention is focused on the molecular

biology of the synthase enzyme rather than on the possibility of alternative chemical routes. Some chemotherapeutic drugs stimulate nitrogen oxide(s) production, and are themselves reactive towards NO_2, and decarboxylate on oxidation.[8,9] This is a possible route by which oxidative damage (e.g. lipid peroxidation) can be 'magnified' by involving drug oxidation to generate peroxyl radicals via decarboxylation. The 'radiation chemistry' of indole-3-acetic acid provides pointers to the design of appropriate drugs.[10]

Clustered DNA damage is a feature of the bioreductive (hypoxia-selective) drug, tirapazamine (SR 4233). Pulse radiolysis experiments provided an explanation for the basis for its selective action, involving radical reaction with oxygen.[11,12] We have now developed a radiolysis model which may explain how a single radical can produce more than one lesion. This exploits the quantitation of radiation chemistry. Although this is taken for granted by chemists, the ability to generate specific radicals at a known, readily-variable zero-order rate using a cobalt source is a feature greatly under-utilized in biochemical studies of drug metabolism and action. Radiation chemists have developed nonhomogeneous kinetics to model 'spur' reactions but the techniques are equally applicable to biological problems with reactions occurring in well-defined organelles, where reactivity and diffusion need both be considered, or at the active site of an enzyme.

This work is supported by the Cancer Research Campaign.

[1] Wardman, P., Dennis, M. F. and White, J., 1989, A probe for intracellular concentrations of drugs: delayed fluorescence from acridine orange. *International Journal of Radiation Oncology, Biology, and Physics*, **16**, 935-938.

[2] Parrick, J., Porssa, M., Davies, L. K., Dennis, M. F., Patel, K. B., Stratford, M. R. L. and Wardman, P., 1993, Targeting radiosensitizers to DNA by minor groove binding: nitroarenes based on netropsin and distamycin. *Bioorganic & Medicinal Chemistry Letters*, 3, 1697-1702.

[3] Everett, S. A., Folkes, L. K., Wardman, P. and Asmus, K.-D., 1994, Free-radical repair by a novel perthiol: reversible hydrogen transfer and perthiyl radical formation. *Free Radical Research*, 20, 387-400.

[4] Everett, S. A. and Wardman, P., 1995, Perthiols as antioxidants: radical-scavenging and pro-oxidative mechanisms. *Methods in Enzymology*, in the press.

[5] Candeias, L. P., Patel, K. B., Stratford, M. R. L. and Wardman, P., 1993, Free hydroxyl radicals are formed on reaction between the neutrophil-derived species superoxide anion and hypochlorous acid. *FEBS Letters*, 333, 151-153.

[6] Candeias, L. P., Stratford, M. R. L. and Wardman, P., 1994, Formation of hydroxyl radicals on reaction of hypochlorous acid with ferrocyanide, a model iron(II) complex. *Free Radical Research*, 20, 241-249.

[7] Wardman, P., 1995, Reactions of thiyl radicals. In: *Biothiols in Health and Disease*. Edited by: L. Packer and E. Cadenas, (Marcel Dekker, New York), in the press.

[8] Candeias, L. P., Everett, S. A. and Wardman, P., 1993, Free radical intermediates in the oxidation of flavone-8-acetic acid: possible involvement in its anti-tumour activity. *Free Radical Biology & Medicine*, **15**, 385-394.

[9] Everett, S. A., Candeias, L. P., Denny, W. A. and Wardman, P., 1994, Decarboxylation of the antitumour drugs flavone-8-acetic acid and xanthenone-4-acetic acid by nitrogen dioxide. *Anti-Cancer Drug Design*, 9, 68-72.

[10] Candeias, L. P., Folkes, L. K., Dennis, M. F., Patel, K. B., Everett, S. A., Stratford, M. R. L. and Wardman, P., 1994, Free-radical intermediates and stable products in the oxidation of indole-3-acetic acid. *Journal of Physical Chemistry*, 98, in the press.

[11] Laderoute, K., Wardman, P. and Rauth, A. M., 1988, Molecular mechanisms for the hypoxia-dependent activation of 3-amino-1,2,4-benzo-triazine-1,4-dioxide (SR 4233). *Biochemical Pharmacology*, 37, 1487-1495.

[12] Wardman, P., Candeias, L. P., Everett, S. A. and Tracy, M., 1994, Radiation chemistry applied to drug design. *International Journal of Radiation Biology*, 65, 35-41.

AUPS15053

A Linac Based Absorbed Dose Calibration Facility

D V Webb, R B Huntley, K Wise and J F Boas

Australian Radiation Laboratory
Lower Plenty Road, Yallambie, Victoria 3085, Australia

Abstract

A 21 MeV Vickers (Radiation Dynamics) electron linear accelerator, previously used by the University of Toronto in the 1970's for physics research, is now operated at ARL. It is a flexible tool for providing electron and x-ray beams primarily for dosimetry studies and applications. Electron beams from energies as low as 7 MeV up to the maximum energy and over a wide range of intensities are available with variable pulse widths and repetition frequencies. A beam line has been developed from which clean, well defined x-ray beams can be produced.

In Australia, the calibration of radiotherapy beams from linear accelerators is referenced to an air kerma calibration at ^{60}Co and the extension to higher energies is made by means of a common, well accepted protocol. For nominal beam energies above 4-6 MV, another approach is to establish standards of absorbed dose directly and compare instruments with a standard at the relevant quality.

An experimental graphite absorbed dose calorimeter has been under development at ARL since about 1980. A second graphite calorimeter was purchased from the Austrian Research Centre Seibersdorf (ARCS) in 1991. This is a fully operational primary standard similar to those supplied by ARCS to the Austrian, Hungarian and Italian National Standards laboratories, and is based on the Domen design.

X-ray beams are being established at several qualities similar to those used by the NPL (UK) calibration service between 6 and 19 MV. Suitable collimation, field flattening and filtration is required at each quality. For calibrations against transfer standard ionisation chambers, a water phantom will be used with a 3-dimensional probe movement system that has been developed at ARL. The PC controller also coordinates data acquisition and a code has been written in 'C' to automate beam profile, depth dose and quality index measurements.

Using the graphite phantom for the Seibersdorf microcalorimeter, a calibration factor has been obtained for our NE2571 cavity chamber against an absorbed dose NE2561 reference chamber calibrated by ANSTO at a nominal energy of 18 MV and a beam quality of 0.781 ($TPR_{20/10}$). A flattened 12 MV x-ray beam should be available later this year and a beam near 6 MV will be developed in 1995.

The linear accelerator also provides high intensity electron beams which are bent vertically through 90° to disperse the beam for studies in radiation damage.

AUS 15054

CHEMISTRY OF ^{99m}Tc NITRIDO COMPLEXES

by
John Baldas

Australian Radiation Laboratory, Yallambie Vic. 3085, Australia

Abstract

The short half-life of 6.01 hours and near ideal physical properties of technetium-99m have resulted in the widespread use of complexes of this radionuclide in diagnostic nuclear medicine. Many important radiopharmaceuticals are either known or thought to contain the $[^{99m}Tc^{V}O]^{3+}$ core. Potential radiopharmaceuticals based on the nitridotechnetium $[^{99m}Tc^{V}N]^{2+}$ and $[^{99m}Tc^{VI}N]^{3+}$ cores are readily prepared by the reaction of $[^{99m}Tc^{VI}NCl_4]^-$ with the ligand and adjustment of pH.[1] With thiolate ligands reduction of Tc(VI) to Tc(V) occurs to give the monomeric ^{99m}TcN-radiopharmaceutical in the lower oxidation state. Studies using the long-lived technetium-99 (half-life 212,000 years and denoted here simply as Tc) have shown that in the case of non-reducing ligands such as phosphonates, gluconate or diethylenetriaminepentaacetic acid the situation is likely to be more complex.

UV-visible spectrophotometric and EPR studies of solutions of $Cs_2[Tc^{VI}NCl_5]$ in a wide variety of inorganic and organic acids (e.g. citric, tartaric, gluconic, glucuronic) have shown that, depending on the nature of the acid and the concentration, the monomeric and two forms of dimeric complexes may be formed at total technetium concentrations as low as 10^{-4} M.[2] The μ-oxo dimers are based on the $[NTc\text{-}O\text{-}TcN]^{4+}$ core and the bis(μ-oxo) dimers on the doubly-bridged cyclic $[NTc(\mu\text{-}O)_2TcN]^{2+}$ core. In particular, the aqua dimer $[\{NTc(OH_2)_3\}_2(\mu\text{-}O)_2]^{2+}$ has been identified. At the low technetium concentration of 10^{-8} to 10^{-7} M present in $^{99m}Tc^{VI}N$-radiopharmaceuticals, dimer formation, which follows second order kinetics, will only be significant if dimerisation is a very fast process. Evidence for the formation of ^{99m}TcN dimers is presented. The aqueous solution chemistry of $[Tc^{VI}N]^{3+}$ is similar to that of the isoelectronic $[Mo^{V}O]^{3+}$ and mixed $Tc^{VI}N/Mo^{V}O$ dimers have been shown to be formed. This raises the novel possibility of the use of microgram amounts of non-radioactive molybdenum to prepare mixed-metal radiopharmaceuticals with picogram quantities of ^{99m}Tc. Paper electrophoretic evidence for the formation of these mixed metal species by the reaction of $[^{99m}TcNCl_4]^-$ with $[MoOCl_5]^{2-}$ is presented.

References

1. Baldas, J. and Bonnyman, J., "Substitution Reactions of $^{99m}TcNCl_4^-$ -- A Route to a New Class of ^{99m}Tc-Radiopharmaceuticals", *Int. J. Appl. Radiat. Isot.* 1985, **36**, 133.

2. Baldas, J., Boas, J. F., Ivanov, Z., and James, B. D., "A spectrophotometric and ESR study of monomer, μ-oxo dimer, di(μ-oxo) dimer interconversion of nitridotechnetium(VI) complexes in solutions of sulfur and phosphorus oxo-acids", *Inorg. Chim. Acta* 1993, **204**, 199.

AU PS15035

Gamma-initiated Radiation Studies of Chain-Length-Dependent Termination Rate Processes in Free-Radical Polymerizations.

Peter A.G.M. Scheren,[§] Gregory T. Russell,[†] David F Sangster,[¶] Robert G. Gilbert,[¶] and Anton L. German[§]

[§]Faculty of Chemical Engineering, Eindhoven University of Technology, 5600 MB Eindhoven, The Netherlands

[†]Chemistry Department, University of Canterbury, Private Bag 4800, Christchurch, New Zealand

[¶]School of Chemistry, Sydney University, Sydney, NSW 2006, Australia

Gamma-radiolysis relaxation experiments were performed to test a model for the kinetics of free-radical polymerization systems, including the dependence of the termination rate coefficients on the lengths of both chains involved. The model has few adjustable parameters, the values of which are moreover confined within fairly narrow limits. The data comprised the rate of polymerization in a seeded emulsion polymerization of styrene, with and without benzene as diluent, with initiation by persulfate and by γ-radiolysis. The latter can be switched off instantly, providing relaxation data which are sensitive to termination kinetics. Data from a single relaxation at a fixed weight-fraction polymer (w_p) were fitted to fix the unknown parameters, of which the only significant one is the probability p of reaction between two radicals upon encounter, incorporating the effect of spin multiplicity; this must lie between 0.25 and 1. Modelling using the value so obtained then successfully fitted: (a) relaxation data at the same w_p but with 15 mol % benzene diluent; (b) relaxation data with and without diluent over the range $0.5 \leq w_p \leq 0.8$; and (c) chemically initiated data over the same w_p range. This provides convincing evidence for the correctness of the termination model, which calculates the termination rate coefficients between two chains from the Smoluchowski equation, incorporating p, with diffusion coefficients (as a function of chain length and of w_p) obtained from a "universal" scaling law inferred from NMR data, and where the interaction distance for termination is the van der Waals radius of a monomeric unit; contributions from "reaction-diffusion" (whereby a chain end moves by propagating) are also important at high conversion. The data also support a model for initiator efficiency in emulsion polymerization, this model being based on competition between aqueous-phase propagation (to a sufficient degree of polymerization for surface activity) and termination.

AU PS 13056

MODE OF CELL DEATH AND RADIOSENSITIVITY

Ian R. Radford, Research Division, Peter MacCallum Cancer Institute, St Andrew's Place, East Melbourne, 3002.

The sensitivity of 10 mouse lymphoid or myeloid cell lines to γ-ray- and DNA-associated ^{125}I-decay-induced clonogenic cell killing have been compared with their rate of loss of viability (membrane integrity), their mode of death, and their putative cell type of origin. The pseudodiploid haematopoietic cell lines showed D_0 values for ^{125}I-induced DNA double-strand breakage (dsb) that ranged from 7.7 ± 0.7 to 40.8 ± 2.8 decays. These lines generally appeared to be more sensitive to killing by radiation-induced DNA dsb than are fibroblast-like cell lines.

The mode of death induced by γ-irradiation in the panel of 10 cell lines was determined, based on the criteria of morphology and DNA degradation pattern. Four of these lines were known to lose viability (membrane integrity) rapidly after irradiation, whilst the others were known to lose viability considerably more slowly. However, all 10 lines showed apoptotic death. The occurrence of apoptosis after irradiation in rapid-dying lymphoid cell lines was consistent with published results, whilst the demonstration of apoptosis in slow-dying lines was unexpected. Cells of slow-dying lymphoid lines underwent one or more mitoses prior to death, a feature also reported for fibroblastoid cell lines. However, the occurrence of radiation-induced necrosis in fibroblasts suggests that the pathways leading to 'mitotic death' can differ between fibroblastoid and lymphoid cell lines.

We also examined the timing of γ-irradiation-induced death in relation to cell cycle progression in the panel of cell lines. Death was found to occur immediately after irradiation ('rapid interphase' death), or after arrest in G_2 phase ('delayed interphase' death), or following one or more mitoses ('mitotoic/delayed mitotic' death). This suggests that different signals can lead to apoptosis in these cell lines. DNA double-strand breakage appeared to directly stimulate the destruction of cell lines susceptible to rapid interphase death, whilst the signal for delayed interphase and mitotic death appeared to be chromosomal aberrations. Several of the cell lines showed different timing of death dependent upon radiation dose used. These differences in the timing of radiation-induced death are shown to be useful indicators of the relative radiosensitivity of haematopoietic cell lines and it is suggested that radiosensitivity is related to the time available for DNA repair prior to induction of apoptosis. Haematopoietic cell lines that undergo rapid interphase apoptotic death showed extreme sensitivity to DNA dsb. The latter cell lines were found to have derived from immature lymphoid cells, and it is speculated that their high radiosensitivity might reflect the action of a mechanism that normally eliminates cells containing illegitimate V(D)J recombinase-induced DNA dsb.

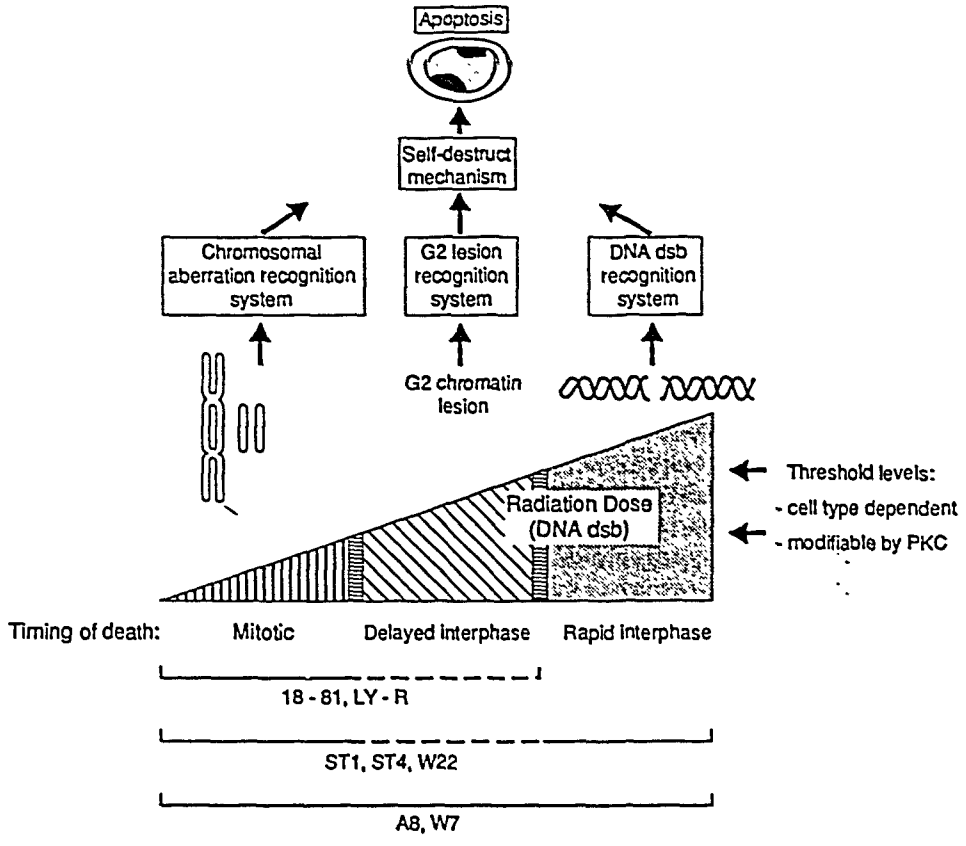

Consistent with the hypothesis that radiosensitivity of lymphoid lines is related to time available for DNA repair, protein kinase C stimulators were found to increase the radioresistance of the mouse pre-T cell-derived line ST4. Increased resistance to γ-ray-induced killing could be produced by addition of 10 nM phorbol 12-myristate 13-acetate (PMA) to ST4 cultures either immediately before or up to 2h after irradiation. Following PMA treatment, ST4 changed from a cell line that underwent rapid interphase apoptosis (i.e. DNA degradation and morphology characteristic of apoptosis were evident 2-3 h after irradiation) to a line that continued to cycle after irradiation and began to die by apoptosis after completing mitosis. Associated with these PMA-induced changes, the D_0 of ST4 cells increased from 7.7 ± 0.7 to 18.8 ± 2.7 ^{125}I decays.

The p53 status of the panel of cell liens was determined by immunoprecipitation with mutant- and wild-type-specific antibodies and was compared with the radiation response of the lines. The more rapidly dying cell lines all contained p53 displaying the wild-type epitope. By contrast, four of six more slowly dying cell lines contained either no or mutant p53 protein. It was of interest that radiation-induced apoptosis occurred, albeit at a considerable time after irradiation, in cells ostensibly lacking p53 protein.

References

Radford, I.R. (1994) Int. J. Radiat. Biol. 65: 203 - 215, 217 - 227, 229 - 239, and 345 - 355.

AU PS15057

Dosimetry for Boron Neutron Capture Therapy

M.G. Carolan[1], S.A.Wallace[1], H.A.Meriaty[2], A.B. Rosenfeld[1], B.J Allen[1,3], J.N. Mathur[1].

(1) Department of Physics University of Wollongong, Wollongong NSW 2526.
(2) Occupational Health and Safety, Ansto, Menai NSW 2234.
(3) St. George Hospital Cancer Care Centre, Kogarah, NSW 2217.

Boron Neutron Capture Therapy (BNCT) is a binary therapy for cancer currently undergoing a resurgence of interest due to the recent commencement clinical trials at the Massachusetts Institute of Technology and the Brookhaven National Laboratory reactors. BNCT uses drugs laden with ^{10}B to localise the ^{10}B within tumour cells which are subsequently irradiated with neutrons to give the $^{10}B(n,\alpha)7Li$ reaction. Thus the energies of the α and Li ions are selectively deposited in the cancer cell. To enable treatment of tumours at depths up to the midline of the brain filtered epithermal neutron beams from reactors or accelerators are used. As a consequence, the primary radiation field that the patient is exposed to includes the following components, photons, fast neutrons, epithermal and thermal neutrons. Each of these needs to be quantified and monitored during treatment.

In this work we have tested the applicability of P-I-N diode and MOSFET semiconductor dosimeters to measure and monitor neutron and photon doses respectively and to validate MCNP Monte Carlo BNCT treatment plans. We have tested the P-I-N diodes in thermal, epithermal and fast neutron fields to determine their sensitivity and energy response function. They were also used to measure the neutron dose distribution in a number of phantoms exposed in an epithermal neutron beam for the purpose of validating a BNCT treatment planning system. The MOSFETs have been tested in the same radiation fields.

A silicon P-I-N diode consists of a section of intrinsic silicon sandwiched between a p-type and an n-type section. For our experiment we used diodes with a $1.3mm^3$ intrinsic silicon base having a resistivity of approximately 100 Ω.cm. Neutrons interact with silicon nuclei in the base section of the diode and cause them to recoil creating defects in the lattice. Such defects introduce new energy states which act as recombination and compensation centres. These centres remove carriers leading to a decrease in carrier lifetime which is manifested macroscopically as an increase in the forward bias voltage V_f of the diode. This change in V_f is measured using a pulsed precision current source to avoid heating the diode which would have the effect of annealing the defects. The relation between dose and ΔV_f is linear up to about 10 Gy of tissue dose with a calibration factor of 1.3 $mV.cGy^{-1}$ $\pm 5\%$ as measured in a ^{252}Cf spectrum.

The KERMA of silicon may be considered to consist of two components, a displacement kerma and an ionisation kerma. It is the former which determines the response of the P-I-N diode with respect to neutron energy. Previous use of P-I-N diodes for accident dosimetry has been based on the fact that the displacement kerma for neutrons of energy >160 keV is in approximately constant proportion with tissue in this range. However for the case of epithermal BNCT, a predominance of neutrons is found in the energy groups <160 keV where the displacement kerma is not proportional to the tissue kerma. Thus the P-I-N cannot be used as a tissue equivalent neutron dosimeter in this case. Photons cause negligible defect production and therefore the gamma sensitivity of ΔV_f is approximately 1000 times lower than the neutron sensitivity of the diodes.

To test that the P-I-N diode ΔV_f response did in fact follow the silicon damage kerma a series of measurements were performed on the Ansto 3MV Van de Graff accelerator using the Li(p,n) reaction in the neutron energy range from 90-200 keV. The diode was positioned 10 cm from the target on the beam axis. The uncertainty in the neutron energy was estimated as ± 40 keV and reasonable agreement with published data was observed. Measurements of the P-I-N response with and without Cd covers were also performed in the TC10 facility on the MOATA reactor. No difference was discernible in these two sets of results presumably since response was dominated in both cases by the neutrons of energy >0.414 eV. The response of the P-I-N to thermal neutrons is 2-3 orders of magnitude lower than for fast neutrons.

The MOSFETs tested as gamma dosimeters are designed with a thick 1 μm SiO_2 insulating layer between the Al gate electrode and the silicon base. Photons impinging on the SiO_2 layer introduce electron hole pairs the holes are immobilised in the insulator particularly in the vicinity of the SiO_2 - Si interface where they produce an electric field

which attracts carriers into the Si below, thus diminishing the threshold voltage between the source and drain electrodes. For the Russian MOSFETs used, a typical sensitivity of 1.5 mV.cGy^{-1} was observed for ^{60}Co photons. The linear range of the MOSFETs when irradiated without any applied bias is approximately 1 Gy. By application of a 15V bias a sensitivity of 11 mV.cGy^{-1} was observed. The linear range of the device is also extended in this case. The photon sensitivity of the MOSFET is flat with respect to energy for photons of E>150 keV. Below this energy the response increases by up to 8 times at energies of ~ 80 keV necessitating some form of filtering (we used Cu in some measurements) to compensate this over response.

The neutron sensitivity of the MOSFETs was tested in the MOATA TC10 facility by exposing them with varying thicknesses of ^{6}LiF covers. The neutron fluence was monitored with Au activation foils. The thermal neutron sensitivity of the MOSFET was approximately 3.6 mV.cGy^{-1}. Thus if the MOSFETs are to be used for photon dosimetry in situations where there is a significant thermal neutron flux then some shielding and/or a correction factor must be employed. ^{6}LiF shielding is probably the best option and was used in the form of a LiF/epoxy encapsulation for the measurements made in phantoms in an epithermal beam. Future applications will include a thin Cu layer within the LiF cover to compensate for low energy photon over response.

The P-I-N diodes and MOSFETs were used to determine the dose distributions in cylindrical, cubic, human head and trunk phantoms which were exposed in the Commission of European Communities Clinical BNCT Facility at Petten in the Netherlands[2]. Convolution of the neutron spectrum of this neutron beam with the damage KERMA for Si shows that all parts of the spectrum contribute to the diode response to about the same order. The phantoms were filled with tissue equivalent gel and dose distributions determined using the MCNP treatment planning system developed by Wallace[1]. The head phantom incorporated a human skull filled with brain equivalent gel and was irradiated from the left side. Arrays of Au, Mn, Cu and In activation foils, P-I-N diodes, MOSFETs, TLD600s and TLD700s were irradiated in the phantoms and in most cases reasonable agreement was achieved between the dose distributions calculated with the treatment planning system and those measured. Results for P-I-N diodes in a cylindrical (fig.1) and a head phantom (fig.2) are shown. The discrepancy at greater depth is being investigated.

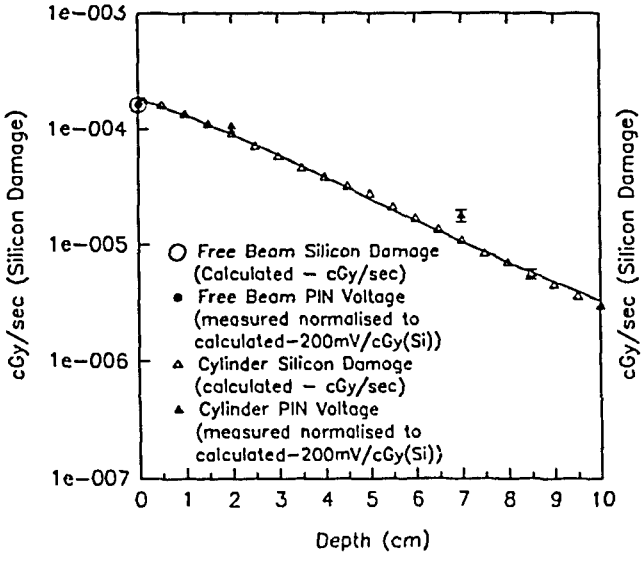

Fig.1 Calculated and observed P-I-N diode responses in 18 cm diameter cylinder phantom exposed in epithermal neutron beam at Petten.

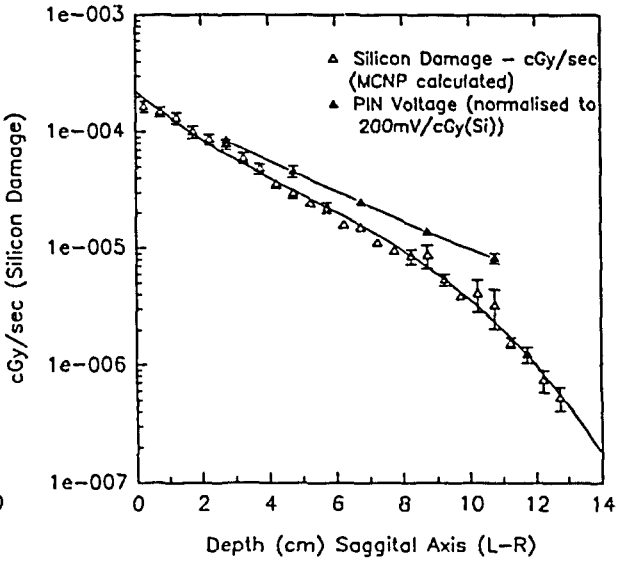

Fig.2 Calculated and observed P-I-N diode responses in human head phantom exposed in epithermal neutron neutron beam at Petten.

1. S.A. Wallace, J.N. Mathur and B.J. Allen, "Monte Carlo Neutron Photon Transport Calculations: Road to Modelling from CT Scans", in proceedings of Sixth International Symposium on Neutron Capture Therapy, October 31-November 4, 1994, Kobe Japan.
2. M.G. Carolan, S.A.Wallace, B.J. Allen, A.B. Rosenfeld, J.N. Mathur, H.A. Meriaty, F. Stecher-Rasmussen and R.L. Moss, "Validation of Monte Carlo Dose Planning Calculations by Epithermal Dose Distribution Measurements in Phantoms", in proceedings of Sixth International Symposium on Neutron Capture Therapy, October 31-November 4, 1994, Kobe Japan.

AU PS 15058

DEFECT IN RADIATION SIGNAL TRANSDUCTION IN ATAXIA-TELANGIECTASIA

M.F. Lavin, K.K. Khanna, H. Beamish, R. Williams, J. Yan and D. Watters. Queensland Cancer Fund Research Unit, Queensland Institute of Medical Research, The Bancroft Centre, 300 Herston Road, Brisbane, QLD, 4029, Australia.

Ataxia-telangiectasia (A-T), a human autosomal recessive disorder, is characterized by cerebellar ataxia, oculocutaneous telangiectasia and sinopulmonary infection, all of which are progressive. Cancer predisposition and hypersensitivity to ionizing radiation are also hallmarks of this disease. Cell cycle anomalies have been described in ataxia-telangiectasia cells at different checkpoints after exposure to ionizing radiation (Beamish and Lavin, 1994). A-T cells fail to show the initial delay in transitions between the G1/S and G2/M phases of the cell cycle and in progression through these phases post-irradiation. In the longer term after passage through S phase they experience a prolonged delay in G2/M. Delay at these cell cycle checkpoints occurs in most organisms after radiation exposure to allow DNA repair to occur and prevent replication of a damaged template or segregation of damaged chromosomes. Further support for the importance of a cell cycle defect in A-T was recently provided by Kastan et al (1992) who showed that A-T cells lacked the ionizing radiation-induced increase in p53, a tumour suppressor protein, seen in normal cells. We have shown that an ionizing radiation-induced p53 response is reduced and/or delayed in cells from different ataxia-telangiectasia complementation groups but not absent (Khanna and Lavin, 1993). On the other hand Lu and Lane (1993) failed to observe a substantive defect in p53 response in A-T. The p53 response to UV was normal in all A-T complementation groups. A delayed response to ionizing radiation was also observed for the cyclin kinase inhibitor WAF1 (p21). As expected this was reflected in a failure to observe inhibition of the cyclinE cdk2 kinase which in turn explains the lack of G1/S checkpoint control. Specific inhibitors of protein kinase C and serine/threonine phosphatases prevented the radiation induction of p53 protein. These results suggest that there is more than one signal transduction pathway responsible for activation of p53, one of which is less efficient in ataxia-telangiectasia cells. We have further investigated the defect in p53 induction at the level of PKC. Protein levels for the PKC_ϵ isoform were reduced or absent in different A-T complementation groups. This pathway of signal transduction is being further elucidated and its possible role on control of different cell cycle checkpoints will be discussed.

REFERENCES

1. Beamish, H. and Lavin, M.F. Radiosensitivity in ataxia-telangiectasia: Anomalies in radiation-induced cell cycle delay. Int. J. Radiat. Biol. 65, 175-184.

2. Kastan, M.B., Zhan, O., El-Deiry, W.S., Carrier, F., Jacks, T., Walsh, W.V., Plunkett, B.S., Vogelstein, B. and Fornace, A.J. A mammalian cell cycle checkpoint pathway utilizing p53 and *Gadd45* is defective in ataxia-telangiectasia. Cell, 71: 587-597, 1992.

3. Khanna, K.K. and Lavin, M.F. Ionizing radiation and UV induction of p53 protein by different pathways in ataxia-telangiectasia cells. Oncogene, 8: 3307-3312, 1993.

4. Lu, X. and Lane, D.P. Differential induction of transcriptionally active p53 following UV or ionizing radiation: Defects in chromosome instability syndromes? Cell, 75:765-778, 1993.

AU PS15 05P

ANSIE Conference on Radiation Biology and Chemistry
University of Melbourne, 16-18 November 1994

Radium-226 in Skeletal Material of Marine Fishes

R. A. Tinker and J. D. Smith
Marine Chemistry Laboratory
School of Chemsitry, University of Melbourne
Parkville, Victoria 3052

Study of ^{226}Ra in fish is significant in two areas of application. Fisheries industry management requires the age estimation of fish as one input into the calculation of sustainable catch size. Ingrowth of ^{210}Pb from ^{226}Ra in otoliths of bony fishes has been used in age estimation (Bennett, Boehlert and Turekian, 1982). ^{226}Ra occurs in the ^{238}U natural decay series and exerts a measure of control on the concentrations of the daughter products ^{210}Pb and ^{210}Po. These are the major source of the weighted absorbed radiation dose in many marine organisms including fish. We are studying the occurrence of ^{226}Ra in skeletal material of fishes as part of an investigation of possible extension of radionuclide age estimation methods. Little is published on the distribution of radionuclides in skeletal material of fishes. Victoria has a large commercial shark fishery and we are concentrating initial effort on a study of ^{226}Ra in skeletal material of the cartilaginous fishes. This includes sharks and rays.

Methods for measurement of ^{226}Ra are being developed for small sample sizes and low concentrations. The three common counting techniques of alpha-spectrometry, gamma-spectrometry and liquid scintillation counting have been compared (Tinker, Smith and Cooper, 1994). We have measured ^{226}Ra in vertebrae of cartilaginous fishes from Port Phillip Bay (Victoria). Three species studied had ^{226}Ra concentrations in the range of 1-3 Bq kg^{-1} (dry weight) with the precision (1 SD) shown based on counting statistics.

Shark Species	^{226}Ra Concentration (Bq kg^{-1})
White Pointer	1.0 ± 0.1
Gummy Shark	2.4 ± 0.2
School Shark	2.9 ± 0.2

The low concentrations of ^{226}Ra found so far show that the method used must have a low limit of detection. Depending on the radiochemical techniques used and the amount of sample available the choice lies between alpha-spectrometry and liquid scintillation counting.

Tinker, R.A., J. D. Smith, and M. B. Cooper. "Selection criteria for an analytical method for radium-226 in environmental samples," *Journal of Radioanalytical and Nuclear Chemistry* In Press (1994).

Bennett, J. T., G. W. Boehlert, and K. K. Turekian. "Conformation of longevity in *Seabastes diploproa* (Pisces: Scorpaenidae) from $^{210}Pb/^{226}Ra$ measurements in otoliths," *Marine Biology* 71, 209-215 (1982).

* * *

ARL'S NATIONAL OVERSIGHT OF RADIATION, ITS USES AND EFFECTS

Dr K H Lokan

Australian Radiation Laboratory, Lower Plenty Road
Yallambie, Vic, Australia

ABSTRACT

The present ARL has been in existence under a variety of names since 1929. It is formally a Branch of the Commonwealth Department of Human Services and Health and maintains oversight of the uses of radiation - ionising and non-ionising - throughout Australia.

Its current scientific programs are briefly described, highlighting some of its more recent activities and responsibilities.

In the course of the next year, ARL will merge with the Nuclear Safety Bureau to form a new Australian Institute for Radiation Protection in a statutory body, embracing the present functions of both and an expanded responsibility to regulate federal uses of radiation and nuclear facilities.

AUPS15 061

The Standardisation of Fluorine-18 and Americium-241

by
H. A. van der Gaast
ANSTO-Physics, PMB 1, Menai, New South Wales, 2234.

$4\pi\beta-\gamma$ coincidence counting is the Australian primary standard method for the measurement of radio-activity. It is commonly used to measure the activity of β^-–γ emitting radionuclides. The method can also be applied to nuclides which decay by other modes. Commonly the literature describes coincidence methods for the standardisation of nuclides which decay by: electron capture (1), α– emission (2), β^+–γ emission (3) and pure β^- emission (4).

The Ansto 4π ionisation chamber calibration factors for pure β^+ emitters (5) have been determined from standardisations of cobalt-60 (6) and sodium-22 (7). Such calibration factors have thus not been directly determined from a primary standardisation of a pure positron emitter.

Activity standardisations of pure β^- emitters can be readily carried out using the efficiency tracer method in conjunction with the $4\pi\beta-\gamma$ coincidence method (4). This involves counting mixed nuclide sources that consist of both β^-–γ and β^- emitters. This method was applied to counting mixed sources of β^-–γ and β^+ (7) emitting nuclides.

The efficiency tracer method was then further developed so those activity estimates using the 4π ionisation chamber were also tested. The ionisation chamber activity estimates of fluorine-18 were confirmed using this method. This result was confirmed using the γ–γ sum peak coincidence counting method (8).

The proportional counter in the $4\pi\beta-\gamma$ coincidence counting system can be used to standardise α-emitters. The system is thus used for $2\pi\alpha$ and $4\pi\alpha$ coincidence counting. The counting efficiency for α– particles is assumed to be 100% (9). Thus the activity of an alpha source is generally the proportional counter - count rate corrected for dead time, counting geometry, radiation absorption by the source and back scatter of the radiation from the source mount (9).

The $2\pi\alpha$ and $4\pi\alpha$ counting methods are only valid for counting sources that are prepared so that the counting efficiency approaches 100%. Commonly, α–sources must be reasonably robust and have a thin covering of plastic. This results in the effective activity rather than the true activity of the source being determined by the above methods.

Coincidence counting overcomes this problem by determining the counting efficiency as well as the α-count rates (2). It is possible then to determine the true activity of an α–source (2). The activity estimate then would have to be corrected for the other events that occur during the decay of an α–source (10). The determination of correction factors can be carried out using efficiency extrapolation of the proportional counter - count rate.

The activities of sources of two non β^- emitting nuclides, fluorine-18 and americium-241, have been absolutely determined using the $4\pi\beta$–γ coincidence counting system at ANSTO. The techniques applicable to each standardisation will be presented.

References

1) Sherlock, S.L. (1987) - "The Absolute Determination of Activity by the Efficiency Extrapolation Method". AAEC/E654.

2) Koskinas, M.F. and Dias, M.S. (1989) - "A Coincidence System for Radionuclide Standardisation using Surface Barrier Detectors". Nucl. Inst. Meth. in Phys. Res., A280, pp327- 331.

3) Campion P.J. (1959) - "The Standardisation of Radioisotopes by the β–γ Coincidence Method using High Efficiency Detectors". Int. J. Appl. Radiat. Isot., 4, pp232.

4) Merrit, J., Taylor, J., Merrit, W. and Campion, P. (1960) - "The Absolute Counting of Sulfur-35". Anal. Chem. Vol. 32, No.3, pp.310 - 313.

5) van der Gaast, H.A., Buckman, S.M., and Sherlock, S.L. (1993) - "The development of the National Radionuclide Dose Calibrator Standardisation Service". Australasian Physical and Engineering Sciences in Medicine, Vol. 16, No. 1.

6) Buckman, S.M. (1994) - "Standardisation of Cobalt-60". - (Thesis to be presented).

7) van der Gaast, H.A.(1994) - "Development of Australian Commonwealth Standards of Measurement for Cyclotron Produced Radionuclides". (Thesis to be Presented).

8) Brinkman, G.A., Aten, A.H.W. (Jr) and Veenboer, J. Th. (1963) - "Absolute Standardisation with a NaI(Tl) Crystal - II, Determination of the Total Efficiency". Int. J. Appl. Radiat. and Isot., (14), pp 433- 437.

9) Sudarsono (1985) - "Standard of Radiation (Main Report of JICA Training Programme)". Radiation Metrology Section, Quantum Technology Division, Electrochemical Laboratory, Ministry of International Trade and Industry of Japan. Tsukuba, Japan.

10) Buckman, S.M. (1994) - ANSTO-Physics (Radiation Standards Project), (Personal Communication).

AU PS15062

RADIATION CROSSLLINKING and GRAFTING of a SWOLLEN POLYMER

Peter Hidi, Donald H. Napper, David F. Sangster
Division of Physical and Theoretical Chemistry F11
University of Sydney NSW Australia 2006

Particles of a poly(vinyl acetate) (PVAc) latex swell up to fifty times their original volume in the presence of an anionic surfactant such as sodium dodecyl sulphate (SDS). PVAc and SDS form polymer micelle complexes (PMCs) on the surface and then throughout the interior of the particles. 96% of the increase is due to water carried in with the SDS. On dilution or dialysis the swelling is reversible and the particles revert to slightly less than their original size, the difference being due to the escape of some low molecular weight material.

If, prior to the swelling, the latex is exposed to gamma radiation it is found that the initial rate of swelling *vs.* SDS concentration is identical to that of the unirradiated control but the final size is much less. This is attributed to crosslinking preventing access by the SDS to the core of each particle to form PMCs. It is noteworthy that the outer layers of the particles are apparently not crosslinked.

In another series of experiments swollen particles were irradiated and then diluted; this would have been expected to cause them to shrink to approximately the original size. However they shrank only slightly yielding a stable structure about forty times the size (volume) of the original particle indicating that the SDS was now attached irreversibly to the PVAc chains. We attribute this to a grafting reaction.

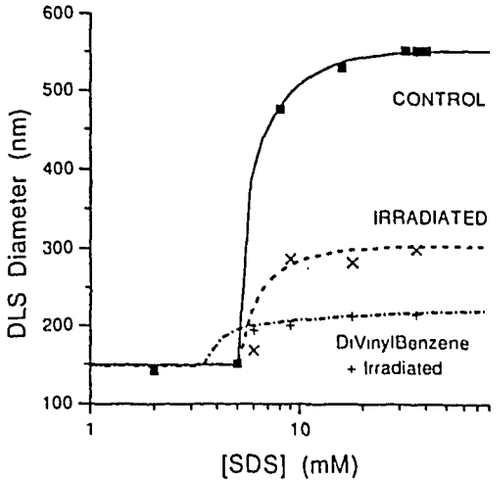

Diameter *v.* log [SDS]. Radiation crosslinked particles swell to a limited extent *c.f.* with control which was not crosslinked.

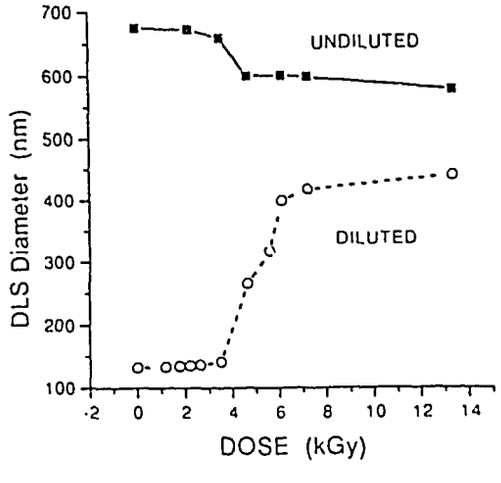

Diameter *v.* Dose. Latex was swollen, irradiated and measured. Then diluted and again measured. The irradiated shrank less.

AU PS15 063

Sequence analysis of ionizing radiation-induced DNA rearrangements.

[a]H. Forrester , [b]N. Deacon and [a]I. Radford.
[a]Research Division, Peter MacCallum Cancer Institute, St Andrews Place, East Melbourne, 3002, and
[b]Macfarlane Burnet Centre for Medical Research, Fairfield Hospital, Fairfield, Vic, 3078, Australia.

We have developed a procedure using the inverse polymerase chain reaction (Ochman et al., 1988, Triglia et al., 1988) that has enabled us to sequence radiation-induced DNA rearrangements in particular genes. Study of DNA rearrangements at a molecular level has, in the past, generally been limited to rearrangements that produce a phenotypic change such as mutations or transformation (Grosovsky et al., 1988, Miles et al., 1990, Ito et al., 1993). Whilst DNA rearrangements that caused cell death or were without marked effect could not be examined. Our procedure potentially allows the detection of DNA rearrangements that previously could not be studied.

This procedure has been used to detect DNA rearrangements 5' to the c-myc gene in human fibroblasts that have been exposed to 30 Gy of γ-irradiation. There was an approximate 10-fold increase in the number of possible DNA rearrangements detected in DNA from irradiated cells that had been allowed to repair the damage compared with DNA extracted from cell immediately after irradiation and DNA from control cells.

Several possible rearrangements have been sequenced. However, only c-myc sequence was detected and no foreign DNA was found rearranged to c-myc sequences. These rearrangements may be the result of deletions, unequal recombination events between the two copies of the gene, or an intra-genic duplication event.

In the diagram below, the breakpoints of six rearrangements that have been sequenced are indicated by letters (**a**, **b**, **c**, **d**, **e** and **f**). The sequences left of these letters were joined to the sequence right of the other breakpoint involved, indicated by the prime of the corresponding letter (i.e. sequence after **a** was joined to the sequence before **a'**). Details of the sequence adjacent to **a**, **b**, and **d** are shown. Stretches of purines or pyrimidines are indicated by solid lines under the sequence, and alternating purine-pyrimidine and A-T rich sequences are underlined by a broken line. Direct repeats of the sequences at sites of recombination are indicated by a solid line above the sequence and inverted repeats by a broken line. The homologous sequences associated with the breakpoint **d'** are indicated by lines above the ones for **a'** and **b'**.

The breakpoints of these products indicated that there were hot spots for ionizing radiation-induced DNA rearrangements that involve a stretch of a few base pairs. These sites were near DNA sequences that may form non-B-DNA conformation as well as possible topoisomerase I and topoisomerase II recognition sequences. For each rearrangement, sequences adjacent to the recombination site was found to contain either direct or inverted homology. In some cases, other homologous sequences were found further from the recombination sites.

The results obtained suggest that the most abundant ionizing radiation-induced DNA rearrangements involve either intrachromosomal DNA deletion or duplication events. At least one breakpoint from each of the rearrangement sequenced was located within 10 nucleotides of a sequence possibly associated with non-B DNA conformation. A combination of homology, topoisomerase sites, and unusual DNA conformation may be necessary for a DNA double strand break to lead to recombination. Position of DNA binding proteins may also contribute to the probability of recombination occurring in particular regions.

Intrachromosomal rearrangements 5' to the c-myc gene

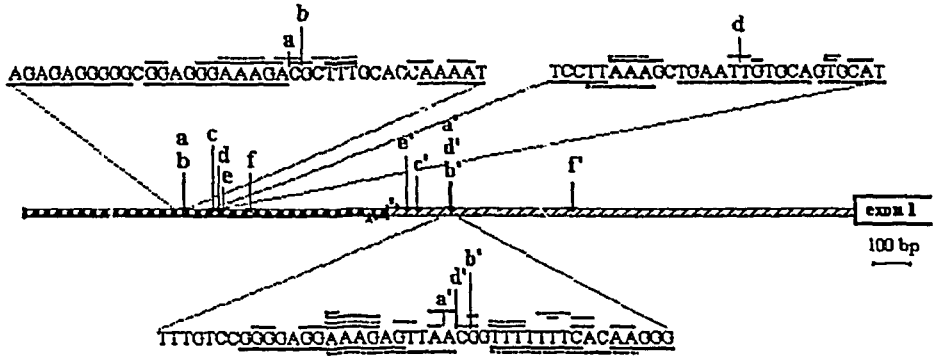

References

Grosovsky, A.J., De Boer, J.G., De Jong, P.J., Drobetsky, E.A., and Glickman, B.W., 1988, Base substitutions, frameshifts, and small deletions constitute ionizing radiation-induced point mutations in mammalian cells. Proc. Natl. Acad. Sci. USA, 85, 185 - 188.

Ito, T., Seyama, T., Mizuno, K.S., Hayashi, T., Iwamoto, N., Dohi, K., Nakamura, N., and Akiyama, M., 1993, Induction of BCR-ABL fusion genes by *in vitro* X-irradiation. Japanese Journal of Cancer Research, 84, 105 - 109.

Miles, C., Sargent, G., Phear, G., and Meuth, M., 1990, DNA sequence analysis of gamma radiation-induced deletions and insertions at the APRT locus of hamster cells. Molecular Carcinogenesis, 3, 233 - 242.

Ochman, H., Gerber, A.S., and Hartl, D.L., 1988, Genetic applications of an inverse polymerase chain reaction. Genetics, 120, 621-623.

Triglia, T., Petersen, M.G., and Kemp, D.J., 1988, A procedure for *in vitro* amplification of DNA segments that lie outside the boundaries of known sequences. Nucleic Acids Research, 16(16), 8186.

AUPS15064

MOLECULAR STRUCTURE AND RADIATION SENSITIVITY OF ELASTOMERS

Tim Bremner, David J.T. Hill, James H. O'Donnell*. M.C. Senake Perera, Peter J. Pomery and Andrew K. Whittaker

Polymer Materials and Radiation Group, Chemistry Department, University of Queensland, Brisbane, QLD 4072

The sensitivity of elastomers to radiation varies greatly, depending on the molecular structure of the elastomer. Moreover, the glass transition temperatures of elastomers, Tg, can be quite different, which also makes irradiation temperature a parameter which affects the radiation sensitivity.

The traditional elastomers are based on a diene backbone, with a H substituent for butadiene, CH_3 for isoprene (natural rubber), etc. The C=C bond, which has such a high concentration in these elastomers, will lead to rapid crosslinking. Earlier studies by IR spectroscopy and chemical analysis have been somewhat contradictory. In recent years the availability of high-resolution NMR spectrometers has provided opportunities to study changes in molecular structure on irradiation. However, this has been difficult in polymers which undergo predominantly crosslinking as the resolution in solid-state NMR spectra is limited, and the amount of change up to the gel dose is small.

Some elastomers have saturated molecular structures, e.g. ethylene-propylene copolymers (which prevent crystallization of sequences of either monomer). The radiation sensitivity should be much less than the diene elastomers and the balance between scission and crosslinking will be in favour of crosslinking.

We have recently obtained extremely interesting NMR spectra from poly(isobutylene), which is an elastomer widely used in the automobile industry as a sealant for tyres on account of its impermeability to air. Scission occurs with high yield, despite the formation of high concentrations of abstraction radicals which would undergo crosslinking in more conventional polymers. Because the polymer remains completely soluble after all radiation doses, excellent NMR spectra are obtained which enable quantitative determinations of the yields of new molecular structures, attributable to chain scission. A major challenge is to assign the many new peaks in the NMR spectra and possible methods are reported.

Dissolution of MnO_2 Colloids by Radicals generated from Ultrasound

by

Joe Sostaric, Paul Mulvaney, and Franz Grieser.

School of Chemistry,
University of Melbourne,
Parkville, VIC., 3052,
Australia.

Abstract

The phenomenon of cavitation which occurs during the absorption of ultrasound by water has been known for some time to lead to chemical reactivity in an otherwise inert system (1). It is well established that this effect is brought about during the final stage of cavitation - that is, the collapse of microbubbles in solution, producing temperatures and pressures that are high enough to lead to the thermal homolysis of water, thus yielding the highly reactive hydrogen and hydroxyl primary radicals (1, 2).

In the presence of certain solutes, these primary radicals can be scavenged to produce secondary radicals which in turn may react with a particular solute in solution, hence leading to further redox processes (3). We have shown that colloidal manganese dioxide can be sonochemically reduced in aqueous solution and this process has been attributed to the reaction of the colloid with either the highly reducing hydrogen radical species or the OOH radical and H_2O_2, which are formed in the presence of oxygen (1), and may also reduce the MnO_2 colloid . An interesting observation is that the amount of MnO_2 reduced can be increased by the presence of aliphatic alcohols in solution. It is proposed, and has previously been shown in γ-radiolysis studies, that this effect is due to the more efficient reduction of the colloid by a secondary radical species which is derived from the alcohol (4). This secondary radical is produced when a primary radical abstracts an α-hydrogen atom from the alcohol (5). More importantly, however, is the observation that the extent of colloidal reduction seemed to be highly dependent on the type and amount of alcohol present.

A number of different alcohols were used, and it was shown that the most effective alcohols in the dissolution process were the longer chain alcohols, n-pentanol, n-butanol and propan-2-ol with the shorter chain ethyl and methyl alcohols

being the least effective. This effect is attributed to the hydrophobicity of the alcohols, which in turn dictates the amount of alcohol at the bubble/water interface and thus its radical scavenging efficiency. Further, for any particular alcohol, it was found that initial increases in the amount of alcohol in solution led to considerable increases in the amount of colloid reduced. Finally, a point was reached where maximum reduction occurred and further increases in bulk alcohol concentration no longer had any effect on the extent of colloid dissolution. These observations are explained in terms of an increasing amount of alcohol at the bubble/water interface with increasing bulk alcohol concentration, and thus an increase in the primary radical scavenging efficiency. A point is eventually reached where saturation of the interface occurs, thus the observation of a maximum in the amount of colloid dissolution.

Ultimately, the above observations can be quantitatively explained in terms of the Gibbs surface excess, where the amount of alcohol at the bubble/water interface is the determining factor in the amount of colloidal dissolution, and not the alcohol type or bulk concentration. This observation is graphically represented in figure 1.

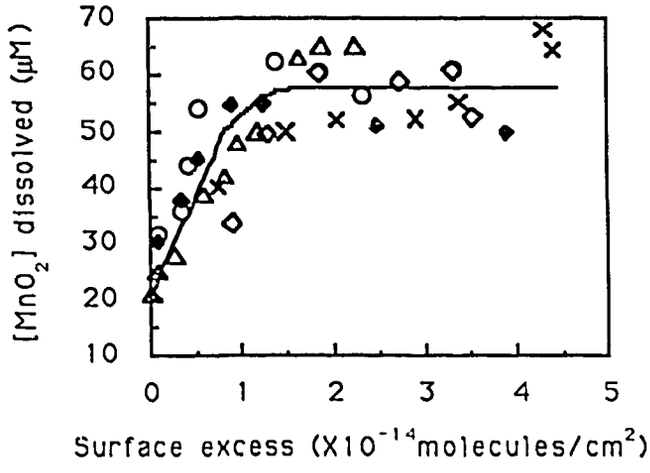

Figure 1. Concentration of MnO_2 dissolved as a function of the surface excess of various alcohols in the colloidal solution: (-x-) n-pentanol; (-◇-) n-butanol; (-♦-) propan-2-ol; (-o-) ethanol; (-Δ-) methanol. The initial solution contained the colloid at 2 x 10^{-4} M and 0.2 % Ludox HS30. Sonication time = 30 minutes; pH 4.5.

---

1. Henglein, A. *Ultrasonics*, 1987, 25, 6.

2. Suslick, K. S.; Hammerton, D. A.; Cline Jr., R. E. *J. Am. Chem. Soc.*, 1986, 108, 5641.

3. Seghal, C.; Sutherland, R. G.; Verrall, R. E. *J. Phys. Chem.*, 1980, 84, 2920.

4. Lume-Pereira, C.; Baral, S.; Henglein, A.; Janata, E. *J. Phys. Chem.*, 1985, 89, 5772.

5. Asmus, K. D.; Mockel, H.; Henglein, A. *J. Phys. Chem.*, 1973, 77, 1218.

AU PS15065

ION RECOMBINATION RATE CONSTANTS IN IRRADIATED GASES

R. N. Bhave and R. Cooper

Chemistry Department
The University of Melbourne
Parkville 3052, Australia.

Pulse radiolysis techniques coupled with time resolved microwave conductivity (TRMC) have been used to measure ion-electron recombination rate constants in Nitrogen and Hydrogen.

The total recombination coefficient is measured as a function of total pressure over the range 50 torr to 1000 torr. The overall rate constant is shown to be resolvable into two-body, α_2, and three- body, α_3, components. The pulse radiolysis technique has distinct advantages over electrical discharge methods since it allows higher pressures than a few torr to be studied. It enables the total rate constants to be accurately resolved into contributions from two- and three body recombination processes.

The particular emphasis in the current work is to study the temperature dependence of the recombination rate constants.

Earlier work at low pressures could not detect any three body effects; this work shows clearly that both two and three body processes are operative in the systems; He, Ne, Ar, N_2 and H_2.

Temperature effects in these systems have been predicted to be negative i.e. rate increases at lower temperatures in keeping with an energy loss process being important in the rate controlling step. A temperature dependence of $T^{-1.5}$ has been determined for α_3 in Nitrogen, and the results of experiments currently underway on Hydrogen will also be presented.

The theoretical calculation for α_3 value using the electron exchange energy coefficient parameter (V_{ll} /N) agrees well with the experimentally determined value for Nitrogen.

AU PS15066

PULSE RADIOLYSIS STUDIES ON THE REACTION BETWEEN DNA-TARGETED COMPOUNDS AND .OH RADICAL-DAMAGED DNA IN AQUEOUS SOLUTION.

R.F. Anderson*[1], W.A. Denny[2], K.B.Patel[3] and W.R. Wilson[4]

[1]Department of Chemistry, [2]Cancer Research Laboratory and [4]Department of Pathology, The University of Auckland, Private Bag 92019, Auckland, New Zealand and [3]Gray Laboratory, Mount Vernon Hospital, Northwood, Middlesex, England.

The reaction between DNA radicals, formed by .OH radical attack, and DNA-targeted cationic heterocycles, which are known hypoxic cell radiosensitizers and hypoxia-selective cytotoxic agents, have been studied in N_2O-saturated aqueous solution. The DNA radicals were produced by keeping the concentration of DNA high (≥ 1 mmol dm^{-3} in base pairs), much greater than that of the added compounds which themselves strongly associate with DNA thus reducing their reactivity with .OH radicals. Oxidation of the essentially immobile DNA radicals by series of regioisomers of nitroacridines (NC) and nitroquinolines (NQ) result in the formation of the one-electron reduced species of the compounds ($NC^{\cdot}$, $NQ^{\cdot}$) in varying amounts.

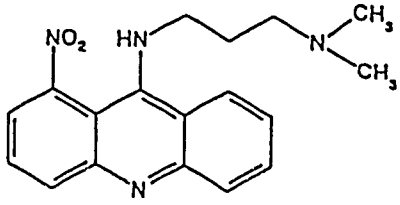

1-NC

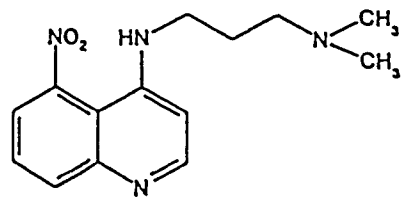

5-NQ

$$H_2O \xrightarrow{\sim\sim\sim} e^-_{aq}, .OH, .H, H_2O_2, H_2, H_3O^+$$
$$e^-_{aq} + N_2O \rightarrow .OH + N_2 + OH^-$$
$$.OH + DNA \rightarrow DNA^{\cdot}$$
$$DNA^{\cdot} + NC(NQ) \rightarrow DNA^+ + NC^{\cdot}(NQ^{\cdot})$$

The observed rate constants for the formation of the $NC^{\cdot}$ / $NQ^{\cdot}$ species were found to be dependent on the concentration of the compounds added to DNA. However a full description of the mechanism by which reaction is occurring must take into account the concentrations of bound and unbound compound in the system. Using the DNA binding parameters of association constant, K and site size, n, it is possible to calculate the concentration of unbound compound, c_f for any concentration added to DNA, from the McGhee and von Hippel equation;

$$\upsilon / c_f = K (1 - n\upsilon)^n / [1 - (n - 1)\upsilon]^{n-1}$$

where υ is the ratio of ligand bound per DNA base pair. The first-order rate constants, k_1, for the formation of $NC^{\cdot}$/ $NQ^{\cdot}$ species increased in line with c_f values for all compounds. The calculated second-order rate constants for the reaction of unbound compounds with the DNA radicals are similar, ranging from 4 - 7.5 x 10^9 dm^3 mol^{-1} s^{-1}. In the case of 6-NQ, an

additional slower kinetic component of oxidation was observed and transients could only be fitted to the expression $k_{obs} = A\exp(k_1 t) + B\exp(k_1')$. The smaller of the first-order rate constants (k_1') did not exhibit a dependency on the concentration of unbound compound, c_f but on the ratio of [6-NQ] / [DNA]. A possible explanation for this "secondary" behaviour in terms of the migration of the compound along the DNA to an oxidisable radical site will be discussed.

The build-up in absorbance due to the formation of the $NC^{\cdot}$ / $NQ^{\cdot}$ species, $OD_{A^{\cdot}-}$, can be used in competition kinetic studies to investigate the reactions of other compounds which also react with the same DNA radical but which do not effect measurable changes in absorbance at accessible wavelengths. This approach has been applied to the study of the repair of the DNA radical through H-atom donation by thiols which gives rise to the weakly absorbing thiyl radical, $RS^{\cdot}$

$$.OH + DNA(H) \rightarrow DNA^{\cdot} + H_2O$$
$$NC + DNA^{\cdot} \rightarrow NC^{\cdot} + DNA^{+} \ (OD_{A^{\cdot}-}) \quad k_1$$
$$DNA^{\cdot} + RSH \rightarrow DNA(H) + RS^{\cdot} \quad k_2$$

where $OD_{A^{\cdot}-}$ is the maximum optical density change on the oxidation of DNA radicals by a fixed concentration of NC. Hence $1/OD.Gy^{-1}$ (absorbance change in the presence of RSH) = $\{1 + k_2[RSH] / k_1\} 1/OD_{A^{\cdot}-}$ from which kinetic plots are used to determine k_2. In a series of experiments, 3 different thiols over a range in concentrations (15-75 μmol dm^{-3}) were added to solutions containing DNA (1.5 mmol dm^{-3} in base pairs) and either 2-NC (150 μmol dm^{-3}) or 4-NC (300 μmol dm^{-3}) as probes. The derived rate constants, k_2, are; glutathione, 1.2×10^6 dm^3 mol^{-1} s^{-1}; cysteine, 6×10^6 dm^3 mol^{-1} s^{-1}; cysteamine, 1.6×10^8 dm^3 mol^{-1} s^{-1}.
These rate constants increase in the order of the overall charges carried by the individual thiols, -1, 0, +1 as would be expected for positive ions accumulating near DNA through counter-ion condensation and of negative ions being repelled from DNA by co-ion depletion. A similar order has been reported for the thiols interacting with pBR 322 plasmid DNA.

A conclusion from these studies is that the targeting of compounds to DNA, through strong DNA association, decreases their reactivity with DNA radicals.

Formation of Q-state CdS Colloids using Ultrasound

Franz Grieser, Rachel A. Hobson and Paul Mulvaney
Advanced Mineral Products Research Centre, School of Chemistry, University of Melbourne, Parkville 3052.

The absorption of high-intensity ultrasound by water can produce significant amounts of H and OH radicals in solution. In the presence of solute in the water these primary radicals can be scavenged, leading to other chemical reactions which are essentially the same as those observed from conventional radiation initiated reactions in water. For example, it has been shown that both the primary and secondary radicals are able to react with aqueous metal ions or metal complexes to yield colloidal metals and metal oxides, much like what has been achieved by γ and electron irradiation of similar solutions[1,2]. The particle sizes obtained from the ultrasound application were quite small <10 nm diameter and this prompted us to investigate the formation of semiconductor particles in the quantum size range - between clusters and bulk size(usually >10 nm diameter)- referred to as Q-state particles. The method we adopted was based on the knowledge gained from radiation chemical studies that have shown that attack of H on certain thiols leads to the release of H_2S. This product can then react further if an aqueous metal ion is present in solution, for example Cd^{2+}. A sequence of reactions leading to particle formation can be written as,

$$H + MeCH(SH)CO_2H \rightarrow H_2 + MeCH(S)CO_2H \quad ...(1)$$

$$H + MeCH(SH)CO_2H \rightarrow H_2S + MeCHCO_2H \quad ...(2)$$

followed by,

$$Cd^{2+} + H_2S \rightarrow CdS + 2H^+ \quad ...(3)$$

$$n\,CdS \rightarrow (CdS)_n \quad ...(4)$$

Our results, using a number of thiols, indicate that Q-state CdS particles are readily formed following sonication of Cd^{2+}/thiol/hexametaphosphate aqueous solutions[3]. Interestingly, we have found that the initial particles formed are near

the cluster size dimensions and relatively stable to further growth unless further sonication is carried out on the solution, where upon Q-state particles are formed. The results also show that sonochemical reactions can mimic the radiation-initiated chemical processes in the same controlled way. It is the low local concentration of H_2S produced in solution by sonication which is conducive to the formation of ultrasmall semiconductor particles. This is probably due to the fact that at low CdS nucleation rates, effective "capping" of Q-state particles by adsorbed thiol occurs, preventing further growth. In contrast, when H_2S is bubbled through a Cd^{2+}/thiol/hexametaphosphate solution larger particles are formed since higher nucleation rates exist under these conditions, and thiol capping has a kinetically weaker impact on limiting particle growth.

[1] S. Au Yeung, R. Hobson, S. Biggs and F. Grieser JCS Chem. Comm. 1993, 378.

[2] M. Gutiérrez, A. Henglein and J.K. Dohrmann J. Phys. Chem. 1987, 91, 6687.

[3] R. Hobson, P. Mulvaney and F. Grieser JCS Chem. Comm. 1994, 823.

Semi-Automated Carbon-11 radioligand synthesis for Positron Emission Tomography

K. S. Phan, H. J. Tochon-Danguy, J. I. Sachinidis and D. Howells#.
Centre for Positron Emission Tomography, Austin Hospital, Heidelberg.
#Department of Medicine, Austin Hospital, Heidelberg.

Introduction

Positron Emission Tomography (PET) is a non-invasive technique to measure quantitative information about normal and diseased organs. The information obtained directly reflects the functional and metabolic state of the organ, which may have important therapeutic consequences. The development of PET, together with an effective choice of physiological radiopharmaceutical, has made possible the study of dynamic biochemical processes. Positron emitting radionuclides such as carbon-11 [^{11}C], nitrogen-13 [^{13}N], oxygen-15 [^{15}O] and fluorine-18 [^{18}F] easily replace the stable equivalents in biological molecules without changing their metabolic behaviour. More than 300 biological substrates and drugs have been already labelled with such radionuclides.

The PET centre at the Austin Hospital has been established and operational for the past two years. The basic equipment consists of a Siemens/CTI PET scanner, a cyclotron from Ion Beam Applications and a radiolabelling facility. The cyclotron accelerates negatively charged particles, hydrogen and deuteron ions, to the energies of 10 MeV and 5MeV respectively. The production of the four positron emitters occurs through the following nuclear reactions:
$^{14}N(p,\alpha)^{11}C$, $^{14}N(d,n)^{15}O$, $^{18}O(p,n)^{18}F$ and $^{16}O(p,\alpha)^{13}N$.

The utilisation of PET [^{11}C]radiopharmaceuticals for brain receptor studies is well recognised[1]. Predominantly the synthesis of choice for [^{11}C]radiolabelling is by the methylation of a desmethyl precursor using [^{11}C]methyl iodide[2]. Many radioligands such as raclopride, flumazenil and SCH23390 had been labelled by this method[3]. Here we report the development of a semi-automated radiolabelling module (figure 1) for a general [^{11}C]radiolabelling synthesis using the [^{11}C]methyl iodide methylation reaction.

[^{11}C]Radiosynthesis and purification

This labelling procedure is carried out in three main stages; radionuclide production, [^{11}C]methyl iodide synthesis and [^{11}C]methylation of the desmethyl precursor.

The proton bombardment of a pressurised target (2%O_2 in N_2) produces carbon-11 in the form of [^{11}C]carbon dioxide. In a typical experiment, the target is irradiated with a 40μA proton beam for 30 mins producing 1Ci (37GBq) of activity.

The [^{11}C]carbon dioxide is transferred to the hotcell and concentrated in a cryogenic trap immersed in liquid nitrogen (-198°C). It is then dispensed into a solution of $LiAlH_4$ in THF where the [^{11}C]carbon dioxide is reduced to "[^{11}C]methanol" trapped as the alkoxide. After evaporating the THF at 120°C under nitrogen, concentrated HI (55%) is added to the alkoxide and the resulting mixture heated at 180°C to produce [^{11}C]methyl iodide. The [^{11}C]methyl iodide is then

distilled into the cooled (-40°C) methylation vial containing the desmethyl precursor and the vial is lowered into an oil bath (80°C) for 5mins to complete methylation. The methylation vial typically could contain 1mg of precursor in its free base form dissolved in 200µl of DMF.

The whole reaction mixture is then injected into a semi-preparative HPLC system (reverse-phase C18-column, 8mL/min, 60/40 0.1M NH_4COOH/CH_3CN) equipped with UV absorbance and radioactivity detectors. The peak corresponding to the pure radiopharmaceutical is collected into a rotary evaporator where the HPLC solvent is removed under vacuum at 120°C. The isolated product is prepared for injection by reconstituting the residue in 5mL of 0.9% sodium chloride solution and passing through a 0.22µm Millipore filter.

In summary, approximately 80mCi of [^{11}C]SCH23390 was prepared from 1Ci of [^{11}C]carbon dioxide (decay corrected yield 26%). The synthesis time from end of bombardment (EOB) to the preparation of injectable product is approximately 30-40mins. The specific activity at the EOS is 0.5Ci/µmoles with a radiochemical purity of greater than 98%. Currently we have succeeded in applying this general semi-automated procedure to a number of different desmethyl precursors to synthesize the corresponding [^{11}C]labelled radioligands.

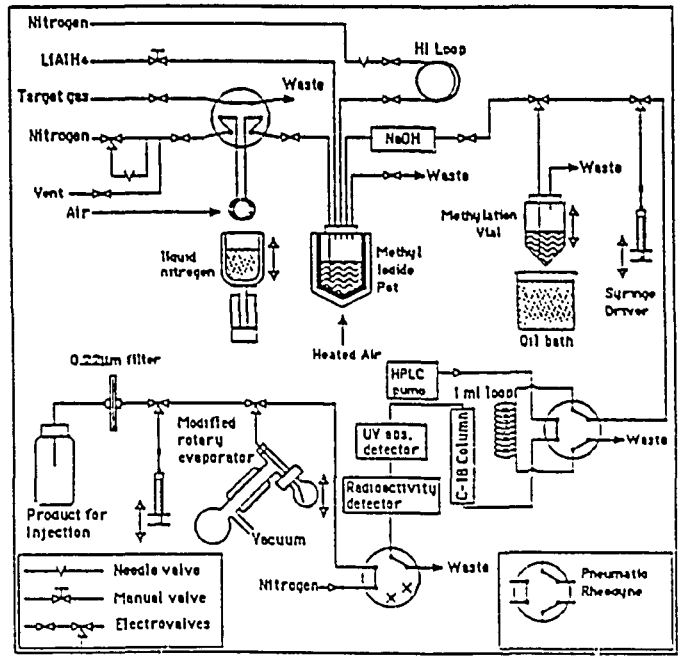

Figure 1: Semi-automated [^{11}C] radiolabelling module. Currently the equipment is controlled by a keyboard located outside the hotcell with provision to connecting onto a computer for a fully automated system.

References

[1]Maziere B. and Maziere M. (1990) Where have we got to with neurorer*ptor mapping of the human brain. *Eur. J. Nucl. Med.* 16:817-835

[2]Marazano C., Maziere M., Berger G. and Comar D. (1977) Synthesis of [^{11}C]methyl iodide and formaldehyde. *Int. J. Appl.Radiat.Isot.* 28,49.

[3]Clark C and Dowsett K. (1991) Automated [^{11}C]radiopharmeutical module. *Targetry '91 Proceedings of the IVth International Workshop on Targetry and Target Chemistry.*

AU 9515068

Calculations of Radiation–induced Scission and Crosslinking Yields from Variations of Molecular Weights of Polymers with Dose

Karen A. Milne and James H. O'Donnell
Polymer and Materials Research Group
Chemistry Department,
University of Queensland Qld 4072, Australia

During the course of a study of the evaluation of scission and crosslinking yields of irradiated polymers by studying the weight–average and z–average molecular weights of polymers with an initial Schulz–Zimm molecular weight distribution[1], it was necessary to develop an approximate method[1] of solution of the general equations for the radiation dose dependence of molecular weights of polymers with an initial Schulz–Zimm distribution[2,3,4].

The present work expands and extends theoretical work reported[1], particularly by developing exact numerical solutions of the general equations. These solutions allow G(S) and G(X), the scission and crosslinking yields to be evaluated exactly using minimization calculations or other numerical methods.

The aim of this study is to find algebraic solutions to the general equations that are suitable for use in computer programs, so that the total work of solving for G(S) and G(X) for a set of experimental results may be automated.

Thus, the general equations for the radiation dose dependence of irradiated polymer molecular weights have been solved exactly. For an initial most probable molecular weight distribution ($\sigma = 1$), the solutions are analytical and exact. For the general case ($\sigma \neq 1$) the solutions are numerical and exact. The present approach has resulted in the solutions for both $\sigma = 1$ and $\sigma \neq 1$ being incorporated into a group of FORTRAN computer programs which will solve experimental data for scission and crosslinking yields by both minimization and exact treatments.

The Equations

The full set of general equations[3] for the dose dependence of each of the molecular weights, $\overline{M}_n$(number average), $\overline{M}_w$(weight average), and $\overline{M}_z$(z average) are given below:

$$\overline{M}_n(D) = \frac{\overline{M}_n(0)}{(1 + (\dot{\tau}/\dot{\chi} - 1)u\dot{\chi}D)} \qquad \text{....(1)}$$

$$\overline{M}_w(D) = \frac{2\,\overline{M}_n(0)\,\phi_1(u\dot{\tau}D, \sigma)}{(u\dot{\tau}D)^2\,[1 - (4\dot{\chi}/u\dot{\tau}^2D)\,\phi_1(u\dot{\tau}D, \sigma)]} \qquad \text{....(2)}$$

$$\overline{M}_z(D) = \frac{3\,\overline{M}_n(0)\,[\phi_2(u\dot{\tau}D, \sigma)/\phi_1(u\dot{\tau}D, \sigma)]}{[1 - (4\dot{\chi}/u\dot{\tau}^2D)\,\phi_1(u\dot{\tau}D, \sigma)]^2} \qquad \text{....(3)}$$

where

$$\phi_1(u\dot{\tau}D,\sigma) = u\dot{\tau}D - 1 + [1+(u\dot{\tau}D/\sigma)]^{-\sigma} \quad \text{....(4a)}$$

and

$$\phi_2(u\dot{\tau}D,\sigma) = 1 + [1+(u\dot{\tau}D/\sigma)]^{-(\sigma+1)} - (2/u\dot{\tau}D)\{1-[1+(u\dot{\tau}D/\sigma)]^{-\sigma}\} \quad \text{....(4b)}$$

D denotes the radiation dose in grays, $\dot{\tau}$ and $\dot{\chi}$ are the respective probabilities per gray of scission and crosslinking of a single monomer unit, and

$\sigma = 1/[(\overline{M}_w(0)/\overline{M}_n(0)) - 1]$ and is a measure of the width of the initial molecular weight distribution. The values of $\dot{\tau}$ and $\dot{\chi}$ determine the values of G(S) and G(X), and are the desired solutions.

Strategies for solution

(*a*) *Initial most probable distribution* ($\sigma = 1$)

For the case of the initial most probable distribution ($\sigma = 1$), the general equations become simplified and are given below:

$$\overline{M}_n(0)/\overline{M}_n(D) = 1 + (\dot{\tau}/\dot{\chi} - 1)u\dot{\chi}D \quad \text{....(1a)}$$

$$\overline{M}_w(0)/\overline{M}_w(D) = 1 + (\dot{\tau}/\dot{\chi} - 4)u\dot{\chi}D \quad \text{....(5)}$$

$$\overline{M}_z(0)/\overline{M}_z(D) = (1 + u\dot{\tau}D - 4u\dot{\chi}D)^2/(1 + u\dot{\tau}D) \quad \text{....(6)}$$

These equations are then amenable to solution as simultaneous equations in pairs by some of the more popular symbolic mathematics computer programs e.g. MATHEMATICA and MACSYMA.

(*b*) *The general case* ($\sigma \neq 1$)

In this case, equations (1),(2) and (3) were taken in pairs and solved simultaneously:

Considering $\overline{M}_w$ *and* $\overline{M}_z$

Squaring both sides of equation (2) and dividing by equation (3) and rearranging eliminates $\dot{\chi}$ and gives,

$$3\phi_2\,(u\dot{\tau}D)^4\,[\overline{M}_n(0)/\overline{M}_z(D)]\,[\overline{M}_w(D)/\overline{M}_n(0)]^2 - 4\phi_1^3 = 0 \quad \text{....(7)}$$

Equation (7) is then suitable to use in the minimization[5] and numerical methods discussed[6].

The procedure for the pair $\overline{M}_n$ and $\overline{M}_z$, and the pair $\overline{M}_w$ and $\overline{M}_n$ is similar.

Simulated data has been treated successfully using these FORTRAN programs. The FORTRAN programs are available from the authors.

References

1. O'Donnell JH, Winzor CL, and Winzor DJ (1990) Macromolecules 23:167
2. Saito A (1972), Chapter 11 in: Dole M (ed) The Radiation Chemistry of Macromolecules Vol 1 Academic Press, New York USA
3. Inokuti M, Dole M (1963) J. Chem. Phys. 38:3006
4. O'Donnell JH, Smith CA, Winzor DJ (1978) J. Polym. Sci., Polym. Phys. Ed. 16:1515.
5. Chandler JP (1975) STEPT: A Family of Routines for Optimization and the Fitting of Data. Obtained from: Department of Computing and Information Sciences, Oklahoma State University, Stillwater, Oklahoma 74074 USA
6. Press WH, Flannery BP, Teukolsky SA, Vetterling WT (1986) Numerical Recipes: The Art of Scientific Computing, Cambridge University Press, Cambridge, London, New York, New Rochelle, Melbourne, Sydney

AUPS15066

Mechanism of Radiation Vulcanisation of Natural Rubber Latex Sensitised by Monoacrylates

D.J.T.Hill, J.H.O'Donnell, M.C.S.Perera and P.J.Pomery
Polymer Materials and Radiation Group, Department of Chemistry, University of Queensland, Q 4072 Australia.

Introduction

Vulcanisation of natural rubber latex can be performed by ionisation radiation, but it requires a dose more than 300 kGy, which is too high a dose to be economical in industrial applications. Halogenated hydrocarbons, such as carbon tetrachloride and chloroform have been used as sensitisers to reduce the dose required for vulcanisation. However, the majority of the carbon tetrachloride remains in the irradiated latex and is released in the working environment. Hence the development of non-toxic sensitisers became a major priority to prevent this pollution of the working environment. Some monofunctional monomers were found to enhance the radiation vulcanisation of natural rubber[1]. It was previously believed that polyfunctionality was essential in order to enhance the radiation crosslinking in latex. Makuuchi [1,2] has reported studies of the mechanism of radiation sensitised crosslinking of natural rubber latex by monofunctional monomers, such as 2-ethyl hexyl acrylate (2-EHA) and n-butyl acrylate (n-BA), with and without carbontetrachloride. In the present study, Electron Spin Resonance (ESR) and Nuclear Magnetic Resonance (NMR) were used to obtain more mechanistic information about this proposal.

Results and discussion

The ESR spectrum of irradiated 2EHA changed shape when the power was increased, indicating the presence of more than one radical. Photobleaching of the samples at a wavelength of 590-900 nm, produced a decrease in the area of the spectrum of approximately 10%. The change in the shape of the spectrum indicate a transition of one radical to another during photobleaching. On annealing the photobleached sample, the radical concentration commenced to drop at a lower temperature than in natural rubber, and no radicals were observed above 280K. The change in the spectral shape during heating from 110 to 150 K is shown in Figure 1. The total width of the spectrum changed from 135 to 90 G. While the central peak and the two outer regions of the spectrum decreased in intensity, the remainder of the peaks in the spectrum have increased in intensity. This indicates that the primary radicals are rapidly converted into new radical intermediates over this temperature region. The change in the total width indicates a conversion of a polypropyl type radical to an acrylate propagating type radical. Above 220K, only a three line spectrum was observed which is assigned to a main chain radical. The ESR spectra of 2EHA/NR mixture indicate the presence of acrylate propagating radical and main chain radical as in pure 2EHA. Further the spectra also indicate the abstraction of allylic hydrogen of the NR molecule by the propagating radical.

The latex sample after irradiation and drying was analysed using solid state NMR and the spectra are shown in Figure 2. It is known that the DD NMR technique is more sensitive to the mobile and uncrosslink regions of the polymer than to the more rigid regions, while the CP techniques are more sensitive to rigid regions. The DD spectrum shows sharp polyisoprene peaks, and peaks due to the pendeat methyl and methylene carbons of the 2EHA. The CP spectrum on the other hand shows peaks corresponding to all the carbons in the 2EHA and polyisoprene. No double bond peaks at 129 ppm were visible, confirming that all the 2EHA had polymerised. These results clearly indicate that the material is heterogeneous and that the 2EHA is in the rigid regions of the material. Thus, even if

the absorption of 2EHA in the NR sheets was found (7) to be very high, quite a large percentage of the 2EHA also remains on the surface of the rubber particles in latex. Therefore the crosslinking, which is sensitised by the acrylate, is higher at the acrylate rich particle surfaces.

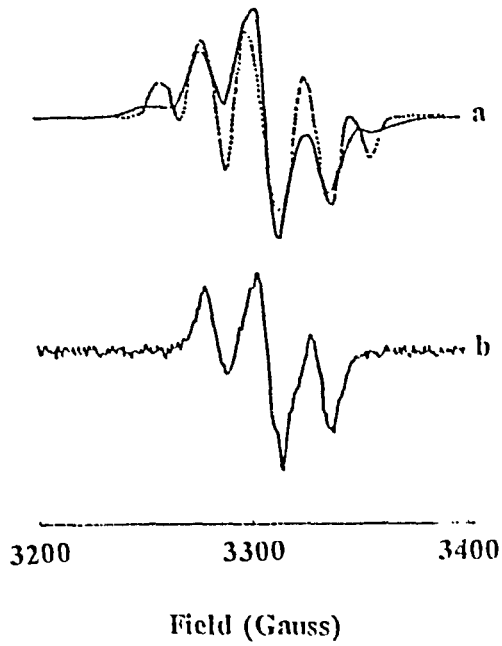

Figure 1: ESR spectra of 2EHA at (a) ——— 110K
..... 150K and (b) 220K

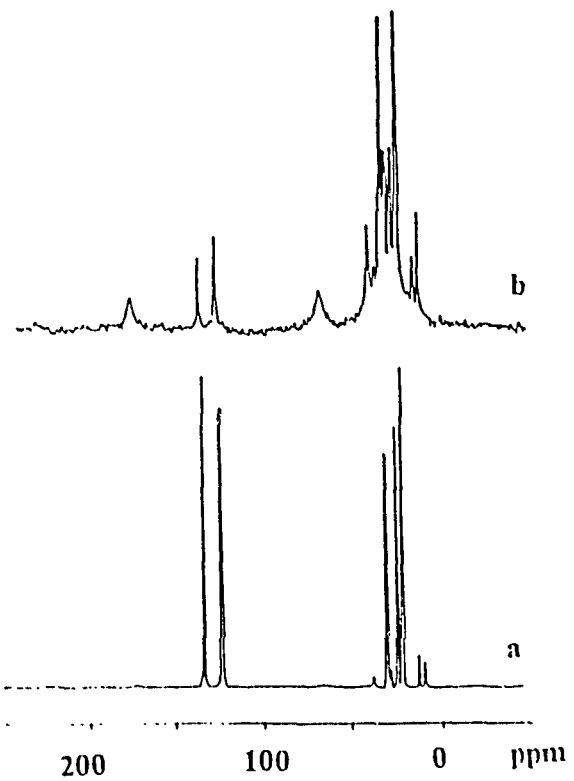

Figure 2: Solid state NMR spectra of irradiated 2EHA/NR
(a) Single pulse dipolar decoupling-DD
(b) cross polarisation-CP

References

1. K.Makuuchi and K Tsushima, Nipon Gomu Kyokaishi, 61,62 (1988)
2. C. Siri-Upathum and K. Makuuchi, Proc. Int. Symp. on Radiation Vulcanisation of Natural Rubber Latex, Tokyo, Japan (1989)

AUPS1507o

Radiation Dosimetry above 1 Gray: A Comparison of Electron-Spin Resonance and Thermoluminescence Dosimetries

John F. Boas and Joseph G. Young

Australian Radiation Laboratory
Lower Plenty Road
Yallambie Victoria 3085

A study of the dose-rate distribution inside the Gammacell 1000 irradiator of the Red Cross Blood Bank in South Melbourne afforded us the opportunity of comparing electron spin resonance dosimetry using alanine (ALD) and thermoluminescence dosimetry (TLD) using TLD-100 (lithium fluoride doped with magnesium and titanium). The doses ranged between ~1 and 50 Gy, which is in the higher range of applicability for LiF based TLD but in the lower range for alanine based esr dosimetry. Good agreement was found between the two methods, with the mean ratio of the two results for the various locations, TLD/ALD, being 1.020±0.025 (1 standard deviation) and the standard deviations being ±3.0% for TLD and ±5.3% for ALD.

For accurate TLD measurements in this dose range, the effects of fading, supralinearity, particle size and annealing procedures need to taken into account, whilst accurate ALD measurements require sample uniformity and consistency. In addition, for best results with ALD, it is necessary that close attention be paid to the conditions of operation of the esr spectrometer to avoid signal distortion.

A study of single crystals of irradiated alanine shows that the so-called "forbidden" transitions have different behaviour to the "allowed" transitions. The former make a significant contribution to the overall intensity of the powder spectrum obtained in dosimetry, a point not often discerned in the ALD literature.[1,2] The factors which lead to complications with the use of alanine as an electron spin resonance dosimetry material have stimulated a search for other, possibly spectroscopically more satisfactory, materials. Some alternatives will be discussed in this paper.

References

1. Wielopski, L., Maryanski, M., Ciesielski, B., Forman, A., Reinstein, L.E. and Meek, A.G., "Continuous three-dimensional radiation dosimetry in tissue-equivalent phantoms using electron paramagnetic resonance in L-α-alanine", Medical Physics, 14, 646-652 (1987).

2. Arber, J.M., Sharpe, P.H.G., Joly, H.A., Morton, J.R. and Preston, K.F., "The ESR/alanine dosimeter-powder dependence of the X-band spectrum", Applied Radiation and Isotopes, 42, 665-668 (1991).

AU 9515071

Rates of Energy Migration in Supramolecular Assemblies

Gregory D. Scholes and Kenneth P. Ghiggino
School of Chemistry, The University of Melbourne, Parkville VIC 3052, Australia

A general rate expression describing microscopic aspects of electronic excitation (energy) transfer (EET) has been developed and used to investigate aspects of superexchange-mediated EET and energy migration (EM). The efficiency of donor-to-trap energy transport processes, for example, in the photosynthetic unit and in various synthetic light-harvesting systems, is discussed from this quantum mechanical viewpoint. In particular, the role of coherent EM pathways, and how they are manifested in the quantum mechanical rate expression, are investigated. The significance of contributions arising through the quantum mechanical interference between pathways is discussed. The theory is related to experiment and compared to various computational models.

In connection with superexchange-mediated EET, for the first time, the possibility of superexchange pathways for EM via higher excited states of the intermediate chromophores is introduced. Experimental studies of through-bond superexchange mediated EET in some rigidly-linked bichromophores using time-resolved fluorescence measurements are also presented.

AU PS15072

The Radiation Chemistry of Organic Herbicides

I. Bokor, K. Cornelius and G.S. Laurence*

Chemistry Department, The University of Adelaide, Adelaide 5005

The chemistry of the degradation of organic herbicides and fungicides in natural systems is important in determining operationally important parameters such as witholding times before planting or consumption. Disappearance rates in the field are frequently many time largerexpected from reactions such as hydrolysis and photchemical- and radical-initiated reactions are frequently cited as causes of the degradation reactions. Apart from the direct photochemistry of the herbicides, reactions of OH and O_2^- radicals are postulated, with the sources of these radicals in natural aqueous systems being suggested as photochemical or transition metal reactions.[1] The reactions of these postulated free radicals with the herbicides are however largely unknown.

We have begun a systematic study of the reactions of OH and O_2^- radicals with important herbicides and fungicides in order to obtain rate constant data for modelling the possible reactions in field conditions and to establish whether the postulated reactions are capable of accounting for the disappearance of the materials in the field.

Some results obtained by pulse radiolysis on aqueous solutions of the pre-emergent herbicides 'Dervinol' ['Napropamide'] (I) and 'Chlorsulfuron' (II) will be presented and the implications for the behaviour of the compounds in natural systems will be discussed.

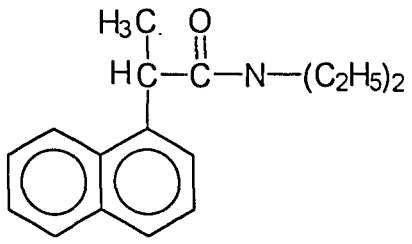

(I) Napropamide

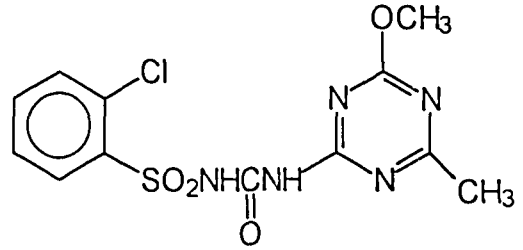

(II) Chlorsulfuron

[1] W.R. Haag and J. Hoigne, *Chemosphere*, 14, 1659-1671 (1985)

AUPS15073

Monte Carlo Neutron Photon Treatment Planning Calculations: Modelling from CT scans

S.A.Wallace[1], J.N.Mathur[1], B.J.Allen[1,2]

1 Physics Department, University of Wollongong, Wollongong NSW 2522
2 St George Cancer Care Centre, Kogarah NSW 2217

The Los Alamos Monte Carlo Neutron Photon radiation transport code MCNP is currently being widely used in the Neutron Capture Therapy (NCT) community for a variety of purposes including treatment planning, diagnostics, beam design, tomographic studies and radiation protection. To date, treatment planning calculations have been based upon simple geometrical shapes such as the elliptical model of Zamenhof et.al.[1]. Extension to significantly more complex geometry, and thus more accurate dose calculations, has been restricted by the computationally intensive nature of the Monte Carlo technique.

This presentation will review the efforts within the Australian NCT group to use CT or MRI scan data to construct MCNP geometry models for treatment planning using the voxel technique. Incorporation of CT scans in the Monte Carlo modelling process has been achieved, including the ability to specify "regions of interest" where higher resolution anatomical structure and dose distribution calculations may be performed. Calculations have been performed for an anthropomorphic head phantom in addition to a whole body phantom. Figure 1 shows a CT scan of the liver region of the whole body phantom. Perspex tubing to house various detectors can be seen penetrating the liver, the dark region to the left is the lowermost part of the lungs, whilst the organ to the right is the spleen. The dark outer layer is simulated adipose tissue. Figure 2 depicts the same slice of the Monte Carlo model. Different materials in the model are represented by differing greyscale values, in addition more detailed modelling can be seen in the liver region - the target of the neutron beam. Neutron and photon dose distributions for the ECN/JRC epithermal neutron beam have been calculated throughout the brain, liver and lungs of these phantoms using the Fujitsu VP2200 supercomputer. Measurements to validate phantom calculations have been performed at the ECN/JRC epithermal neutron beam. Additionally, application of this technique to treatment planning for BNCT of cervical cancer with ^{252}Cf brachytherapy is being examined.

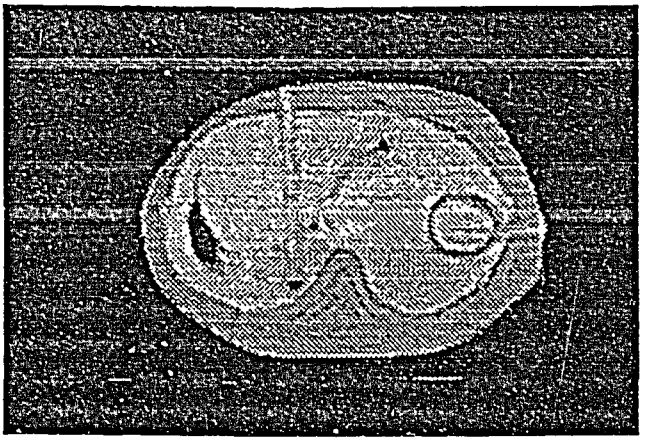

Figure 1. CT scan of the liver region of the whole body phantom

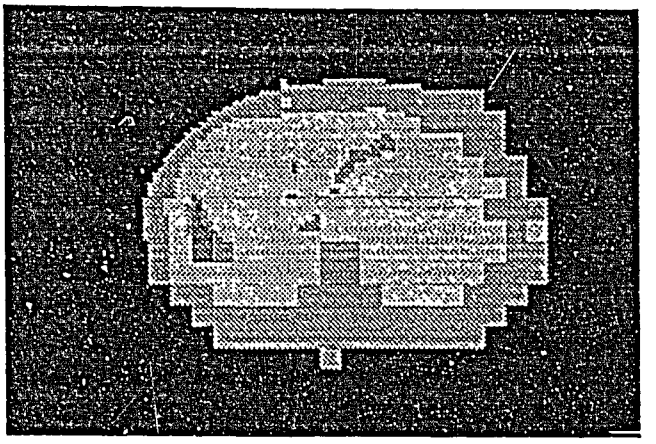

Figure 2. Slice of the Monte Carlo model equivalent to the CT scan of figure 1. Adipose, lung and other soft tissues are modelled, in addition to more accurate geometric representation in the area of the liver - the target of the epithermal neutron beam.

[1] R.G.Zamenhof, S.D.Clement, O.K.Harling, J.F.Brenner, D.E.Wazer, H.Madoc-Jones, and J.C.Yanch, "Monte Carlo Based Dosimetry and Treatment Planning for Neutron Capture Therapy of Brain Tumours", in Neutron Beam Design, Development and Performance for Neutron Capture Therapy, O.K.Harling, J.A.Bernard and R.G.Zamenhof, eds.,Plenum Press, New York (1990).

Acknowledgements
Thanks to Martin Carolan, Paul Miskelly, Haider Meriaty, Ned Blagojevic and Julia Mallesch for assistance during this project.

Financial support by the Australian Institute of Nuclear Science and Engineering (AINSE) and an Australian Research Council (ARC) small grant is gratefully acknowledged.

AUPS15074

RECENT ADVANCES IN RADIATION CHEMISTRY & PHYSICS

Dr R Cooper
School of Chemistry
University of Melbourne

Recent international conferences have shown how widely radiation chemistry is being used by chemists, physicists, biologists and engineers in a wide range of situations. Fundamental chemical-physics has spread widely into areas of molecular biology , chemical engineering, and recently into the physics of plasmas and electrical discharges. The breakdown of electrical insulators has now come under scrutiny by radiation chemical techniques.
At the 1994 Gordon Conference on Radiation Chemistry, the 1993/4 meetings on Gaseous Electronics in Montreal & Canberra and most lately the 3rd Japan Australia workshop on gaseous electronics and applications , the impact of ionic and excited state chemistry has become apparent. It has ranged from ion impact reactions on the surface of the planet Mercury and Jupiters moons, through plasma etching of silicon surfaces ; to the clean up of flue-gases; direct high energy "hits" on biological targets; free radicals and redox chemistry in cells; synchrotron radiation to explore single high energy events in DNA etc.

One of the original R.L. Platzmann predictions in the 1960's was the time evolution of radiation action. This gave scientists a time map of the processes evolving from the initial deposition of energy from the radiation into the medium to the conventional chemical physics relaxations of 10^{-12} - 10^{-6} seconds which followed into the chemical reaction times which initiated the final biological phase.
Initial electronic excitation and ionisation of molecules was placed in the 10^{-15} sec time domain. Now this process can be directly seen by picosecond time resolved spectroscopy asoociate with pulse radiolysis techniques. In the simplest chemical systems - a pure rare gas- this process takes ~ 30 ps. Molecular systems are much faster. The reaction sequence can now be modelled quite reliably.
The relaxation of excited initial species can now be directly observed as hot electrons in a plasma relax and allow recombination processse to proceed. The rate of such processes can now be directly monitored by pulse radiolysis techniques and has implications stretching beyond simple radiation chemstry into the domain of the relaxation of the ionosphere which affects the range and quality of radio transmissions in the atmophere.
Laser photochemistry has had its impact and it is now possible to generate single ion pairs by photoionisation in liquids. This mimics radiation action and helps solve a long standing problem concerning the dynamics of ion recombination in close neighbour or geminate situations. In radiation chemistry/biology, the possibilty exists of multi-ion pair radical reactions occurring in so called "spurs".
More recently free radicals have been shown to be produced by sonic events where extremely high temperatures can be generated by acoustic radiation.
In solid state chemical physics, the etching of surfaces is done by reactive ions and radicals produced by electrical discharge ionisation of a gaseous system. This type of chemical process is currently extremely important industrially.
In polymers the energy migration along polymer chains is a perennial source of interest as light harvesting; energy localistaion in biological"hot spots" must finallly come down to energy transfer.
This paper will present a review of the up to date topics and dilemma's facing radiation science today.

LIST OF PARTICIPANTS

LIST OF PARTICIPANTS
(as at time of printing)

OVERSEAS VISITORS	PAPER NO
Dr R F Anderson (Faculty of Science, The University of Auckland)	51
Dr K-D Asmus (Hahn-Meitner Institut, Berlin)	1
Dr A Singh (AECL Research, Canada)	11
Dr P Wardman (CRC Gray Laboratory, Mt Vernon Hospital, London)	36
THE UNIVERSITY OF ADELAIDE (Dept of Chemistry)	
Professor G S Laurence	58
ANSTO	
Mr J Twining	12
Mr G Gant	6
Dr J S Prosser	27
Dr R W Garrett	6
Mr H van der Gaast	17, 45
PET CENTRE, AUSTIN HOSPITAL	
Dr J Sachinidis	16, 13, 53
Dr H J Tochon-Danguy	16, 13, 53
Dr K S Phan	13, 53
AUSTRALIAN RADIATION LABORATORY	
Dr K Lokan	44
Dr J Baldas	38
Dr J Boas	37, 56
Dr D V Webb	37
GRIFFITH UNIVERSITY (Faculty of Science & Technology)	
Mr G Watson	9
MACQUARIE UNIVERSITY (School of Biological Sciences)	
A/Professor J M Gebicki	2, 30
Mrs S Gebicki	30

THE UNIVERSITY OF MELBOURNE
(Dept of Civil & Environmental Engineering)
Mrs F Dyer

(School of Chemistry)
A/Professor R Cooper 4, 50, 60
Miss P Nel 4
Mr D Edmondson 10
Dr P Mulvaney 20, 49, 52
Dr R N Bhave 50
Dr F Grieser 19, 49, 52
Miss R Hobson 19, 52
Mr J Sostaric 49
Mr G Scholes 57
Dr K Ghiggino 57
Mr P Towler 18
Mr R Tinker 43
Dr J D Smith 18, 43

MONASH UNIVERSITY
(Gippsland Campus)
Mr B McEniery
Dr R Markiewicz

PETER MACCALLUM CANCER INSTITUTE
Dr R F Martin 4, 23, 25
Mr G C D'Cunha 23, 24
Dr R Budd 25
Mr D R Aldridge 26
Dr I R Radford 26, 40, 47
Ms H Forrester 47

THE UNIVERSITY OF QUEENSLAND
(Chemistry Department)
Professor J H O'Donnell 7, 8, 31, 32, 33, 34, 48, 54, 55
Dr S Perera 48, 55
Dr K Milne 54
Dr K Y Kim 31
Mr L Dong 8
Mr M Killeen 32
Mr J Hopewell 7
Ms G Saadat 34
Mr J Forsythe 33
Mr J Kwiatkowski 35
Dr E-J Choi 31

THE UNIVERSITY OF QUEENSLAND
(QIMR)
Professor M Lavin 3, 42
Ms H Beamish 3, 42

THE UNIVERSITY OF SYDNEY
(Faculty of Health Sciences)
Mr D McLean 15
Ms D Strain 27

(School of Chemistry)
Mr D F Sangster 39, 46
Professor R G Gilbert 39

UNIVERSITY OF WESTERN SYDNEY, NEPEAN
(Faculty of Science & Technology)
Dr F Z Company 5

THE UNIVERSITY OF WOLLONGONG
(St George Cancer Care Centre)
Professor B J Allen 5, 21, 28, 29, 41, 59

(Department of Physics)
Mr S A Wallace 41, 59
Mr M G Carolan 41

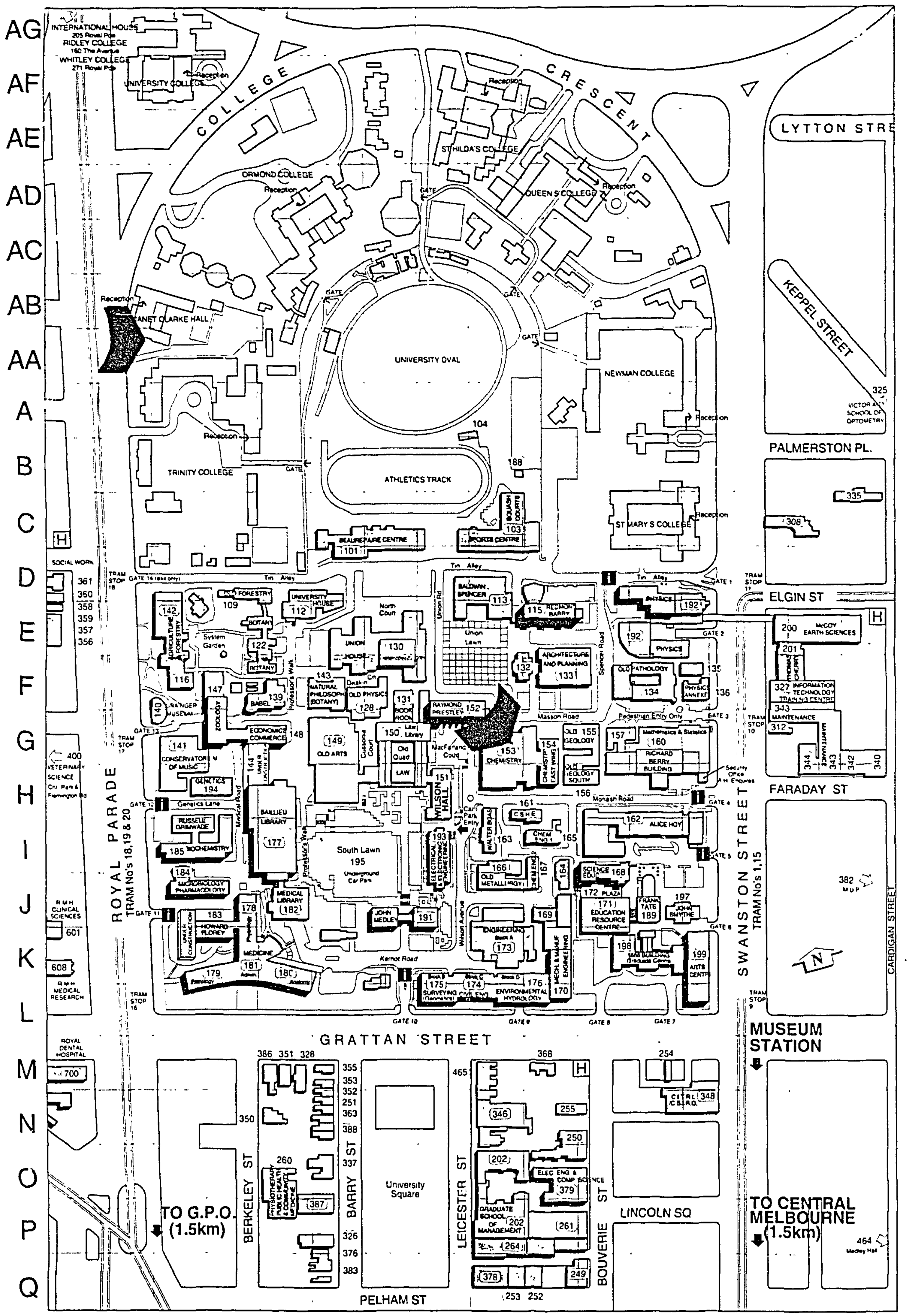

AG
AF
AE
AD
AC
AB
AA
A
B
C
D
E
F
G
H
I
J
K
L
M
N
O
P
Q
INTERNATIONAL HOUSE
RIDLEY COLLEGE
WHITLEY COLLEGE
UNIVERSITY COLLEGE
COLLEGE CRESCENT
LYTTON STREET
ST HILDA'S COLLEGE
ORMOND COLLEGE
QUEEN'S COLLEGE
Reception
GATE
JANET CLARKE HALL
UNIVERSITY OVAL
NEWMAN COLLEGE
KEPPEL STREET
VICTORIAN COLLEGE OF OPTOMETRY
TRINITY COLLEGE
ATHLETICS TRACK
PALMERSTON PL.
ST MARY'S COLLEGE
BEAUREPAIRE CENTRE
SPORTS CENTRE
SOCIAL WORK
Tin Alley
ELGIN ST
FORESTRY
UNIVERSITY HOUSE
BALDWIN SPENCER
REDMOND BARRY
PHYSICS
McCOY EARTH SCIENCES
System Garden
BOTANY
UNION HOUSE
Union Lawn
North Court
ARCHITECTURE AND PLANNING
OLD PATHOLOGY
PHYSICS ANNEXE
INFORMATION TECHNOLOGY TRAINING CENTRE
NATURAL PHILOSOPHY (BOTANY)
OLD PHYSICS
ZOOLOGY
BABEL
GRAINGER MUSEUM
RAYMOND PRIESTLEY
Masson Road
Pedestrian Entry Only
MAINTENANCE
ECONOMICS & COMMERCE
OLD ARTS
Law Library
Old Quad
LAW
CHEMISTRY
OLD GEOLOGY
Mathematics & Statistics
RICHARD BERRY BUILDING
400 VETERINARY SCIENCE
CONSERVATORIUM OF MUSIC
GENETICS
WILSON HALL
FARADAY ST
Genetics Lane
BAILLIEU LIBRARY
Monash Road
RUSSELL GRIMWADE
ALICE HOY
BIOCHEMISTRY
South Lawn 195 Underground Car Park
ELECTRICAL & ELECTRONIC ENGINEERING
CHEM ENG
OLD METALLURGY
MICROBIOLOGY PHARMACOLOGY
MEDICAL LIBRARY
ROYAL PARADE
TRAM No's 18,19 & 20
SWANSTON STREET
TRAM No's 1,15
EDUCATION RESOURCE CENTRE
FRANK TATE
JOHN SMYTHE
R M H CLINICAL SCIENCES
HOWARD FLOREY
JOHN MEDLEY
ENGINEERING
MECH & MANUF ENGINEERING
ARTS CENTRE
MEDICINE
Kernot Road
R M H MEDICAL RESEARCH
Pathology
Anatomy
SURVEYING
CIVIL ENG
ENVIRONMENTAL HYDROLOGY
CARDIGAN STREET
N
GRATTAN STREET
MUSEUM STATION
ROYAL DENTAL HOSPITAL
TO G.P.O. (1.5km)
BERKELEY ST
BARRY ST
University Square
LEICESTER ST
BOUVERIE ST
LINCOLN SQ
TO CENTRAL MELBOURNE (1.5km)
GRADUATE SCHOOL OF MANAGEMENT
ELEC ENG & COMP SCIENCE
PHYSIOTHERAPY PUBLIC HEALTH & COMMUNITY MEDICINE
CITRL CSIRO
PELHAM ST
464 Medley Hall